

Supramolecularly Self-Organized Nanomaterials: a Voyage from
Inorganic Particles to Organic Light-Harvesting Materials

by

ALESSANDRO VAROTTO

A dissertation submitted to the Graduate Faculty in Chemistry in partial fulfillment
of the requirements for the degree of Doctor of Philosophy, The City University of
New York

2009

© 2009

ALESSANDRO VAROTTO

All Rights Reserved

This manuscript has been read and accepted for the Graduate Faculty in Chemistry in satisfaction of the dissertation requirement for the degree of Doctor of Philosophy.

<u>08/21/2009</u>	<u>Dr. Charles M. Drain</u>
Date	Chair of Examining Committee
<u>08/21/2009</u>	<u>Dr. Mahesh K. Lekshman</u>
Date	Executive Officer

Dr. T. Carofiglio

Dr. T. Francesconi

Dr. I. Kretzschmar

Dr. H. Matsui

Dr. L. Todaro

Supervision Committee

THE CITY UNIVERSITY OF NEW YORK

Abstract

Supramolecularly Self-Organized Nanomaterials: a Voyage from
Inorganic Particles to Organic Light-Harvesting Materials

by

Alessandro Varotto

Adviser: Professor Charles Michael Drain

In 2009 the U.S. National Science Foundation announced the realignment of the Chemistry Divisions introducing the new interdisciplinary program of “*Macromolecular, Supramolecular and Nanochemistry.*” This statement officially recognizes a field of studies that has already seen the publication of many thousands of works in the past 20 years. Nanotechnology and supramolecular chemistry can be found in the most diverse disciplines, from biology to engineering, to physics. Furthermore, many technologies rely on nanoscale dimensions for more than one component. Nanomaterials and technologies are on the market with a range of applications from composite materials, to electronics, to medicine, to sensing and more. This thesis will introduce a variety of studies and applications of supramolecular chemistry to form nanoscale photonic materials from soft matter.

We will first illustrate a method to synthesize metallic nanoparticles using plasmids DNA as a mold. The circular DNA functions as a sacrificial template to shape the particles into narrowly monodispersed nanodiscs. Secondly, we will describe the synthesis of a highly fluorinated porphyrin derivative and how the fluorines improve the formation of ultra thin films when the porphyrin is blended with fullerene C₆₀. Finally, we will show how to increase the short-circuit current in a solar cell built with an internal parallel tandem light harvesting design. A blend of phthalocyanines, each with a decreasing optical band gap, is supramolecularly self-organized with pyridyl-C₆₀ within thin films. The different band gaps of the single phthalocyanines capture a wider segment of the solar spectrum increasing the overall efficiency of the device.

In conclusion, we have presented a number of studies for the preparation of inorganic and organic nanomaterials and their application in supramolecularly organized photonic devices.

Dedicated to my parents, Renato and Mariella

Dedicata ai miei genitori, Renato e Mariella

Acknowledgments

I would like to express a special thank to my mentor Professor Drain, not only for giving me the chance to work in his laboratory but also for the freedom and trust he granted me in managing the research. I am also very grateful for having the opportunity to visit and work in other laboratories such as Dr. Liu's in University of California at Davis, Dr. Smith's at Haverford College and Dr. Black's from the Center of Functional Nanomaterial at Brookhaven National Labs. In particular, I thank Dr. Black and Dr. Nam for their vital contribution to this work.

I thank the member of my committee, Dr. Carofiglio, Dr. Francesconi, Dr. Kretzschmar, Dr. Matsui and Dr. Todaro for their help, support and suggestions that helped me achieve the results presented in this book. In particular, I thank Dr. Carofiglio for the countless and precious ideas, hours spent in discussion and for his friendship; Dr. Francesconi for her helpful comments during our meetings; Dr. Kretzschmar for her advice; Dr. Matsui for his guidance, suggestions and personal help; and Dr. Todaro for his assistance in solving the crystal structures of the compounds and for his kind friendship.

A special thank to Dr. Grohmann for being a portable encyclopedia of organic chemistry and for helping me carry out some delicate reactions.

Thank you so very much to my friends and colleagues Jacopo, Ivana, Giorgio, Amit, Sunanina, Sebastian, Gabriela and Matt. Thank you for bringing laughs and fun every day in the lab.

Finally, I thank my parents, Renato and Mariella, for supporting me in pursuing my dreams.

Table of Contents

Chapter 1. Introduction

1. Introduction	1
1.1 Porphyrinoids	1
1.2 The electronic properties of porphyrinoids	4
1.3 Supramolecularly self-organized systems	8
1.4 Self-Assembly and Self-Organization of Porphyrin thin films on surfaces	11
1.5 Porphyrins and Fullerenes Architectures	14
1.6 Conclusions and Outlook	24
References	25

Chapter 2. Fabrication of Metal Nanoparticles using Plasmid DNA as a

Sacrificial Mold

2.1 Introduction	35
2.2 Characterization of the Nanoparticles	38
2.3 Use of different Plasmids	44
2.4 Conclusions	49
2.5 Two-particle Lithography	50
2.6 Conclusions	52
References	50

Chapter 3. Self-Organization of a New fluorous Porphyrin and C₆₀ Films on

Indium-Tin-Oxide Electrode

3.1 Introduction	55
3.2 Synthesis	57
3.3 Preparation of Films on ITO and Characterization	59
3.4 Role of the Fluorines Moieties on the Stability of the film	70
3.5 Conclusions	72
3.6 Experimental Section: Syntheses and Characterization of the compounds	73
References	80

Chapter 4. Phthalocyanines Blends Parallel Tandem Solar Cells

4.1 Introduction: Solar Cells	82
4.2 Scope of the Work	90
4.3 Design of the Solar Cell	98
4.4 AFM	103
4.5 Experimental Section: Syntheses and Characterization of the Compounds	107
References	116

Chapter 5. Self-Organization of Pc787 and Fullerene C₆₀ on ITO

5.1 Introduction	118
5.2 Preparation of the Slides	120
5.3 Pc787 and Fullerene C ₆₀	120
5.4 Conclusions and Outlook	133
References	134

Chapter 6. Synthesis of Novel Chromophores for the Preparation of

Organic Solar Cells

6.1 Synthesis of Porphyrin-Phthalocyanine Dyads	135
6.2 Synthetic procedures	139
6.3 Synthesis of Zn-Pc bearing long perfluoroalkanes	141
References	142

Bibliography

I - XXVIII

List of Figures

Figure 1.1 Structures of 4 of the most common porphyrinoids	2
Figure 1.2. Typical UV–vis spectra of porphyrins	6
Figure 1.3. Typical UV–vis spectra for a phthalocyanine	7
Figure 1.4. Electrostatic self-assembly of multilayers on quartz	13
Figure 1.5. Example of a covalently bound porphyrin-fullerene complex	16
Figure 1.6. X-ray crystal structure of a porphyrin dyad	17
Figure 1.7. Porphyrin dyad with spacer: 1.2 nm separation	19
Figure 1.8. Films of a highly fluorinated porphyrin and C ₆₀	21
Figure 1.9. Self-assembly of porphyrin-fullerene materials	23
Figure 2.1 AFM of Plasmids DNA	37
Figure 2.2 AFM of metal nanoparticles	38
Figure 2.3 TEM images of metal nanodiscs	38
Figure 2.4. AFM height image of plasmid pcDNA 3.1	41
Figure 2.5. AFM amplitude images of metal nanoparticles	42
Figure 2.6. TEM images of metal nanodiscs	43
Figure 2.7. AFM image of Ni and Co nanoparticles	44
Figure 2.8. AFM images (1.5X1.5 μm) of plasmid DNA/NiCl ₂ on HOPG	46
Figure 2.9. Gel electrophoresis	47
Figure 2.10. ED patterns of the prepared nanodiscs	49
Figure 2.11. Average heights of gold, nickel and cobalt nanoparticles	51
Figure 2.12. (A) Height analysis of (B) AFM image of nickel nanoparticles	52

Figure 2.13. TEM images of the control experiments	46
Figure 2.14. Schematic steps for the nanopatterning of rings	48
Figure 2.15. AFM images of the nanorings on MICA	49
Figure 3.1. Ellipsoid crystal structure of TPPF ₁₀₀ 1	55
Figure 3.2. Absorption spectrum of 1 in CCl ₄	59
Figure 3.3. Fluorescence spectra of film of 1 on ITO	63
Figure 3.4. Combined laser scanning and atomic force microscopy	67
Figure 3.5. Nanoshaving of films of 1 : C ₆₀ (1:1) on ITO electrode	68
Figure 3.6. 10x10 μm AFM image of a film of 1 and C ₆₀ on ITO	69
Figure 3.7. AFM image - section analysis of co-deposition of 2 and C ₆₀	71
Figure 3.8. UV-Vis spectra of the co-deposition of compound 2 and C ₆₀	71
Figure 3.9. High resolution ESI-MS of compound 1	75
Figure 3.10. ¹ H NMR of 1 in CDCl ₃ 5% TFA	76
Figure 3.11. ¹⁹ F NMR of 1 in CDCl ₃ 5% TFA	77
Figure 3.12. ¹ H-NMR of compound 2	78
Figure 3.13. FAB spectrum of compound 2	79
Figure 3.14. ¹ H-NMR of compound 2	80
Figure 4.1. Scheme of the charge transfer processes	85
Figure 4.2. An ideal solar cell modeled by a current source	86
Figure 4.3. Principles of device function for organic layers	87
Figure 4.4. Current–voltage characteristics	88

Figure 4.5. Schematic of a bi-layer device	89
Figure 4.6. Schematic of a Bulk Heterojunction	89
Figure 4.7. Optical absorbances and Q-band HOMO-LUMO gap of Pcs	92
Figure 4.8. Relative energy levels of the device components	93
Figure 4.9. IPCE compared to the absorbance of the blend device	97
Figure 4.10. Absorption spectra of the films of Pc derivatives	98
Figure 4.11. Variation of the V_{oc} and J_{sc} versus content of py-C ₆₀	102
Figure 4.12. Absorption of the blended film on ITO	102
Figure 4.13. Plot of the efficiencies versus the concentration	103
Figure 4.14. AFM height analysis of films of active materials	106
Figure 4.15. MALDI MS of Pc707	109
Figure 4.16. MALDI MS of Pc735	110
Figure 4.17. MALDI HRMS of Pc787 with 16 thioalkanes	111
Figure 4.18. Cyclic voltammogram of Pc677	113
Figure 4.19. Cyclic voltammogram of Pc707	114
Figure 4.20. Cyclic voltammogram of Pc735	115
Figure 4.21. Structure of py-C ₆₀	115
Figure 5.1. AFM heights analysis (tapping mode) of a film	121
Figure 5.2. UV-Vis absorption spectra of Pc787 on ITO	122
Figure 5.3. UV-Vis absorption spectra of Pc787 blended with C ₆₀	102
Figure 5.4. AFM height analysis of Pc735 on ITO	123
Figure 5.5. Nanoparticles formed by soaking a slide of ITO	124

Figure 5.6. Larger scan of the same sample described in Figure 5.5	126
Figure 5.7. AFM height analysis of four different samples	127
Figure 5.8. AFM images of nanoparticles	127
Figure 5.9. AFM images (5x5 microns, height mode) of nanoparticles	128
Figure 5.10. (A) AFM images of nanoparticles	129
Figure 5.11. AFM images of nanoparticles formed from Pc787/C ₆₀	130
Figure 5.12. AFM image (Amplitude, tapping mode) of particles	132
Figure 5.13. AFM height analysis of the particles described in Figure 5.12	133
Figure 6.1. Synthetic schemes	136
Figure 6.2. Synthesis of the porphyrin-phthalocyanine conjugate	137
Figure 6.3. Maldi of perfluoroalkylated ZnPc	142
Figure 6.4. Maldi of alkylated ZnPc	143

List of schemes, tables and charts

Chart 2.1. Histograms of the height distribution determined by AFM	40
Chart 2.2. Histograms of the height and diameter	48
Scheme 3.1. Reagents and conditions	57
Table 4.1. Optical bandgaps and HOMO-LUMO energy levels	85
Table 4.2. Solar cell PV characteristics	89
Scheme 5.2. Structures of phthalocyanine Pc787 and fullerene C ₆₀	114

CHAPTER 1

1. INTRODUCTION

In this chapter, the nomenclature, properties and applications of a vast class of compounds, called porphyrinoids, will be introduced. Porphyrinoids include porphyrins, phthalocyanines, porphyrazines, corroles and more. Nevertheless, the main focus of this thesis will be on porphyrins and phthalocyanines. A brief overlook on the supramolecular self-organization of porphyrinoids, with their use and applications, will be presented. Finally, since most of the thesis will be devoted to the description of porphyrinoids and fullerenes assemblies, a few paragraphs will illustrate the chemistry and relevance of these adducts.

1.1. PORPHYRINOIDS

A porphyrin is a heterocyclic macrocycle derived from four pyrroline subunits interconnected via their α carbon atoms via methine bridges ($=CH-$). Porphyrins are aromatic and they obey Hückel's rule for aromaticity in that they possess $4n+2$ π electrons which are delocalized over the macrocycle.¹⁻³ The macrocycle, therefore, is a highly-conjugated system, and, as a consequence, is deeply coloured - the name porphyrin comes from a Greek word for purple. The macrocycle has 22 π electrons. The parent porphyrin is porphine, and substituted porphines are called porphyrins. Many porphyrins occur in nature, such as in

green leaves and red blood cells, and in bio-inspired synthetic catalysts and devices.

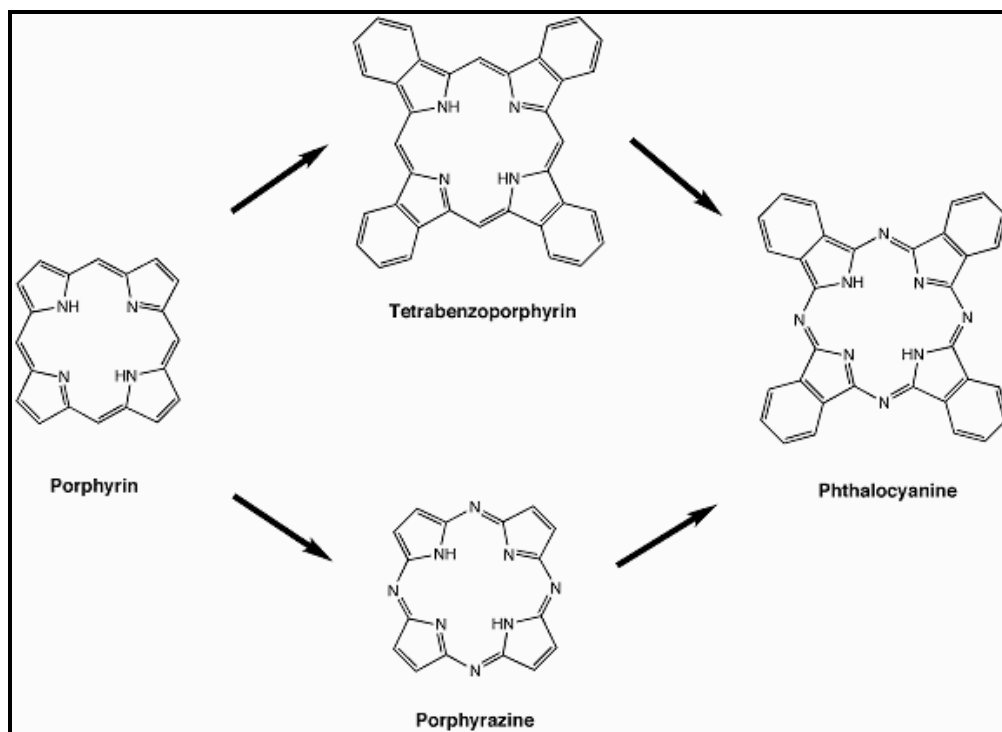
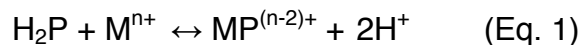


Figure 1.1 Structures of 4 of the most common porphyrinoids

Porphyrins bind metals to form complexes. The metal ion, usually with a charge of 2+ or 3+, resides in the central N4 dianion cavity formed by the loss of two protons. Most metals can be inserted. A schematic equation for these syntheses is shown:



A porphyrin in which no metal is inserted in its cavity is called a free base. Some iron-containing porphyrins are called hemes; and heme-containing proteins, or hemoproteins, are found extensively in nature. Hemoglobin and myoglobin are two O₂ binding proteins that contain iron porphyrins.

Related to porphyrins are several other heterocycles, including corrins, chlorins, bacteriochlorophylls, and corphins. Chlorins (2,3-dihydroporphyrin) are more reduced than porphyrins, featuring a pyrroline subunit. This structure occurs in chlorophyll. Replacement of two of the four pyrrolic subunits with pyrrolic subunits results in either a bacteriochlorin (as found in some photosynthetic bacteria) or an isobacteriochlorin, depending on the relative positions of the reduced rings. Some porphyrin derivatives follow Hückel's rule, but many do not.¹⁻³

Porphyrinoids are characterized by unique absorption spectra in the visible, denoted as B- and Q-bands. In porphyrins the B-band appears in the blue and it is much more intense than the Q-bands (approximately 5-10 times depending on the specific derivative), whereas in phthalocyanines the opposite is true and the B-band is shifted towards the UV.⁴ The differences arise mostly from the shape and number of the frontier molecular orbitals which affect the electronic transitions. The number of Q-bands is normally four for free base and two for metallo-porphyrinoids, where the latter is due to a degeneracy of the energy levels arising from the increased symmetry.⁴

Syntheses of porphyrins have been known for decades, while phthalocyanines have been used as dyes for over 100 years. Many derivatives are commercially available and relative inexpensive or relatively easy to synthesize; features that make them appealing for the fabrication of devices useful for everyday applications.

1.2. THE ELECTRONIC PROPERTIES OF PORPHYRINOIDS

As anticipated above, the UV-Vis spectra of porphyrinoids consist of two absorptions, one in the near UV to blue (ca. 380 nm to 430 nm) and one in the visible. The location and intensity depend on a variety of factors, such as substitution of the macrocycle, metallation, protonation and environment. Martin Gouterman successfully described the electronic spectra of porphyrinoids by using theoretical concepts.⁵ The so-called four-orbital model uses two HOMO's and LUMO's generated by Huckel theory and the electronic transition from the former to the latter accounts for the spectra of porphyrinoids. In porphyrins, the dominant spectral feature appears between 400-430 nm because it is an allowed transition, whereas the Q-bands are weakly allowed because of vibronic coupling and therefore less intense.⁴ In phthalocyanines the forbidden transition acquires significant intensity and therefore the Q-bands are the predominant spectral absorption, whereas the B-band is shifted toward shorter wavelengths. This behavior is also confirmed by more complex theoretical calculations, which account for the mixing of the frontier molecular orbitals. The electronic spectra of

free base porphyrins and phthalocyanines are characterized by split Q-bands, due to a reduction of the symmetry from D_{4h} to D_{2h} when going from the metal complexes to the free bases. Figures 1.2 and 1.3 summarize graphically these concepts.

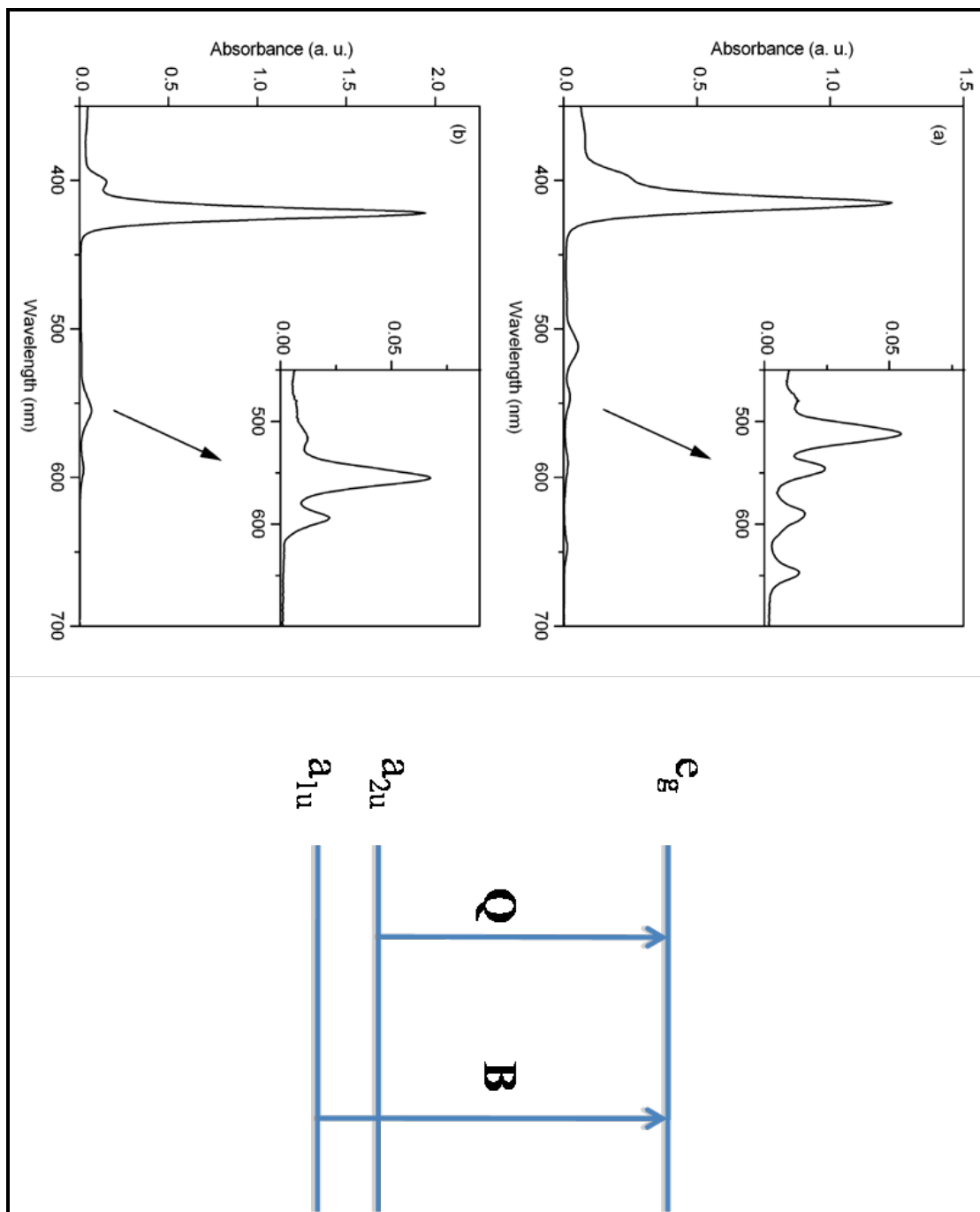


Figure 1.2. Typical UV-vis spectra for (a) a free-base porphyrin and (b) a porphyrin-metal complex (left) and scheme of energy levels in metallated porphyrins with the first two π - π^* transitions, the Q- and B-bands, marked (right). Adapted from reference 4.

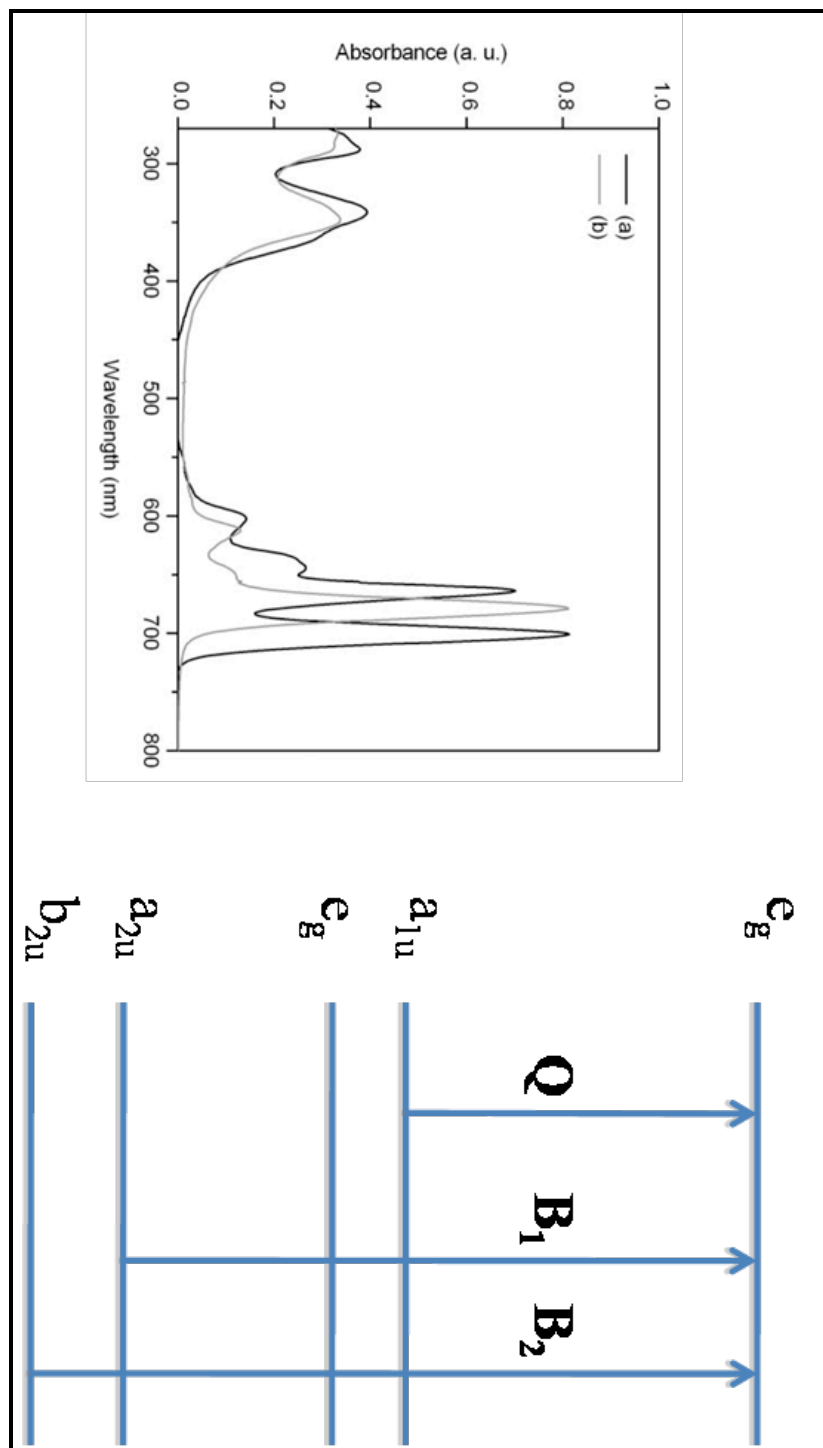


Figure 1.3. Typical UV-vis spectra for a phthalocyanine as (a) a free-base and (b) a metal complex (left). The scheme of energy levels in metallated phthalocyanines with the first two π - π^* transitions, the Q- and B-bands, marked (right). Adapted from reference 4.

1.3. SUPRAMOLECULARLY SELF-ORGANIZED SYSTEMS

One key feature in the chemistry of porphyrinoids^a is the substitution of the periphery of the macrocycle with different moieties. The substitution can be tailored to change the optical properties, increase solubility in particular solvents, distort the planarity of the ring, and for many other reasons. Furthermore, it is possible to functionalize the ring with a variety of groups that can direct the self-organization of the molecules into discrete nanostructures via supramolecular interactions such as H-bonding, π - π , electrostatic, coordination, and other types of non-covalent forces. One of the most common moieties used to self-organize the molecules via H-bonding is the carboxylic group. There are a number of reports about the formation of nano-wires, -sheets and other 3-D networks by employing this functionality. Other common substituents include long alkylic chains, to promote the formation of mesogenic materials and H-bond acceptors, for instance the pyridyl group.

For some applications, such as solar energy harvesting,⁶ several chromophores are needed to collect light from the entire solar spectrum and to maximize optical density.⁷ Therefore as in nature, construction of multi chromophoric systems or materials is important to ensure maximum use of solar energy. Arrays containing different kinds of dyes can be engineered in several ways. (1) To assure vectoral energy/electron transfer, the architectural organization of the chromophores must be specifically designed such that molecules with the greatest HOMO-LUMO gap can funnel energy/electrons to

^a Adapted from reference: Chem. Rev., 2009, 109 (5), pp 1630–1658

those with the lowest HOMO-LUMO gap next to the electrode. Supramolecular systems afford a viable means to accomplish this. (2) Spatially separated chromophores in patterns with periodicity less than ca. 400 nm may assure maximal charge injection into the electrode without competing energy/electron transfer to neighboring dyes with different electronic properties. The latter strategy can be accomplished by adsorbing the dyes onto different nanoparticles and by nanolithography. The former strategy is employed in natural light-harvesting systems in photosynthesis,⁸⁻¹¹ wherein the photonic properties of the antenna systems are controlled by the spatial arrangement and orientation of the various chromophores self-assembled on a protein scaffold.

Given the potential applications and the need for better theoretical frameworks, the design and construction of novel multi porphyrin architectures by self-assembly and self-organization continues to be an active research area. The self-organization of a single type of porphyrin into crystalline materials using non-specific intermolecular interactions and HOMO coordination has a long, rich history.^{1, 12-16} More recent efforts have incorporated exocyclic moieties for specific intermolecular interactions that direct the organization of a given porphyrin into more ordered and/or more robust crystalline systems.^{17, 18} An early example of discrete porphyrin arrays are those self-assembled using electrostatic interactions in the liquid crystalline matrix of lipid bilayers, which functioned as photogated ion conductors.¹⁹⁻²¹ Later, arrays assembled by specific intermolecular interactions such as H-bonds²²⁻²⁴ and metal ion coordination were

reported.^{23, 25-27} Linear tapes assembled with H-bonds and with coordination chemistry placed in lipid bilayers exhibit photogated electronic conductivity wherein the function of the device relies on the hierarchical structure: molecule, tape, alignment of the tapes in the bilayer, and the organization of the device itself.²⁸ Self-organized systems with different topologies can be formed using designed intermolecular interactions, but additionally, long chain hydrocarbons can be used for the formation of liquid crystals. Covalent attachment to surfaces results in self-assembled monolayers, and packing forces in crystalline materials, can be designed. New venues towards the crystal engineering of porphyrins into crystal lattices include iodo-pyridyl and iodophenyl halogen bonding, but the robustness of these interactions needs to be further investigated.^{29, 30}

Supramolecular synthetic methods and strategies have developed rapidly, and porphyrins are particularly amenable to the design of complex and robust architectures because of their rigid framework. 1-, 2-, and 3-dimensional materials are now routinely accessible. Strategies to make hierarchically organized porphyrinic materials, wherein the local structure is different than the global organization,²⁷ are now a research focus. These porphyrin assemblies are of fundamental importance not only as models for the study of light harvesting antenna and photosynthetic reaction centers but also as building blocks for the construction of a variety of functional photonic devices.⁷

1.4. SELF-ASSEMBLY AND SELF-ORGANIZATION OF PORPHYRIN THIN FILMS ON SURFACES

Because of the potential applications of porphyrinic nanomaterials in areas such as molecular electronics, photonics, and for semiconductor sensitization, there has been a great interest in utilizing supramolecular chemistry as a means to fabricate components for nanoscale devices. However, in order to make stable and useful solid nanoarchitectures, the self-assembled and self-organized systems have to be transferred from solution onto surfaces while maintaining the same or at least predictable structure and function. Deposition onto surfaces can be challenging since the equilibria, therefore structures, in supramolecular systems can significantly change upon altering the environment. These factors include solvent, concentration, temperature, moisture, and evaporation rate. For weakly interacting molecules deposited from solvents (drop cast, spin cast and dipping), solvent dynamics, in terms of microscopic flow and shear play a crucial role in the morphology of the resultant film. Microscale and nanoscale rings, rods, and fibers can be formed as a consequence of both intermolecular interactions and solvent dynamics.^{31,32} The angle of the substrate during deposition, whether it is held horizontal or vertical, can make significant differences. Since surface energetics and surface structure can have a significant influence on the organization of molecules on surfaces, from a different standpoint, surface properties can be used as another design tool. Matching surface chemistry to linking groups, e.g. gold and thiols, and energetics to molecules, e.g. HOPG and

large aromatic molecules, can yield highly organized monolayers. Additionally, useful nanomaterials should be long lasting and resistant to environmental influences like humidity, dioxygen, or redox chemistry.^{33, 34}

There have been many reports on self-assembled and self-organized porphyrinic systems deposited on surfaces.³⁴ Recent work using H-bonds between stereogenic centers probed the role of chiral centers on surface-assembly in two dimensions, where it was found by STM that only one of the two porphyrin faces is oriented toward the HOPG surface.³⁵ We focus on multicomponent, two-dimensional porphyrin materials, self-organized into multilayer thin films, as well as 2D ordering of molecules on solid surfaces. Various degrees of molecular organization can be obtained through several deposition methods.^{33, 34, 36} (1) Multilayer thin films on surfaces can be fabricated by layer-by-layer and sequential dipping methods that rely on noncovalent electrostatic, ionic, coordination, or H-bonding interactions,³⁴ and (2) Self-assembled monolayers (SAMs), bound to a surface via covalent or coordination bonds or by absorption. Scanning probe microscopy (AFM or STM) are key tools in examining the structure of these materials on a surface.

1.4.1. LAYER-BY-LAYER METHODS

Generally, layer-by-layer (LBL) methods consist of dipping a charged substrate into a solution containing a molecule or polyelectrolyte of the opposite charge, resulting in the formation of a layer of material on the surface.^{37, 38} After

annealing and rinsing, the substrate is immersed into a second solution containing a molecule or polyelectrolyte of opposite charge than in the first solution. Thus, each dipping results in a film electrostatically absorbed onto the surface. The films are not a priori complete and often they interdigitate. This method enables formation of multilayer films since the same procedure can be repeated many times. A large number of layers is possible, but the fidelity and structure of the films can change, usually decrease, with an increasing number of layers.^{33, 34, 36, 39} While charged supports such as mica allow more rapid development of the initial layers, polar oxide surfaces such as glass and ITO can be used, but several dipping cycles are usually necessary to form complete films of charged molecules.

There are many reports on LBL-organized porphyrin materials for use as sensors⁴⁰⁻⁴⁷ for modification of electrodes,³⁶ for photovoltaics,⁴⁸⁻⁵⁰ and for non-linear optic (NLO) materials (Figure 1.4).^{40, 51}

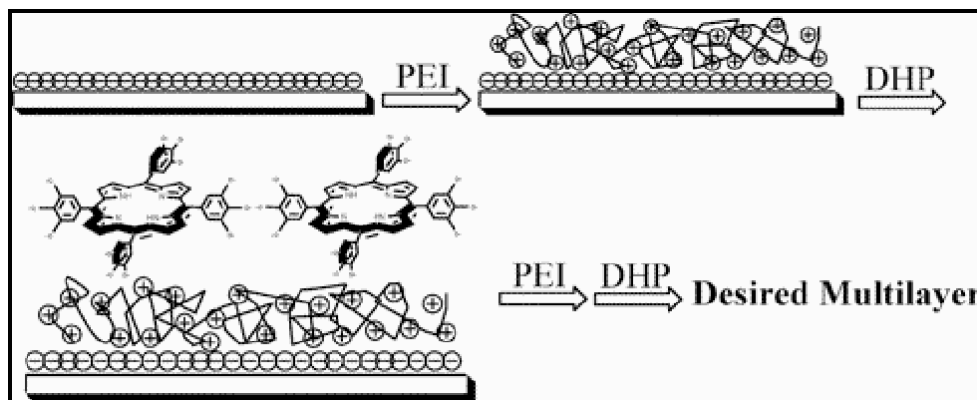


Figure 1.4. Electrostatic self-assembly of multilayers on quartz can result in porphyrinic films with good NLO properties. Taken from reference 51.

1.5. PORPHYRIN AND FULLERENE ARCHITECTURES

The primary focus of this thesis is on supramolecular porphyrinoids/fullerene adducts, therefore the next few paragraphs will be dedicated to the description of these materials. Examples wherein the fullerene is coordinated to metalloporphyrins via a ligand will be discussed. Great efforts have been devoted to the preparation and the study of complexes formed between porphyrins and fullerenes because these constructs and materials can exhibit efficient charge-separation.⁵² Thus, porphyrin-fullerene architectures have been studied as photovoltaic devices and proposed to be viable components for the conversion and utilization of solar energy.⁵³⁻⁵⁵

The nature of the bonding between the porphyrin and fullerene is an important director of the photonic properties of materials composed of these molecules. Constructs that use covalent bonds to link the porphyrin to the fullerene, which may or may not include a functional linker/spacer, are widely studied. In supramolecular porphyrin–fullerene materials the components are spontaneously self-assembled and self-organized by non-covalent interactions.^{56,}
⁵⁷ There are non-directional interactions such as π - π interactions and van der Waals forces as found in co-crystallized materials. There are also specific intermolecular interactions mediated by coordination chemistry, for example the axial coordination of a substituted fullerene to a metalloporphyrin. In solid-state materials a combination of several intermolecular interactions dictate the arrangement of the molecules in the material.

1.5.1. COVALENT BONDING

There are numerous studies on porphyrins covalently bound to C₆₀.⁵⁸⁻⁶⁶ The nature of covalent bonds to the fullerene and to the porphyrin, e.g. the functional groups used, can be exploited as a means to fine-tune the properties of the dyads (see Figure 1.5).⁶⁷ The linking moiety also can provide a versatile handle to impart additional functions to covalently linked dyads. The synthetic chemistry of these systems is well developed, can proceed in good yields, and facilitates characterization of the molecule by a variety of spectroscopic techniques. One significant disadvantage of the covalent approach includes the modification of the fullerene to form a covalent bond, which decreases the spherical orbital symmetry and causes an increase in the reorganization energy to be overcome in the formation of charge transfer species with an electron donor. The decreased efficiency is generally deleterious to the function of the materials, but these dyads can have better charge separation than many other donor-spacer-acceptor systems.⁶⁸

Many of these covalent structures have been deposited on surfaces in the form of chemisorbed or physisorbed materials.⁶⁹ Some porphyrin-fullerene compounds can self-organize into ordered arrays, and some are further modified to allow the formation of SAMs on solid surfaces such as gold electrodes or indium-tin-oxide (ITO).⁷⁰⁻⁷² Considering the chemical differences in covalently bound systems, it is difficult to discern which mode of surface binding (adsorption or SAM) results in the more efficient charge injection into band gap materials.

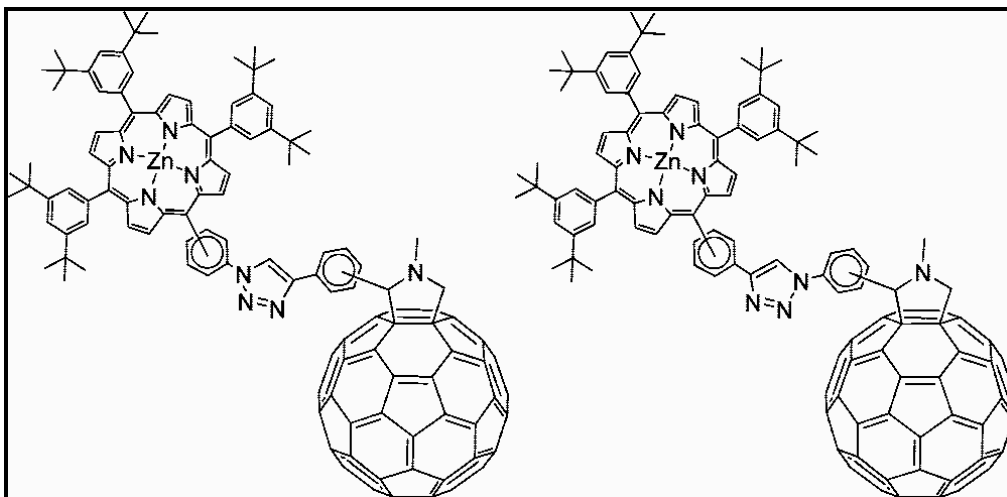


Figure 1.5. Example of a covalently bound porphyrin-fullerene complex. Taken from reference 67.

1.5.2. DISPERSION FORCES

Fullerenes and porphyrins are spontaneously attracted to each other via π - π intermolecular interactions between the curved surface of a fullerene and the center of a porphyrin. There are also electrostatic interactions between the electropositive center of the porphyrin or some metalloporphyrin macrocycles and fullerenes such as C_{60} .^{73, 74} The combination of these two attractive forces shortens the distance between the C_{60} and the center of the porphyrin compared to the distance expected from the π - π interactions alone (see Figure 1.6). This supramolecular motif is used for the design of a variety of new solid-state porphyrin-fullerene nanoarchitectures.⁷³⁻⁷⁶

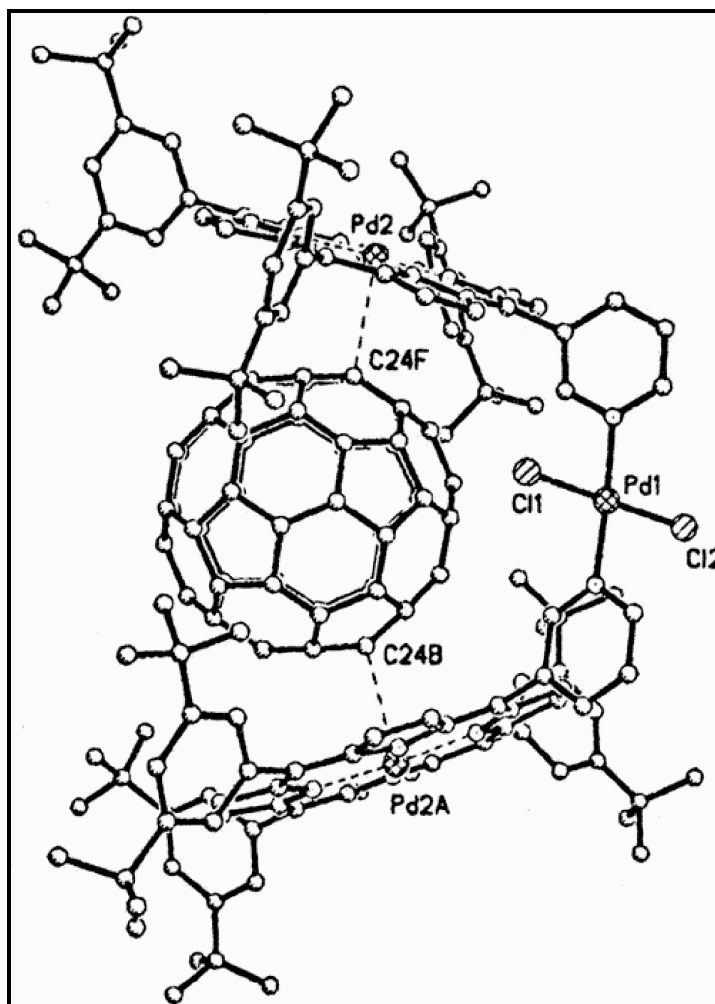


Figure 1.6. X-ray crystal structure of a porphyrin dyad with encapsulated C_{60} . The Pd2...C24F distance is 2.856(10) Å. A combination of π - π interactions and electrostatic forces between the porphyrins in the tweezers allow the complexation of the fullerene. Taken from reference 77.

Fullerenes such as C_{60} are efficient electron acceptors and differ from other widely used electron acceptor molecules because of the spherical shape, large size, polarizability, and lack of a dipole.^{52, 78} These properties result in small molecular and solvent reorganization energies upon accepting electron(s) from metallo- and free-base porphyrin electron donors.⁵² Though much of this work has been done on the covalently bonded dyads, supramolecular porphyrin- C_{60}

constructs can also lead to the formation of long-lived charge separated states which exhibit desirable electronic and photophysical properties.⁵² Consequently, porphyrin-C₆₀ systems can be used as dyes that serve to photosensitize charge transport in band gap materials such as TiO₂ and ITO using solar light.^{79, 80} Photoelectronic applications and dye-sensitized solar cells are well reviewed.⁸¹

Depending on the environment, the peripheral substituents on the macrocycle, and the mode of assembly, several different nano to micro scaled structures have been made. These structures range from nanotubes,^{82, 83} nanoporous networks,⁶⁹ host-guest complexes,⁸⁴⁻⁸⁸ to highly ordered framework solids.^{43, 89-98} Varying the conditions used to self-organize these materials can lead to the formation of different architectures using the same starting compounds. For instance, Imahori and coworkers demonstrated that altering the ratio of porphyrin:C₆₀ results in different structures of the composite clusters which display different photoelectrochemical properties.⁸⁷ Two important considerations in the supramolecular synthesis of host-guest complexes containing porphyrins and fullerene are the size of the chromophores and the separation between them. For example, crystal structure analysis shows the approach of a fullerene C₆₀ to the center of the porphyrin mean molecular plane to be ca. 0.27 nm,⁷³ so a minimum of ca. 1.2 nm between the two porphyrins is needed to host the fullerene (Figure 1.7).⁷⁷ It has been shown that shorter or greater spacings lower the binding constants, in the former case because there is

not enough space to accommodate the buckyball and in the latter because of an increased flexibility.

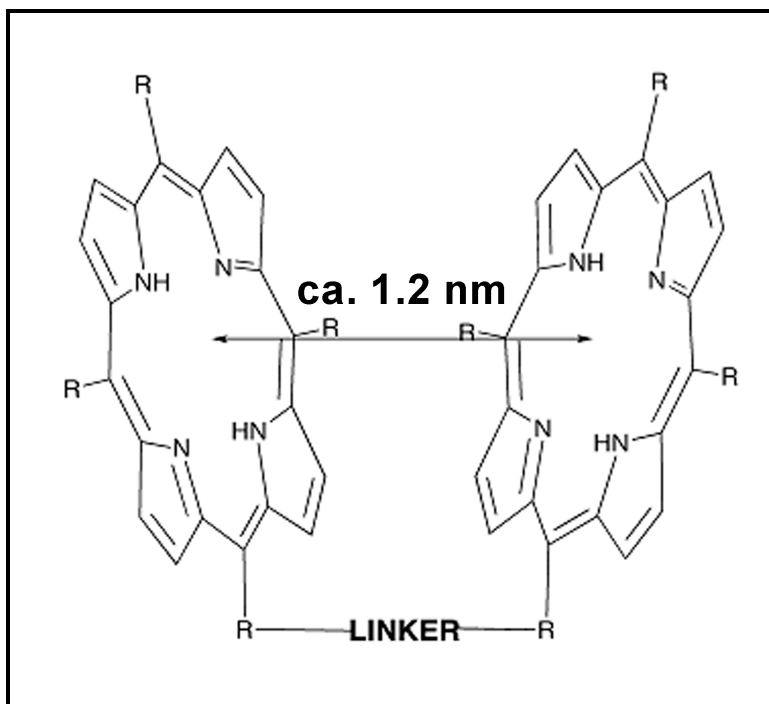


Figure 1.7. Porphyrin dyad with spacer: 1.2 nm separation. Taken from reference 99.

To assemble porphyrins and fullerenes into architectures more complex than discrete host-guest systems such as nanotubes, other specific intermolecular interactions are used. For instance, Naruta et al.⁸² described a tubular structure formed between a cyclic porphyrin dimer and C_{60} that takes full advantage of several non-covalent interactions. The porphyrin nanotubes are self-organized by both the formation of non-classical H-bonds between the pyrrole β -H and the nitrogen of a pyridyl group and weak π - π interactions between the pyridyl groups. The C_{60} molecules are held within the tubular

structure by π - π and C-H $\cdots\pi$ interactions. In this case the host reinforces the structure of the guest. Recently, a rotaxane-porphyrin conjugate has been used as a molecular tweezers to host C₆₀ through π - π interactions.¹⁰⁰ This assembly is interesting because the scaffold can be immobilized onto gold surface through a thio-terminated linker to create a functionalized electrode for photoelectrochemical applications. In another report, porphyrins have been attached to a cellulose motif designed to encapsulate C₆₀, and the films of this material fabricated by a LB technique exhibited photo-currents.¹⁰¹ Most of the self-assembled structures are also driven by crystal packing forces. Mixtures of C₆₀ with simple tetraphenylporphyrins, and those appended with long alkyl chains, cast on ITO or other surfaces do not form films and often separate into the two components because the π - π interactions are insufficient to maintain an organized structure. However, we found that perfluoro alkanes appended on the para positions of tetrakis-(tetrafluorophenyl)porphyrin drive the formation of thin films containing C₆₀.¹⁰² The films are organized by the low surface energy due to the fluorinated alkanes, and fullerene C₆₀ is held in the film through a combination of π - π interactions and C-F $\cdots\pi$ interactions (see Figure 1.8 and chapter 3).^{75, 76, 102}

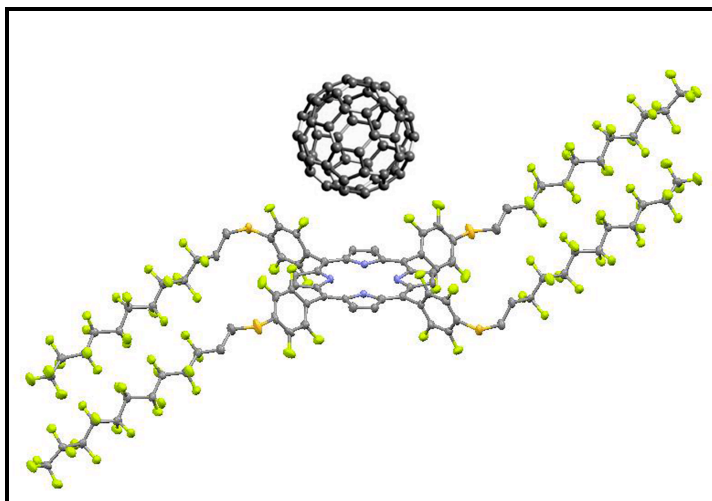


Figure 1.8. Films of a highly fluorinated porphyrin and C₆₀ form when cast on ITO due to both π - π interactions and the additional van der Waal's interactions between the fluorinated alkanes and the fullerene. Taken from reference 99.

1.5.3. AXIAL COORDINATION

There are numerous reports on the formation of porphyrin-C₆₀ architectures mediated by axial coordination of a ligand substituent on the fullerene to the metal center or a metalloporphyrin.^{41, 92, 103-115} The nature of the ligand is matched to the binding and geometry of the target metal ion. Moreover, it is possible to place more than one ligand on the C₆₀ core, thereby increasing the topological diversity of self-assembled structures and affording a compound that can be in the backbone of a coordination polymer or assembled into a triad with two different donor molecules.¹¹⁶

Axial coordination offers a versatile approach to the rapid preparation and photophysical characterization of self-assembled porphyrin-C₆₀ structures in solution. While some supramolecular systems are not very stable in solution and may reorganize when deposited onto surfaces, the stability and solid state

structure can be modulated by designing ligands with greater binding constants and/or different topologies. As anticipated above, in many cases the self-organization of porphyrin-C₆₀ complexes takes advantage of more than one kind of designed interaction simultaneously. An elegant example of a supramolecular structure assembled by a set of designed intermolecular interaction is offered by D'Souza et al. (Figure 1.9)¹⁰⁵ In this work, two zinc-porphyrins bearing four substituent crown ethers are pre-assembled into a co-facial dimer upon binding four potassium ions, and then a fullerene bi-substituted with a pyridyl and alkylammonium groups are added to the porphyrin assembly. The 2x2 array forms when the pyridyl moieties bind the zinc ion center and the ammonium groups electrostatically interact with the crown ether cation binding centers. (Figure 1.9).

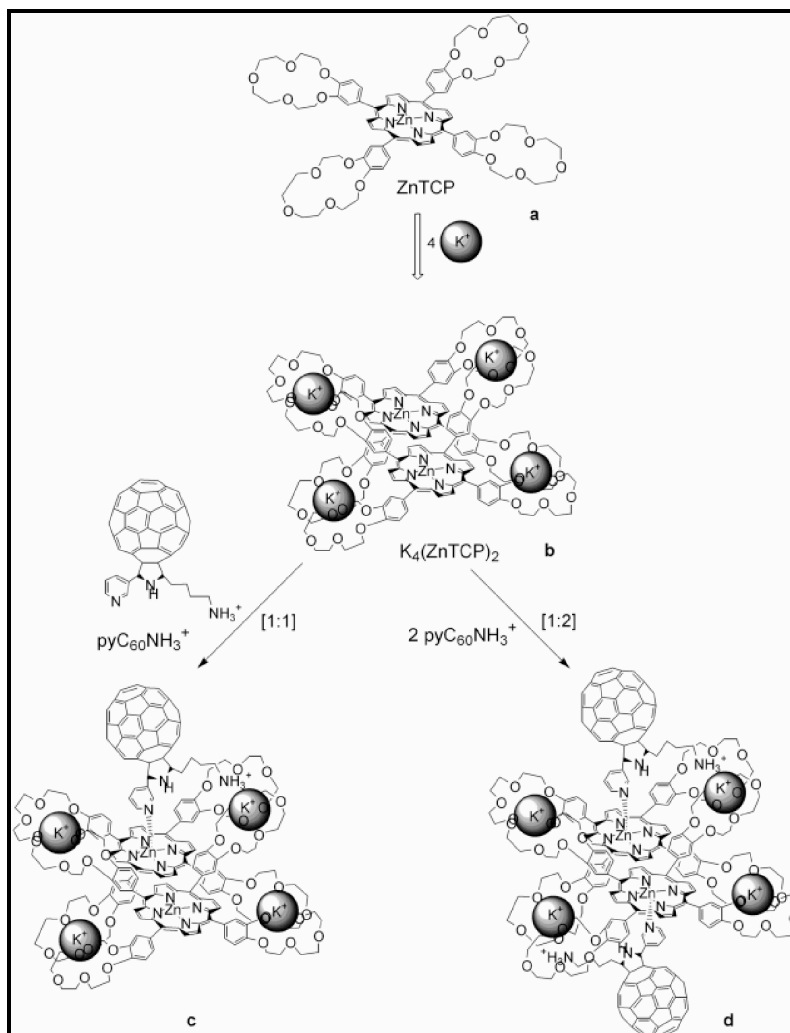


Figure 1.9. Self-assembly of porphyrin-fullerene materials can be mediated by synergic interactions using metal ion coordination and ionic recognition. First the tetra-crown ethers substituted porphyrin (a) pre-assembles into a cofacial arrangement where the potassium ion is sandwiched between crown ethers (b). Second, a fullerene, bis-substituted with a pyridyl and alkylammonium groups, coordinates to the Zn and one of the crown ether entities yielding the formation of a triad if the ratio is 1:1 (c), or tetrad if the ratio is 1:2 (d). Taken from reference 105.

1.6. CONCLUSIONS AND OUTLOOK

Due to their tunable optical and electronic properties, stability and versatility, porphyrinoids are excellent candidates for use in a variety of applications from organic electronics, catalysis, sensors, to photodynamic therapy and more. Nonetheless, to-date there are very few examples of commercially available devices fabricated using porphyrinoids. Therefore, much effort has to be devoted to the improvement of the properties of this class of compounds. Nanomaterials based of porphyrinoids, such as particles or wires, have shown enhanced and exotic characteristics and perhaps this is the route to the needed improvement.

For real-world applications, the organic materials need to be robust, and as importantly, be cost effective in terms of synthesis. These considerations dictate the design constraints on the dyes such that compounds requiring multi-step synthetic procedures, low yields, and complex separations are likely unsuitable. The hypotheses of this manuscript are that self-organized systems obviate the need for complex molecular designs and by extension syntheses, but can afford similar functionalities.

References.

1. Kadish, K.; Smith, K. M.; Guillard, R., *The Porphyrin Handbook*. Academic Press: New York, 2000, 2003; Vol. 1-20.
2. Kimura, M.; Shirai, H., *The Porphyrin Handbook*. In Kadish, K. M.; Smith, K. M.; Guillard, R., Eds. Academic Press: New York, 2003; Vol. 19, pp 151-174.
3. Dolphin, D., *The Porphyrins*. Academic Press: New York, 1978.
4. Rio, Y.; Rodriguez-Morgade, M. S.; Torres, T., Modulating the electronic properties of porphyrinoids: a voyage from the violet to the infrared regions of the electromagnetic spectrum. *Org. Biomol. Chem.* **2008**, 6, 1877-1894.
5. Ceulemans, A.; Oldenhof, W.; Gorller-Walrand, C.; Vanquickenborne, L. G., Gouterman's "four-orbital" model and the MCD spectra of high-symmetry metalloporphyrins. *J. Am. Chem. Soc.* **2002**, 124, (6), 1155-1163.
6. Alstrum-Acevedo, J. H.; Brennaman, M. K.; Meyer, T. J., Chemical Approaches to Artificial Photosynthesis. 2 *Inorg. Chem.* **2005**, 44, 6802-6827.
7. Wasielewski, M. R., Energy, Charge, and Spin Transport in Molecules and Self-Assembled Nanostructures Inspired by Photosynthesis. *J. Org. Chem.* **2006**, 71, (14), 5051-5066.
8. Cogdell, R. J.; Isaacs, N. W.; Howard, T. D.; McLusky, K.; Fraser, N. J.; Prince, S. M., How Photosynthetic Bacteria Harvest Solar Energy. *J. Bacteriol.* **1999**, 181, 3869-3879.
9. Law, C. J.; Roszak, A. W.; Southall, J.; Gardiner, A.; Isaacs, N. W.; Cogdell, R. J., The structure and function of bacterial light harvesting complex. *Mol. Membr. Biol.* **2004**, 21, 183-191.
10. Zuber, H.; Brunisholz, R. A., *Chlorophylls*. CRC: Boca Raton: 1991; p 627-704.
11. Zuber, H.; Cogdell, R. J., *An oxygenic photosynthetic Bacteria*. Kluwer Academic: Boston, 1995; p 315-348.
12. Byrn, M. P.; Curtis, C. J.; Hsiou, Y.; Khan, S. I.; Sawin, P. A.; Tendick, S. K.; Terzis, A.; Strouse, C. E., Porphyrin sponges: conservative of host structure in over 200 porphyrin-based lattice clathrates *J. Am. Chem. Soc.* **1993**, 115, (21), 9480-9497.
13. Shmilovits, M.; Vinodu, M.; Goldberg, I., Porphyrin clathrates. Crystal structures of two unexpected products obtained by solvothermal reactions of Pt-tetra(4-carboxyphenyl)porphyrin with copper acetate. *J. Incl. Phenom. Macro. Chem.* **2004**, 48, (3-4), 165-171.
14. Vinodu, M.; Goldberg, I., Complexes of hexamethylenetetramine with zinc-tetraarylporphyrins, and their assembly modes in crystals as clathrates and hydrogen-bonding network polymers. *New J. Chem.* **2004**, 28, (10), 1250-1254.
15. Abrahams, B. F.; Hoskins, B. F.; Michail, D. M.; Robson, R., Assembly of porphyrin building blocks into network structures with large channels. *Nature* **1994**, 369, 727-729.

16. Fleischer, E. B.; Shachter, A. M., Coordination oligomers and a coordination polymer of zinc tetraarylporphyrins. *Inorg. Chem.* **1991**, 30, 3763-3769.
17. Goldberg, I., Crystal engineering of porphyrin framework solids. *Chem. Commun.* **2005**, (10), 1243-1254.
18. Goldberg, I., Crystal engineering of nanoporous architectures and chiral porphyrin assemblies. *CrystEngComm* **2008**, 10, 637-645.
19. Drain, C. M.; Christensen, B.; Mauzerall, D. C., Photogating of ionic currents across a lipid bilayer. *Proc. Natl. Acad. Sci. USA* **1989**, 86, 6959-6962.
20. Drain, C. M.; Mauzerall, D. C., Photogating of ionic currents across lipid bilayers: hydrophobic ion conductance by an ion chain mechanism. *Biophys. J.* **1992**, 63, 1556-1563.
21. Drain, C. M.; Mauzerall, D. C., Photogating of ionic currents across lipid bilayers: electrostatics of ions and dipoles inside the membrane. *Biophys. J.* **1992**, 63, 1544-1555.
22. Drain, C. M.; Russel, K. C.; Lehn, J.-M., Self-assembly of a multi-porphyrin supramolecular macrocycle by hydrogen bond molecular recognition. *Chem. Commun.* **1996**, 337-338.
23. Drain, C. M.; Batteas, J. D.; Flynn, G. W.; Milic, T.; Chi, N.; Yablon, D. G.; Sommers, H., Designing supramolecular porphyrin arrays that self-organize into nanoscale optical and magnetic materials. *Proc. Natl. Acad. Sci. U S A* **2002**, 99 Suppl 2, 6498-6502.
24. Samaroo, D.; Soll, C. E.; Todaro, L. J.; Drain, C. M., Efficient Microwave-Assisted Synthesis of Amine-Substituted Tetrakis(pentafluorophenyl)porphyrin. *Org. Lett.* **2006**, 8, 4985-4988.
25. Drain, C. M.; Lehn, J., M., Self-assembly of square multiporphyrin arrays by metal ion coordination. *Chem. Commun.* **1994**, 2313-2315 (correction 1995, p503).
26. Drain, C. M.; Nifatis, F.; Vasenko, A.; Batteas, J. D., Porphyrin tessellation by design: Metal-mediated self-assembly of large arrays and tapes *Angew. Chem.* **1998**, 37, 2344-2347.
27. Milic, T.; Garno, J. C.; Batteas, J. D.; Smeureanu, G.; Drain, C. M., Self-organization of self-assembled tetrameric porphyrin arrays on surfaces. *Langmuir* **2004**, 20, (10), 3974-3983.
28. Drain, C. M., Self-organization of self-assembled photonic materials into functional devices: Photo-switched conductors. *Proc. Natl. Acad. Sci. USA* **2002**, 99, 5178-5182.
29. Lipstman, S.; Muniappan, S.; Golberg, I., Supramolecular Reactivity of Porphyrins with Mixed Iodophenyl and Pyridyl mesa-Substituents. *Cryst. Growth Des.* **2008**, 8, 1682-1688.
30. Stang, P. J.; Olenyuk, B., Self-Assembly, Symmetry, and Molecular Architecture: Coordination as the Motif in the Rational Design of Supramolecular Metallacyclic Polygons and Polyhedra. *Acc. Chem. Res.* **1997**, 30, (12), 502-518.

31. van Hameren, R.; Schön, P.; van Buul, A. M.; Hoogboom, J.; Lazarenko, S. V.; Gerritsen, J. W.; Engelkamp, H.; Christianen, P. C.; Heus, H. A.; Maan, J. C.; Rasing, T.; Speller, S.; Rowan, A. E.; Elemans, J. A.; Nolte, R. J., Macroscopic hierarchical surface patterning of porphyrin trimers via self-assembly and dewetting. *Science* **2006**, 314, (5804), 1433-1436.
32. Elemans, J. A. A. W.; Van Hameren, R.; Nolte, R. J. M.; Rowan, A. E., Molecular materials by self-assembly of porphyrins, phthalocyanines, and perylenes. *Adv. Mater.* **2006**, 18, (10), 1251-1266.
33. Drain, C. M.; Chen, X., Self-Assembled Porphyrinic Nanoarchitectures. In *Encyclopedia of Nanoscience & Nanotechnology*, Nalwa, H. S., Ed. American Scientific Press: New York, 2004; Vol. 9, pp 593-616.
34. Drain, C. M.; Batteas, J. D.; Smeureanu, G.; Patel, S., Self-Assembled Porphyrinic Materials on Surfaces. In *Encyclopedia of Nanoscience and Nanotechnology*, Marcel Dekker: New York, 2004; pp 3481-3502.
35. Linares, M.; Iavicoli, P.; Psychogiopoulou, K.; Beljonne, D.; Feyter, S. D.; Amabilino, D. B.; Lazzaroni, R., Chiral Expression at the Solid-Liquid Interface: A Joint Experimental and Theoretical Study of the Self-Assembly of Chiral Porphyrins on Graphite. *Langmuir* **2008**, 24, (17), 9566–9574.
36. Drain, C. M.; Bazzan, G.; Milic, T.; Vinodu, M.; Goeltz, J. C., Formation and Applications of Stable 10 nm to 500 nm Supramolecular Porphyrinic Materials. *Isr. J. Chem.* **2005**, 45, 255–269.
37. Izquierdo, A.; Ono, S. S.; Voegel, J.-C.; Schaaf, P.; Decher, G., Dipping versus Spraying: Exploring the Deposition Conditions for Speeding Up Layer-by-Layer Assembly. *Langmuir* **2005**, 21, 7558-7567.
38. Decher, G.; B.Schlenoff, J., *Multylayer thin films*. Wiley-VCH, Weinheim: 2003.
39. Drain, C. M.; Goldberg, I.; Sylvain, I.; Falber, A., Synthesis and applications of supramolecular porphyrinic materials. *Topics in Current Chemistry* **2005**, 245, 55-88.
40. Jiang, L.; Changa, Q.; Ouyanga, Q.; Liub, H.; Wanga, Y.; Zhanga, X.; Songa, Y.; Lib, Y., Fabrication and nonlinear optical properties of an ultrathin film with acceptor–donor periodically overlapping structure *Chem. Phys.* **2006**, 324, 556-562.
41. Xiang, Y.; Wei, X.-W.; Zhang, X.-M.; Wang, H.-L.; Wei, X.-L.; Hu, J.-P.; Yin, G.; Xu, Z., Synthesis of new pyridinofullerene ligands capable of forming complexes with zinc tetraphenyl porphyrin. *Inorg. Chem. Commun.* **2006**, 9, (5), 452-455.
42. Zhang, B.; Mu, J.; Li, X., Linear assemblies of aged CdS particles and cationic porphyrin in multilayer films. *Appl. Surf. Sci.* **2006**, 252, 4990–4994.
43. Zhang, S.; Echegoyen, L., Supramolecular immobilization of fullerenes on gold surfaces: receptors based on calix[n]arenes, cyclotrimeratrylene (CTV) and porphyrins. *C. R. Chimie* **2006**, 9, (7-8), 1031-1037.

44. Zhao, S.; Zhang, K.; Yang, M.; Sun, Y.; Sun, C., Fabrication of photosensitive self-assembled multilayer films based on porphyrin and diazoresin via H-bonding. *Mater. Lett.* **2006**, 60, (19), 2406.
45. Splan, K. E.; Hupp, J. T., Permeable Nonaggregating Porphyrin Thin Films That Display Enhanced Photophysical Properties. *Langmuir* **2004**, 20, 10560-10566.
46. Splan, K. E.; Massari, A. M.; Hupp, J. T., A porous multilayer dye-based photoelectrochemical cell that unexpectedly runs in reverse. *J. Phys. Chem. B* **2004**, 108, 4111-4115.
47. Splan, K. E.; Stern, C. L.; Hupp, J. T., Two coordinately linked supramolecular assemblies constructed from highly electron deficient porphyrins. *Inorg. Chim. Acta* **2004**, 357, (13), 4005-4014.
48. Badjic, J. D.; Nelson, A.; Cantrill, S. J.; Turnbull, W. B.; Stoddart, J. F., Multivalency and cooperativity in supramolecular chemistry. *Acc. Chem. Res.* **2005**, 38, (9), 723-732.
49. Balaban, T. S.; Linke-Schaetzel, M.; Bhise, A. D.; Vanthuyne, N.; Roussel, C.; Anson, C. E.; Buth, G.; Eichhöfer, A.; Foster, K.; Garab, G.; Gliemann, H.; Goddard, R.; Javorfi, T.; Powell, A. K.; Rösner, H.; Schimmel, T., Structural characterization of artificial self-assembling porphyrins that mimic the natural chlorosomal Bacteriochlorophylls c, d, and e. *Chem. Eur. J.* **2005**, 11, 2267-2275.
50. Ahn, S.; Hupp, J. T., Assembles of porphyrin layers on ITO and deposition of polyaniline on porphyrin layered ITO. *Bull. Kor. Chem. Soc.* **2006**, 27, (9).
51. Jiang, L.; Lu, F.; Li, H.; Chang, Q.; Li, Y.; Liu, H.; Wang, S.; Song, Y.; Cui, G.; Wang, N.; He, X.; Zhu, D., Third-Order Nonlinear Optical Properties of an Ultrathin Film Containing a Porphyrin Derivative. *J. Phys. Chem. B* **2005**, 109, 6311-6315.
52. Guldi, D. M., Fullerene-porphyrin architectures; photosynthetic antenna and reaction center models. *Chem. Soc. Rev.* **2002**, 31, 22-36.
53. Hasobe, T.; Fukuzumi, S.; Hattori, S.; Kamat, P. V., Shape- and Functionality-Controlled Organization of TiO₂-Porphyrin-C60 Assemblies for Improved Performance of Photochemical Solar Cells. *Chem. As. J.* **2007**, 2, (2), 265-272.
54. Campbell, W. M.; Burrell, A. K.; Officer, D. L.; Jolley, K. W., Porphyrins as light harvesters in the dye-sensitized TiO₂ solar cell. *Coord. Chem. Rev.* **2004**, 248, 1363-1379.
55. Hasobe, T.; Saito, K.; Kamat, P. V.; Troiani, V.; Qiu, H.; Solladie, N.; Kim, K. S.; Park, J. K.; Kim, D.; D'Souza, F.; Fukuzumi, S., Organic solar cells. Supramolecular composites of porphyrins and fullerenes organized by polypeptide structures as light harvesters. *J. Mater. Chem.* **2007**, 17, 4160-4170.
56. Bonifazi, D.; Kiebele, A.; Stöhr, M.; Cheng, F.; Jung, T.; Diederich, F.; Spillmann, H., Supramolecular Nanostructuring of Silver Surfaces via Self-Assembly of [60]Fullerene and Porphyrin Modules. *Adv. Func. Mater.* **2007**, 17, (7), 1051-1062.

57. Tong, L. H.; Wietor, J.-L.; Clegg, W.; Raithby, P. R.; Pascu, S. I.; Sanders, J. K. M., Supramolecular Assemblies of Tripodal Porphyrin Hosts and C60. *Chem. Eur. J.* **2008**, 14, (10), 3035-3044.
58. Umeyama, T.; Imahori, H., Self-Organization of Porphyrins and Fullerenes for Molecular Photoelectrochemical Devices. *Photosyn. Res.* **2006**, 87, 63-71.
59. Imahori, H.; Yamada, H.; Ozawa, S.; Ushidab, K.; Sakata, Y., Synthesis and photoelectrochemical properties of a self-assembled monolayer of a ferrocene–porphyrin–fullerene triad on a gold electrode. *Chem. Commun.* **1999**, 1165-1166.
60. Yamada, H.; Imahori, H.; Nishimura, Y.; Yamazaki, I.; Ahn, T. K.; Kim, S. K.; Kim, D.; Fukuzumi, S., Photovoltaic Properties of Self-Assembled Monolayers of Porphyrins and Porphyrin-Fullerene Dyads on ITO and Gold Surfaces. *J. Am. Chem. Soc.* **2003**, 125, (30), 9129-9139.
61. Wang, N.; Li, Y.; Lu, F.; Liu, Y.; He, X.; Jiang, L.; Zhuang, J.; Li, X.; Li, Y.; Wang, S.; Liu, H.; Zhu, D., Fabrication of novel conjugated polymer nanostructure: Porphyrins and fullerenes conjugately linked to the polyacetylene backbone as pendant groups. *J. Poly. Sci.* **2005**, 43, (13), 2851-2861.
62. Akiyama, T.; Matsuoka, K.-i.; Arakawa, T.; Kakutani, K.; Miyazaki, A.; Yamada, S., Facile Fabrication and Photoelectrochemical Properties of Porphyrin–Fullerene Assemblies by Self-Assembly and Surface Sol–Gel Processes. *Jap. J. Appl. Phys.* **2006**, 45, (4b), 3758.
63. Nakagawa, H.; Ogawa, K.; Satake, A.; Kobuke, Y., A supramolecular photosynthetic triad of slipped cofacial porphyrin dimer, ferrocene, and fullerene. *Chem. Commun.* **2006**, 14, 1560-1562.
64. Isosomppi, M.; Tkachenko, N. V.; Efimov, A.; Kaunisto, K.; Hosomizu, K.; Imahori, H.; Lemmetyinen, H., Photoinduced electron transfer in multilayer self-assembled structures of porphyrins and porphyrin–fullerene dyads on ITO. *J. Mater. Chem.* **2005**, 15, 4546-4554.
65. Chukharev, V.; Vuorinen, T.; Efimov, A.; Tkachenko, N. V.; Kimura, M.; Fukuzumi, S.; Imahori, H.; Lemmetyinen, H., Photoinduced Electron Transfer in Self-Assembled Monolayers of Porphyrin-Fullerene Dyads on ITO. *Langmuir* **2005**, 21, (14), 6385-6391.
66. Schuster, D. I.; Li, K.; Guldi, D. M.; Palkar, A.; Echegoyen, L.; Stanisky, C.; Cross, R. J.; Niemi, M.; Tkachenko, N. V.; Lemmetyinen, H., Azobenzene-Linked Porphyrin-Fullerene Dyads. *J. Am. Chem. Soc.* **2007**, 129, (51), 15973-15982.
67. Fazio, M. A.; Lee, O. P.; Schuster, D. I., First Triazole-Linked Porphyrin-Fullerene Dyads. *Org. Lett.* **2008**, 10, (21), 4979-4982.
68. Hayes, R. T.; Wasielewski, M. R.; Gosztola, D., Ultrafast Photoswitched Charge Transmission through the Bridge Molecule in a Donor-Bridge-Acceptor System. *J. Am. Chem. Soc.* **2000**, 122, (23), 5563-5567.
69. Kiebele, A.; Bonifazi, D.; Cheng, F.; Stohr, M.; Diederich, F.; Jung, T.; Spillmann, H., Adsorption and Dynamics of Long-Range Interacting Fullerenes in a Flexible, Two-Dimensional, Nanoporous Porphyrin Network. *Chem. Phys. Chem.* **2006**, 7, 1462-1470.

70. Conoci, S.; Guldi, D. M.; Nardis, S.; Paolesse, R.; Kordatos, K.; Prato, M.; Ricciardi, G.; Vicente, M. G. H.; Zilbermann, I.; Valli, L., Langmuir-Shäfer Transfer of Fullerenes and Porphyrins: Formation, Deposition, and Application of Versatile Films. *Chem. Eur. J.* **2004**, 10, (24), 6523-6530.
71. Zilbermann, I., Anderson, G.A., Guldi, D.M., Yamada, H., Imahori, H. and Fukuzumi, S., Layer-by-layer assembly of porphyrin-fullerene dyads. *J. Porph. Phth.* **2003**, 7, 357-364.
72. Kaunisto, K.; Vuorinen, T.; Vahasalo, H.; Chukharev, V.; Tkachenko, N. V.; Efimov, A.; Tolkki, A.; Lehtivuori, H.; Lemmetyinen, H., Photoinduced Electron Transfer and Photocurrent in Multicomponent Organic Molecular Films Containing Oriented Porphyrin-Fullerene Dyad. *J. Phys. Chem. C* **2008**, 112, (27), 10256-10265.
73. Boyd, P. D. W.; Reed, C. A., Fullerene-Porphyrin Constructs. *Acc. Chem. Res.* **2005**, 38, (4), 235-242.
74. Boyd, P. D. W.; Hodgson, M. C.; Rickard, C. E. F.; Oliver, A. G.; Chaker, L.; Brothers, P. J.; Bolskar, R. D.; Tham, F. S.; Reed, C. A., Selective Supramolecular Porphyrin/Fullerene Interactions. *J. Am. Chem. Soc.* **1999**, 121, (45), 10487-10495.
75. Hosseini, A.; Hodgson, M. C.; Tham, F. S.; Reed, C. A.; Boyd, P. D. W., Tapes, Sheets, and Prisms. Identification of the Weak C-F Interactions that Steer Fullerene-Porphyrin Cocrystallization. *Cryst. Growth Des.* **2006**, 6, (2), 397-403.
76. Olmstead, M. M.; Nurco, D. J., Fluorinated Tetraphenylporphyrins as Cocrystallizing Agents for C₆₀ and C₇₀. *Cryst. Growth Des.* **2006**, 6, (1), 109-113.
77. Sun, D.; Tham, F. S.; Reed, C. A.; Chaker, L.; Burgess, M.; Boyd, P. D. W., Porphyrin-Fullerene Host-Guest Chemistry. *J. Am. Chem. Soc.* **2000**, 122, 10704-10705.
78. Bonifazi, D.; Enger, O.; Diederich, a. F., Supramolecular [60]fullerene chemistry on surfaces. *Chem. Soc. Rev.* **2007**, 36, 390-414.
79. Imahori, H.; Fukuzumi, a. S., Porphyrin- and Fullerene-Based Molecular Photovoltaic Devices. *Adv. Funct. Mater.* **2004**, 14, (6), 525-536.
80. Sgobba, V.; Giancane, G.; Conoci, S.; Casilli, S.; Ricciardi, G.; Guldi, D. M.; Prato, M.; Valli, L., Growth and Characterization of Films Containing Fullerenes and Water Soluble Porphyrins for Solar Energy Conversion Applications. *J. Am. Chem. Soc.* **2007**, 129, (11), 3148-3156.
81. Grätzel, M., Dye-sensitized solar cells. *J. Photochem. Photobiol. C: Photochem. Rev.* **2003**, 4, 145-153.
82. Nobukuni, H.; Shimazaki, Y.; Tani, F.; Naruta, Y., A Nanotube of Cyclic Porphyrin Dimers Connected by Nonclassical Hydrogen Bonds and Its Inclusion of C₆₀ in a Linear Arrangement. *Angew. Chem., Int. Ed.* **2007**, 46, (47), 8975-8978.
83. Yamaguchi, T.; Ishii, N.; Tashiro, K.; Aida, T., Supramolecular Peapods Composed of a Metalloporphyrin Nanotube and Fullerenes. *J. Am. Chem. Soc.* **2003**, 125, (46), 13934-13935.

84. Shirakawa, M.; Fujita, N.; Shimakoshi, H.; Hisaeda, Y.; Shinkai, S., Molecular Programming of Organogelators Which Can Accept [60]Fullerene by Encapsulation. *Tetrahedron* **2006**, 62, (9), 2016-2024.
85. Dudi, M.; Lhoták, P.; Stibor, I.; Petíková, H.; Lang, K., (Thia)calix[4]arene-porphyrin conjugates: novel receptors for fullerene complexation with C70 over C60 selectivity. *New J. Chem.* **2004**, 28, 85-90.
86. Tashiro, K.; Aida, T., Metalloporphyrin hosts for supramolecular chemistry of fullerenes. *Chem. Soc. Rev.* **2007**, 36, (2), 189-197.
87. Imahori, H.; Fujimoto, A.; Kang, S.; Hotta, H.; Yoshida, K.; Umeyama, T.; Matano, Y.; Isoda, S.; Isosomppi, M.; Tkachenko, N. V.; Lemmetyinen, H., Host-Guest Interactions in the Supramolecular Incorporation of Fullerenes into Tailored Holes on Porphyrin-Modified Gold Nanoparticles in Molecular Photovoltaics. *Chem. Eur. J.* **2005**, 11, (24), 7265-7275.
88. Marois, J. S.; Cantin, K.; Desmarais, A.; Morin, J. F., [3]Rotaxane-Porphyrin Conjugate as a Novel Supramolecular Host for Fullerenes. *Org. Lett.* **2008**, 10, (1), 33-36.
89. Taylor, S. K.; Jameson, G. B.; Boyd, P. D. W., A New Polymeric Framework Formed by the Self Assembly of 5,10,15,20-tetra(3-pyridyl)porphyrin, Hg₂ And C₆₀. *Supramol. Chem.* **2005**, 17, 543-546.
90. Bonifazi, D.; Spillmann, H.; Kiebele, A.; Wild, M. d.; Seiler, P.; FuyongCheng; Guntherodt, H.-J.; Jung, T.; Diederich, F., Supramolecular Patterned Surfaces Driven by Cooperative Assembly of C[60] and Porphyrins on Metal Substrates. *Angew. Chem., Int. Ed.* **2004**, 43, 4759-4763.
91. Hasobe, T.; Imahori, H.; Kamat, P. V.; Fukuzumi, S., Quaternary self-organization of porphyrin and fullerene units by clusterization with gold nanoparticles on SnO₂ electrodes for organic solar cells. *J. Am. Chem. Soc.* **2003**, 125, 14962-14963.
92. Trabolsi, A.; Elhabiri, M.; Urbani, M.; Delgado de la Cruz, J. L.; Ajamaa, F.; Solladié, N.; Albrecht-Gary, A. M.; Nierengarten, J. F., Supramolecular click chemistry for the self-assembly of a stable Zn(II)-porphyrin-C60 conjugate. *Chem. Commun.* **2005**, 46, 5736-5738.
93. Zhang, S.; Echegoyen, L., Supramolecular Incorporation of Fullerenes on Gold Surfaces: Comparison of C₆₀ Incorporation by Self-Assembled Monolayers of Different Calix[n]arene (n = 4, 6, 8) Derivatives. *J. Org. Chem.* **2005**, 70, (24), 9874-9881.
94. Sánchez, L.; Sierra, M.; Martín, N.; Myles, A. J.; Dale, T. J.; Jr, J. R.; Seitz, W.; Guldi, D. M., Exceptionally Strong Electronic Communication through Hydrogen Bonds in Porphyrin-C₆₀Pairs. *Angew. Chem., Int. Ed.* **2006**, 45, (28), 4637-4641.
95. Schmittel, M.; He, B.; Mal, P., Supramolecular Multicomponent Self-Assembly of Shape-Adaptive Nanoprisms: Wrapping up C60 with Three Porphyrin Units. *Org. Lett.* **2008**, 10, (12), 2513-2516.
96. Hasobe, T.; Sandanayaka, A. S. D.; Wada, T.; Araki, Y., Fullerene-encapsulated porphyrin hexagonal nanorods. An anisotropic donor-acceptor

composite for efficient photoinduced electron transfer and light energy conversion. *Chem. Commun.* **2008**, 3372-3374.

97. Furutsu, D.; Satake, A.; Kobuke, Y., A giant supramolecular light-harvesting antenna-acceptor composite. *Inorg. Chem.* **2005**, 44, (13), 4460-4462.

98. Ohmura, T.; Usuki, A.; Fukumori, K.; Ohta, T.; Ito, M.; Tatsumi, K., New porphyrin-based metal-organic framework with high porosity: 2-D infinite 22.2-A square-grid coordination network. *Inorg. Chem.* **2006**, 45, (20), 7988-7990.

99. Drain, C. M.; Varotto, A.; Radivojevic, I., Self-Organized Porphyrinic Materials. *Chem. Rev.* **2009**, 109, (5), 1630-1658.

100. Marois, J.-S.; Morin, J.-F., Synthesis and Surface Self-Assembly of [3]Rotaxane-Porphyrin Conjugates: Toward the Development of a Supramolecular Surface Tweezer for C60. *Langmuir* **2008**, 24, (19), 10865-10873.

101. Sakakibara, K.; Nakatsubo, F., Effect of Fullerene on Photocurrent Performance of 6-O-Porphyrin-2,3-di-O-stearoylcellulose Langmuir-Blodgett Films. *Macromol. Chem. Phys.* **2008**, 209, (12), 1274-1281.

102. Varotto, A.; Todaro, L.; Vinodu, M.; Koehne, J.; Liu, G.-y.; Drain, C. M., Self-organization of a new fluoros porphyrin and C60 films on indium-tin-oxide electrode. *Chem. Commun.* **2008**, 4921 - 4923.

103. Regev, A.; Galili, T.; Levanon, H.; Schuster, D. I., Triplet Topology of Self-Assembled Zinc Porphyrin-Pyridylfullerene Complex. *J. Phys. Chem. A* **2006**, 110, (27), 8593-8598.

104. Sandanayaka, A. S.; Araki, Y.; Ito, O.; Chitta, R.; Gadde, S.; D'Souza, F., Electron transfer switching in supramolecular porphyrin-fullerene conjugates held by alkylammonium cation-crown ether binding. *Chem. Commun.* **2006**, 4327-4329.

105. D'Souza, F.; Chitta, R.; Gadde, S.; Rogers, Lisa M.; Karr, Paul A.; Zandler, Melvin E.; Sandanayaka, Atula S. D.; Araki, Y.; Ito, O., Photosynthetic Reaction Center Mimicry of a 'Special Pair' Dimer Linked to Electron Acceptors by a Supramolecular Approach: Self-Assembled Cofacial Zinc Porphyrin Dimer Complexed with Fullerene(s). *Chem. Eur. J.* **2007**, 13, (3), 916-922.

106. D'Souza, F.; Chitta, R.; Gadde, S.; Zandler, M. E.; McCarty, A. L.; Sandanayaka, A. S. D.; Araki, Y.; Ito, O., Effect of Axial Ligation or pi-pi-Type Interactions on Photochemical Charge Stabilization in 'Two-Point' Bound Supramolecular Porphyrin-Fullerene Conjugates. *Chem. Eur. J.* **2005**, 11, (15), 4416-4428.

107. D'Souza, F.; E.El-Khouly, M.; Gadde, S.; Zandler, M. E.; McCarty, A. L.; Araki, Y.; Itoh, O., Supramolecular Triads Bearing Porphyrin and Fullerene via 'Two-Point' Binding Involving Coordination and Hydrogen Bonding. *Tetrahedron* **2006**, 62, (9), 1967-1978.

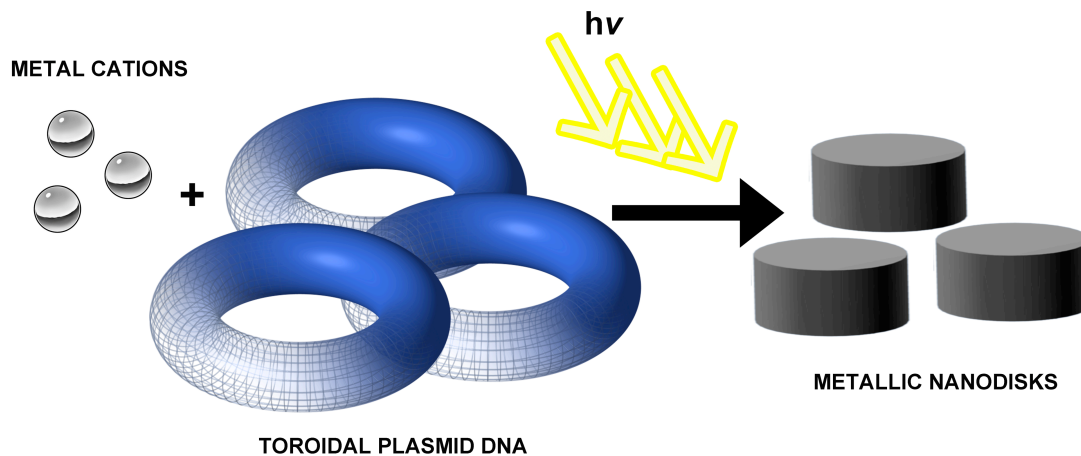
108. D'Souza, F.; Chitta, R.; Gadde, S.; McCarty, A. L.; Karr, P. A.; Zandler, M. E.; Sandanayaka, A. S. D.; Araki, Y.; Ito, O., Design, Syntheses, and Studies of Supramolecular Porphyrin-Fullerene Conjugates, Using Bis-18-crown-6

- Appended Porphyrins and Pyridine or Alkyl Ammonium Functionalized Fullerenes. *J. Phys. Chem. B* **2006**, 110, (12), 5905-5913.
109. D'Souza, F.; El-Khouly, M. E.; McCarty, A. L.; Gadde, S.; Karr, P. A.; Zandler, M. E.; Araki, Y.; Ito, O., Self-Assembled via Axial Coordination Magnesium Porphyrin-Imidazole Appended Fullerene Dyad: Spectroscopic, Electrochemical, Computational, and Photochemical Studies. *J. Phys. Chem. B* **2005**, 109, (20), 10107-10114.
110. D'Souza, F.; Chitta, R.; Gadde, S.; Shafiqullslam, D. M.; Schumacher, A. L.; Zandler, M. E.; Araki, Y.; Ito, O., Design and Studies on Supramolecular Ferrocene-Porphyrin-Fullerene Constructs for Generating Long-Lived Charge Separated States. *J. Phys. Chem. B* **2006**, 110, (50), 25240-25250.
111. Terazono, Y.; Kodis, G.; Liddell, P. A.; Garg, V.; Gervaldo, M.; Moore, T. A.; Moore, A. L.; Gust, D., Photoinduced Electron Transfer in a Hexaphenylbenzene-Based Self-Assembled Porphyrin-Fullerene Triad. *Photochem. Photobiol. Sci.* **2006**, 83, (2), 464-469.
112. Schmittel, M.; Kishore, R. S.; Bats, J. W., Synthesis of supramolecular fullerene-porphyrin-Cu(phen)₂-ferrocene architectures. A heteroleptic approach towards tetrads. *Org. Biomol. Chem.* **2007**, 5, (1), 78-86.
113. Mateo-Alonso, A.; Sooambar, C.; Prato, M., Fullerene photoactive dyads assembled by axial coordination with metals. *Comptes Rendus Chimie* **2006**, 9, (7-8), 944-951.
114. Schumacher, Amy L.; Sandanayaka, A. S. D.; Hill, Jonathan P.; Ariga, K.; Karr, Paul A.; Araki, Y.; Ito, O.; D'Souza, F., Supramolecular Triad and Pentad Composed of Zinc-Porphyrin(s), Oxoporphyrinogen, and Fullerene(s): Design and Electron-Transfer Studies. *Chem. Eur. J.* **2007**, 13, (16), 4628-4635.
115. Gadde, S.; Islam, D. M. S.; Wijesinghe, C. A.; Subbaiyan, N. K.; Zandler, M. E.; Araki, Y.; Ito, O.; D'Souza, F., Light-Induced Electron Transfer of a Supramolecular Bis(Zinc Porphyrin)-Fullerene Triad Constructed via a Diacetylamidopyridine/Uracil Hydrogen-Bonding Motif. **2007**, 111, (34), 12500-12503.
116. Imahori, H.; Tamaki, K.; Guldi, D. M.; Luo, C.; Fujitsuka, M.; Ito, O.; Sakata, Y.; Fukuzumi, S., Modulating Charge Separation and Charge Recombination Dynamics in Porphyrin-Fullerene Linked Dyads and Triads: Marcus-Normal versus Inverted Region. *J. Am. Chem. Soc* **2001**, 123, (11), 2607-2617.

CHAPTER 2

FABRICATION OF METAL NANOPARTICLES USING TOROIDAL PLASMID

DNA AS A SACRIFICIAL MOLD



This work was carried out in collaboration with another graduate student, Jacopo Samson, who contributed to the synthesis of the gold nanoparticles and the electron diffraction (ED) characterization of the particles.

This chapter was adapted from Jacopo Samson, Alessandro Varotto, Patrick C. Nahirney, Alfredo Toschi, Irene Piscopo and Charles Michael Drain. *ACS Nano*, **2009**, 3 (2), pp 339–344.

2.1. INTRODUCTION

The fabrication of nanomaterials of metals, ceramics, inorganics, and organic dyes is widely investigated because these materials possess unusual or unexpected properties that can be exploited for a wide range of applications.¹⁻⁴ There are diverse methods of fabricating metal nanoparticles including reduction of the metal salts with reducing agents,⁵ pyrolysis,⁶⁻⁸ laser ablation,^{9, 10} and photoreduction.^{11, 12} The average nanoparticle size ranges from few nanometers to over 100 nm. The size, shape and dispersity depend on the synthetic methods, and can be controlled by adjusting thermodynamic as well as kinetic parameters.⁶

A variety of templates can be employed in the preparation of nanoparticles to control the size, and special distribution. Nanostructured materials such as carbon nanotubes,¹³ aggregates,¹⁴ organic polymers, biopolymers¹⁵⁻¹⁷ and biological systems such as viruses¹⁸ can be used as a platform on which nanoparticles can be adsorbed or synthesized as a means to order the nanoparticles in two or three dimensions. Nanoparticles can be formed and stabilized in a variety of matrixes such as gels,^{19,20} polymers,²¹ and biopolymers,²² which can also induce specific shapes. Nanoparticles can be formed inside self-organized biomimetic rings that control the growth of the nanoparticle, but these rings are formed in low yields.²³ For molding nanomaterials in nanocavities or templates, the ideal mold can be made in high yields, are monodispersed, and topologically well defined.

A plasmid is a circular extra-chromosomal DNA molecule capable of replicating autonomously in bacterial hosts,²⁴ and can be made in large quantities using standard molecular biology procedures.²⁵ Besides being monodispersed biopolymers, plasmid DNA adopts a variety of topologies such as relaxed, linear supercoiled, and toroidal depending on environmental conditions such as temperature, pH, and ionic strength. A recent report demonstrated that ionic strength can maximize the toroidal topology of plasmid DNA.²⁶ Also, the toroid thickness is a salt-dependent phenomenon that can be controlled with the ionic strength and a given plasmid will always form the same size toroids under the same conditions.²⁶ In general, the size of the toroid depends on the number of base pairs, the sequence of the plasmid, and environmental factors. As a proof-of-principle, we present herein the use of the toroidal form of pcDNA 3.1(+) plasmid DNA (Figure 2.1) as a monodispersed biopolymer nanocavity mold for the formation of disc-shaped nanoparticles of several types of metals.

In addition to being monodispersed and easy to synthesize in high yields, this approach exploits several properties of plasmid DNA: (1) DNA is well known to bind cations at the negatively charged phosphate backbone with various affinities,²⁷ (2) metal ion binding favors formation of toroidal plasmid DNA structures,²⁶ (3) the size of plasmid, therefore the size of the toroid, is easy to vary,^{18,19} (4) DNA has a well established UV light initiated oxidation chemistry.²⁸⁻

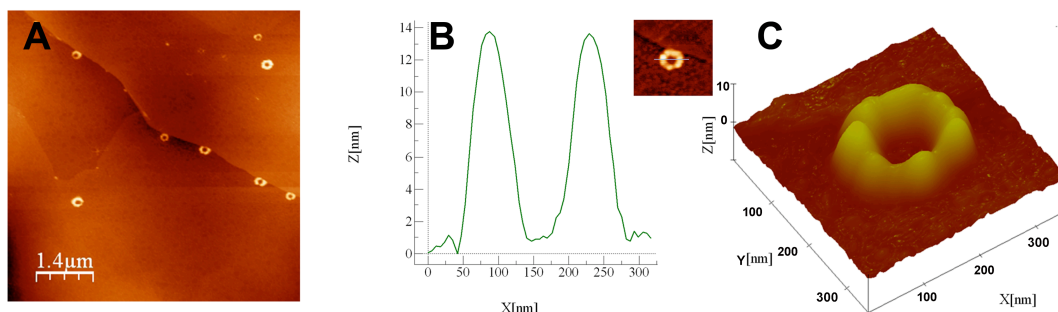


Figure 2.1. (A) AFM height image of the toroidal topology of plasmid pcDNA 3.1 on a HOPG substrate. (B) Height analysis of inset (top right corner). (C) 3-D AFM image of the plasmid shown in B.

Incubation of low concentrations of Me_3PAuCl , $\text{NiCl}_2 \cdot (\text{H}_2\text{O})_6$, or $\text{CoCl}_2 \cdot (\text{H}_2\text{O})_6$ with pcDNA 3.1(+) plasmid DNA, which has 5,428 base pairs, does not affect the distribution of the three main topologies significantly. 254 nm UV irradiation of the plasmid shows a redistribution of the conformations and degradation in the presence of the three metal ions. Photo-oxidation and degradation of the DNA mold upon exposure of the sample to 254 nm UV light results in reduction of the metal ions such that the plasmid DNA acts as a sacrificial mold, and drives the formation of the nanoparticles.

After incubation of the plasmid DNA suspension (10 μL of a 1 $\mu\text{g}/\text{mL}$ original solution) with the gold, nickel, or cobalt salts (12 mM) overnight in the dark at 4° C, the nanoparticles were prepared by irradiating the solution for one hour with UV light ($\lambda=254$, 10 $\mu\text{W}/\text{cm}^2$ using a UVGL-25 compact UV lamp by UVP). The solutions were then cast onto AFM or TEM substrates through a 0.2 μm syringe filter. (See Figure 2.10 for controls without the plasmid.)

2.2. CHARACTERIZATION OF THE NANOPARTICLES

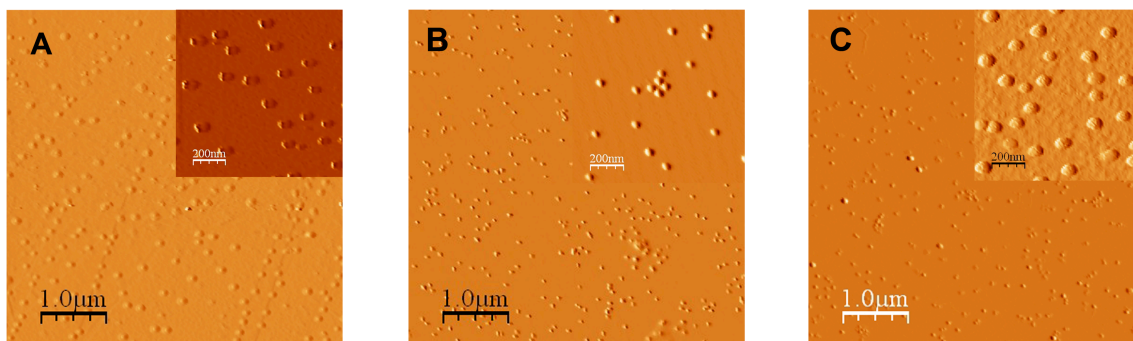


Figure 2.2. AFM amplitude images of metal nanoparticles obtained from photo-initiated reduction of metal ions bound to plasmid pcDNA 3.1 sacrificial mold: (A) gold; (B) nickel; (C) cobalt particles.

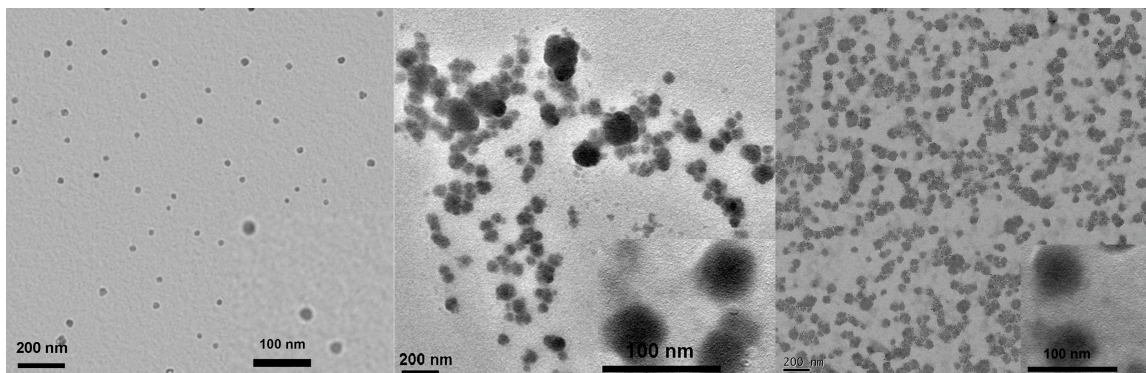


Figure 2.3. TEM images were used to assay the diameters of metal nanodiscs obtained from photo-initiated reduction of metal ions bound to plasmid pcDNA 3.1 sacrificial mold: (A) gold nanoparticles, (B) nickel nanoparticles, and (C) cobalt nanoparticles.

The sizes of the nanoparticles were characterized with both AFM (Figure 2.2) and TEM (Figure 2.3) to get accurate measurements of the heights and widths of the metal nanoparticles, respectively. The histograms of the AFM-measured heights and the TEM-measured horizontal dimensions are presented

in Chart 2.1. The vertical and horizontal dimensions of the metal nanoparticles reveal that these nanoparticles are disc-shaped. The average height of the nickel and cobalt nanodiscs obtained from pcDNA 3.1(+) templates is 13 ± 2 nm, while for gold the average height is 8 ± 2 nm. These nanoparticle heights correspond with the 12-14 nm vertical dimension of the plasmid. The 40-60 diameters of the metallic nanodiscs correspond to the inner diameter of the toroidal plasmid (Figure 2.1), and the differences are discussed below.

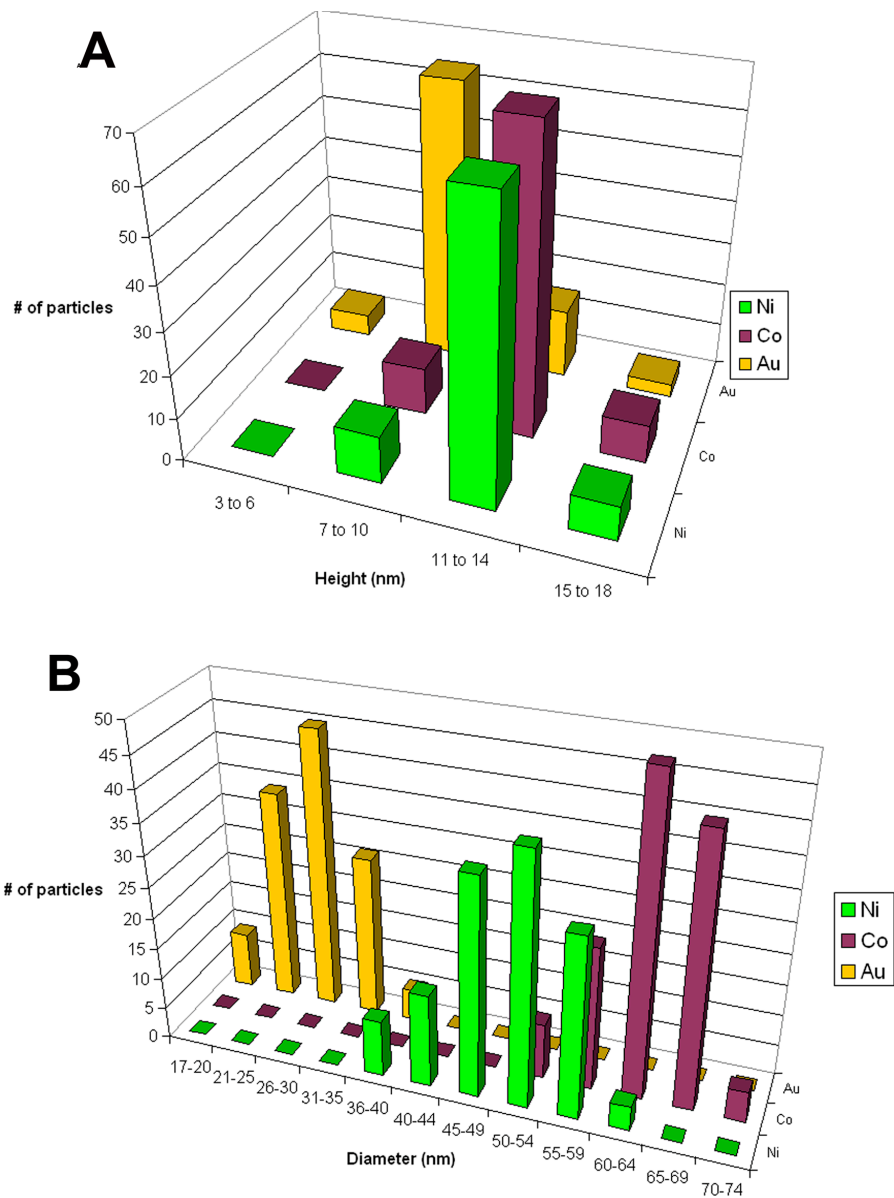


Chart 2.1. (A) Histograms of the height distribution determined by AFM and (B) histograms of the diameter distribution determined by TEM: nickel (green), cobalt (purple), and gold (yellow) nanoparticles obtained using a pcDNA 3.1 template.

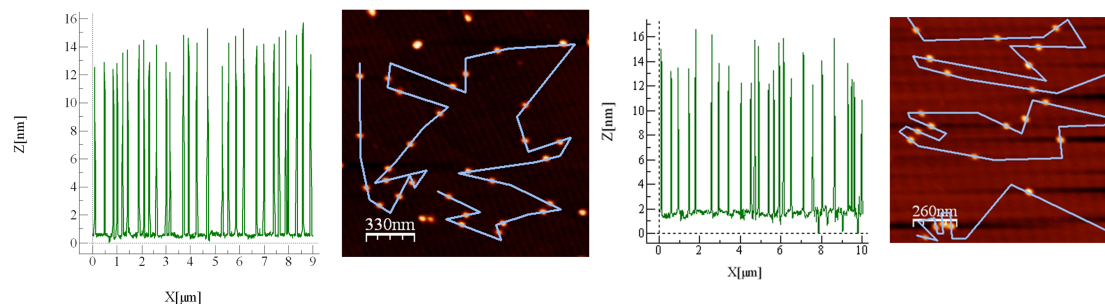


Figure 2.4. The left panel shows the average heights of nickel nanoparticles synthesized using pcDNA 3.1(+) with corresponding AFM image. The size ranges between 13 ± 1 . On the right, height analysis of cobalt nanoparticles synthesized using pcDNA 3.1(+) with corresponding AFM image. The size ranges between 12 ± 2 .

The small differences in the nanoparticle heights and widths for the three metals can be attributed to several factors. As mentioned before, the relative distribution of the toroidal/supercoiled condensation state versus the linear and relaxed forms does not significantly change upon binding of low concentrations of these metals, and in agreement with a previous study.²⁶ However the dimensions of the toroidal condensation state of the plasmid is sensitive to the binding of the different metal ions,³¹⁻³³ and the morphology of the plasmid changes during the formation of the nanoparticles as it is degraded under UV irradiation. Photoinduced metal coating of linear DNA with concomitant photo-oxidation of DNA to yield nanowires has been reported.^{34,35} In our study, even though the mechanism of photoreduction of the metal may occur in a similar fashion, the circular morphology of the toroidal DNA clearly drives the formation of nanodisc topologies. The size of the nanodisc is correlated to the inner diameter of the plasmid and circular DNA, but is not exactly the same. When the plasmid is

incubated with the nickel salt and irradiated for 5-20 minutes with the UV light there is a significant contraction in the plasmid height. After UV irradiating for 20 minutes, the forming particle is still surrounded by filaments of DNA. In order to probe the possible mechanism(s) for the formation of nanoparticles, we used AFM scans of a drop of solution containing pcDNA and NiCl₂ on HOPG after UV irradiation for 20, 40 and 60 minutes. The images suggest that there is a contraction of the plasmid soon after irradiation. After 20 and 40 minutes filaments of DNA are still visible, whereas after 60 minutes the photodegradation process is complete and only nanoparticles are visible (Figure 2.5).

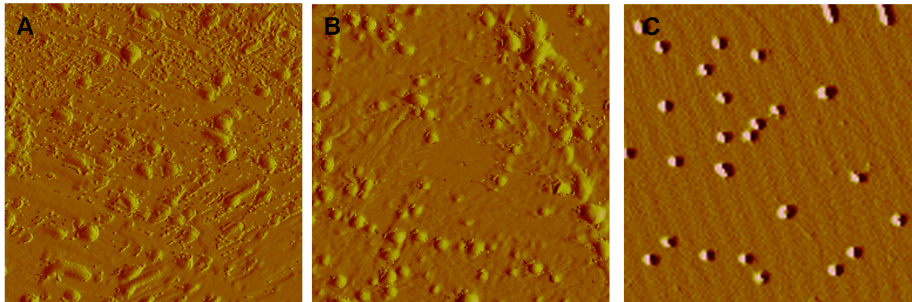


Figure 2.5. AFM images (1.5X1.5 μm) of plasmid DNA/NiCl₂ on HOPG after different time of exposure to UV light: A. 20 minutes, B. 40 minutes, C. 60 minutes. Figure A and B suggest that after UV irradiation the plasmids undergo a contraction with concomitant formation of the nanoparticles of nickel. Only after some time (60 minutes, figure C) the process is complete and the plasmids have been degraded whereas the particles are formed.

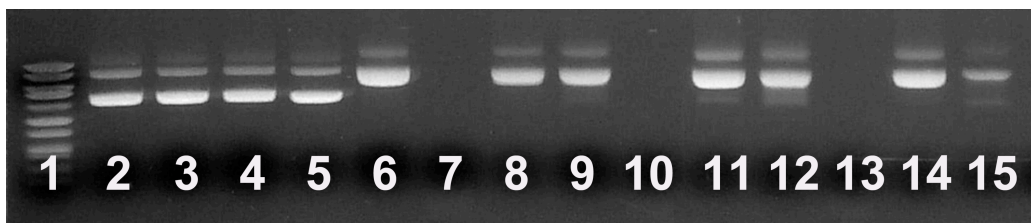


Figure 2.6. Gel electrophoresis (GE, 0.8% agarose) of pcDNA 3.1(+). Lanes: [1] 1kb ladder; [2] naked pcDNA 3.1(+); [3] naked pcDNA 3.1(+) + UV (5 min); [4] pcDNA + Me₃PAuCl + UV (5min); [5] pcDNA + NiCl₂ +UV (5 min); [6] pcDNA + CoCl₂ +UV (5 min); [7] naked pcDNA 3.1(+) + UV (20 min); [8] pcDNA(+) + Me₃PAuCl + UV (20 min); [9] pcDNA(+) + NiCl₂ +UV (20 min); [10] pcDNA(+) + CoCl₂ + UV (20 min); [11] naked pcDNA 3.1(+) + UV (40 min); [12] pcDNA(+) + Me₃PAuCl + UV (40 min); [13] pcDNA(+) + NiCl₂ +UV(40 min); [14] pcDNA(+) + CoCl₂ +UV (40 min); [15] naked pcDNA(+) 3.1(+) + UV (60 min).

Electron diffraction analysis (Figure 2.7) suggests that most of the nanodiscs are composed only of the metal atoms. Some DNA fragments adsorbed to the outside of the nanoparticle are occasionally observed in both AFM and TEM images. As noted above, incomplete degradation of the plasmid DNA, and DNA decorated with small metal nanoparticles is observed in experiments with shorter UV irradiation times. Only amorphous clusters of various sizes are observed in control experiments with no plasmid DNA. Chemical reduction of these metal ions with hydrazine anhydrous results in similar nanodiscs with similar shapes, but the plasmid DNA surrounds the nanoparticles or is entrained in the nanoparticles depending on growth conditions (Figure 2.5). Taken together, this data suggests that small changes in the toroid dimensions of the plasmid DNA can be induced by the binding of different metal ions,¹⁹⁻²² and that the detailed mechanism and kinetics of nanodisc formation may be somewhat metal ion dependent. As with other template methods,²³ it is

likely that the increased concentration of metal ion inside the toroid relative to the outside drives the formation of the nanodiscs. In the case of a sacrificial mold, the competing rates of nanoparticle formation versus mold degradation, which also may be metal ion dependent, will also influence the size and morphology of the products.

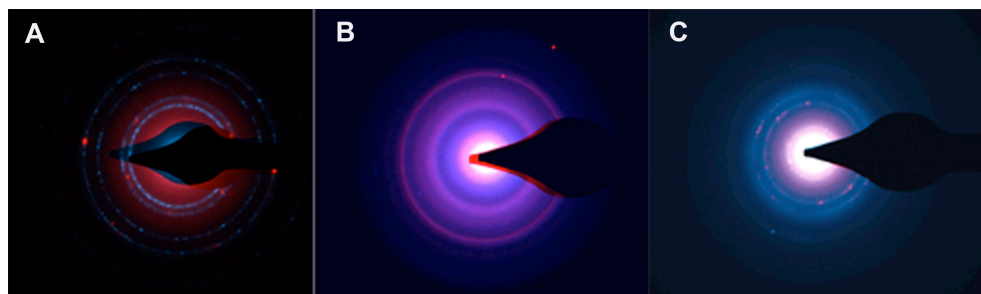


Figure 2.7. ED patterns in red of the prepared nanodiscs of (A) gold, (B) nickel, and (C) cobalt. The corresponding standards are superimposed and are in blue.

2.3. USE OF DIFFERENT PLASMIDS

Other plasmids with different numbers of base pairs and sequences can adopt similar structures but with different sizes, though the size of the toroidal condensation state does not linearly scale with the number of base pairs. The plasmid pRc/CMV-(HA)-pVHL,¹ abbreviated as pVHL, has ca. 8,000 base pairs and also adopts toroidal conformations. The same procedures as above using the larger pVHL plasmid results in larger gold, nickel and cobalt nanodiscs with different heights (Figure 2.8). A much smaller circular DNA containing 70 base

¹ pRc/CMV-(HA)-pVHL was a generous gift of Dr. Michael Ohh (University of Toronto, Toronto, ON, Canada), and the 70bp circular DNA was a generous gift of Dr. Smita Patel (University of Medicine and Dentistry of New Jersey, Piscataway, New Jersey).

pairs,^a is able to mold the formation of 3 ± 0.5 nm high by 13 ± 5 nm wide nanoparticles of nickel (Figure 2.9). Note that the AFM error for these smallest nanoparticles is greater due to convolution with the 10 nm tip curvature so that the actual diameter is less than observed. Chart 2.2 shows the histogram of the height as well as the diameter distribution of nanoparticles using the three different plasmids.

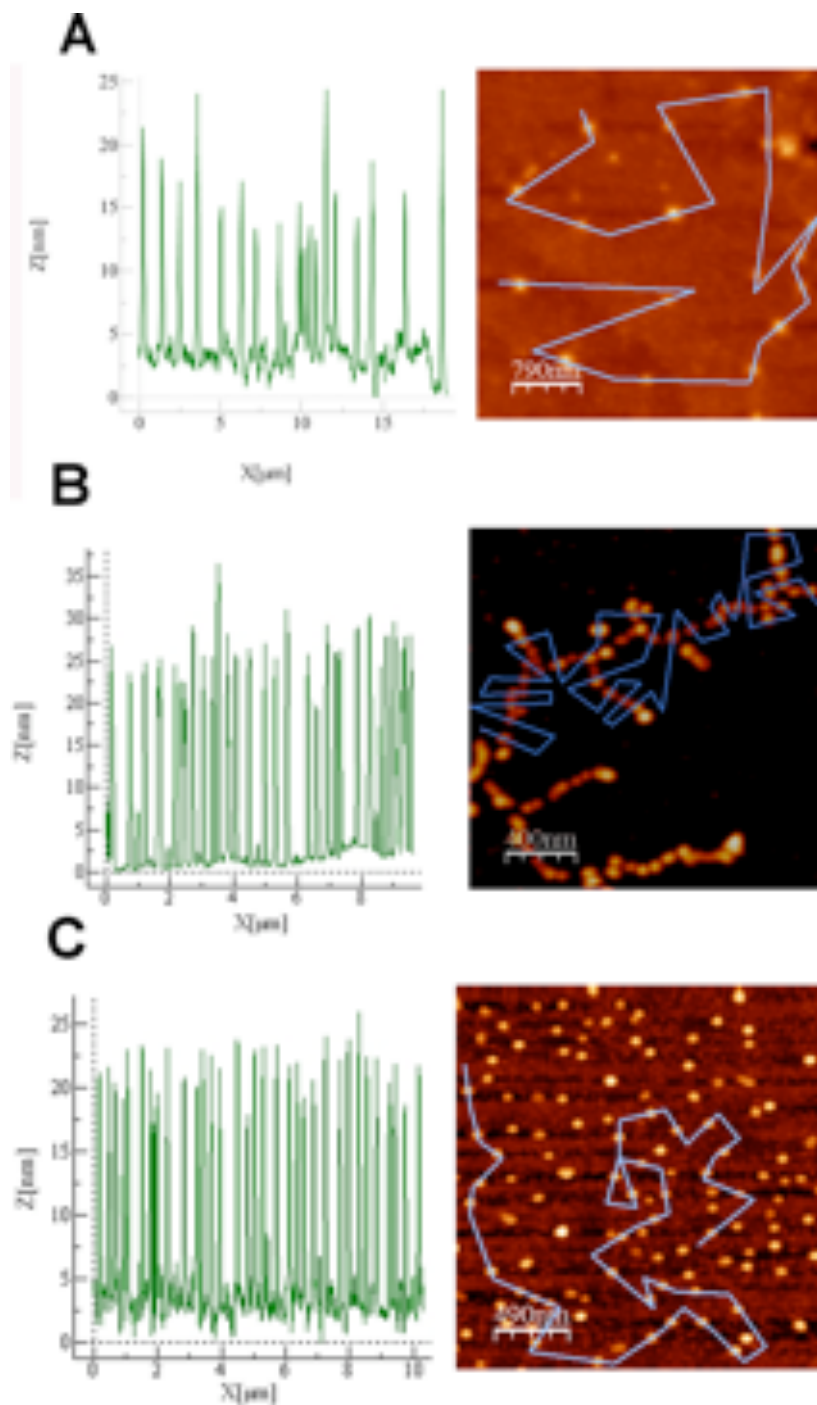


Figure 2.8. The three panels show the average heights of gold (A), nickel (B) and cobalt (C) nanoparticles synthesized using plasmid pVHL with corresponding AFM image. The average height of the gold nanoparticles is 18 ± 3 nm, of the nickel nanoparticles is 25 ± 2 and of the cobalt nanoparticles is 20 ± 3 .

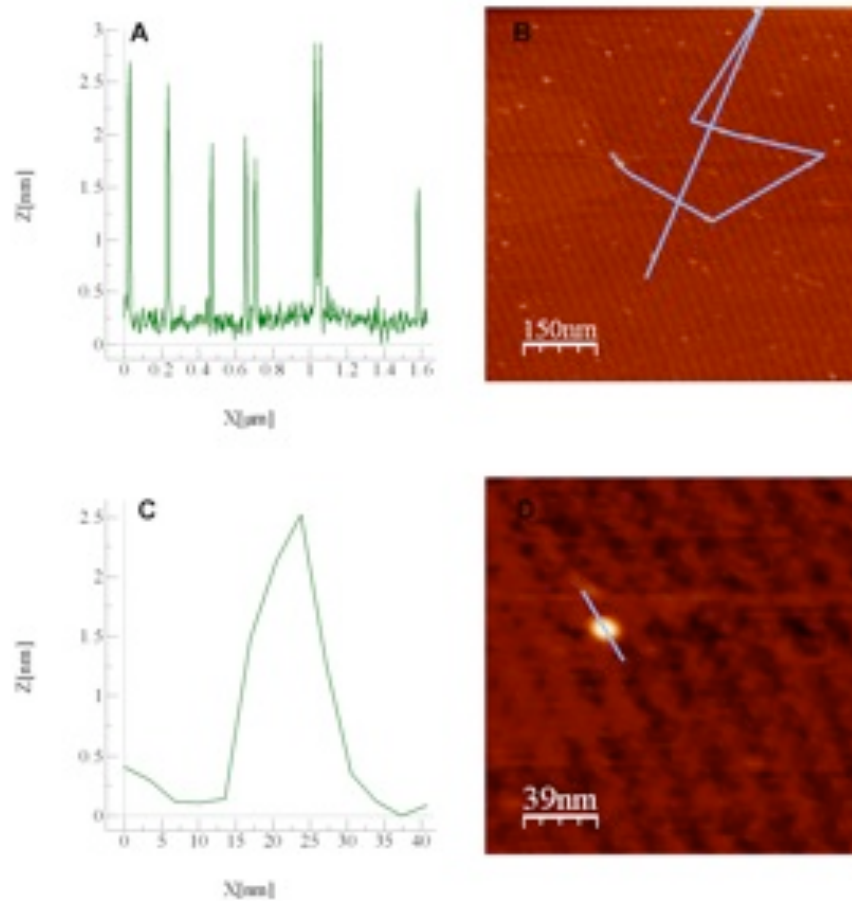


Figure 2.9. (A) Height analysis of (B) AFM image of nickel nanoparticles fabricated using a 70bp circular DNA as a template. (C) Height analysis of (D) AFM height image single nickel nanoparticle.

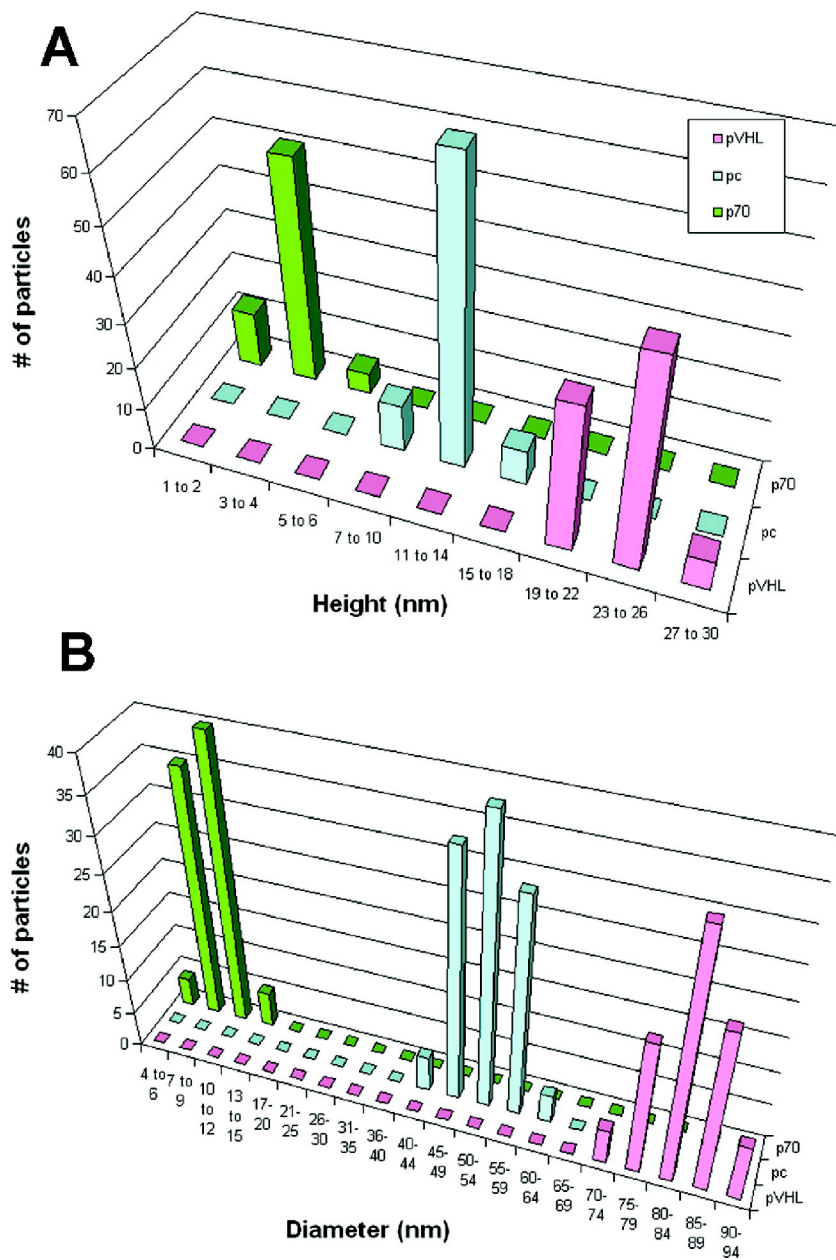


Chart 2.2. (A) Histograms of the height and (B) histogram of the diameter distribution determined by AFM of nickel nanoparticles using p70 (olive green), pcDNA (light blue), and pVHL (pink) as molds. The diameter measurements were estimated from the AFM height images; a 10 nm ultra-sharp tip was utilized to minimize the error due to the tip convolution effect.

2.4. CONCLUSIONS

In conclusion we have synthesized narrowly dispersed nanodiscs at room temperature using UV light and a biological sacrificial toroidal plasmid DNA mold. Toroidal plasmids are readily available in large quantities, easy to purify, rigid, and monodispersed. The size of the particles is dictated by the topology of the template, metal ion binding, and the mechanism of formation. The method is quite general and may be applicable to DNA/RNA structures with more complex topologies. Future studies will investigate the formation of other types of nanoparticles, e.g. this work suggests that it may be possible to form nanorings by controlling the synthetic conditions. The method uses materials and equipment found in most undergraduate teaching laboratories.

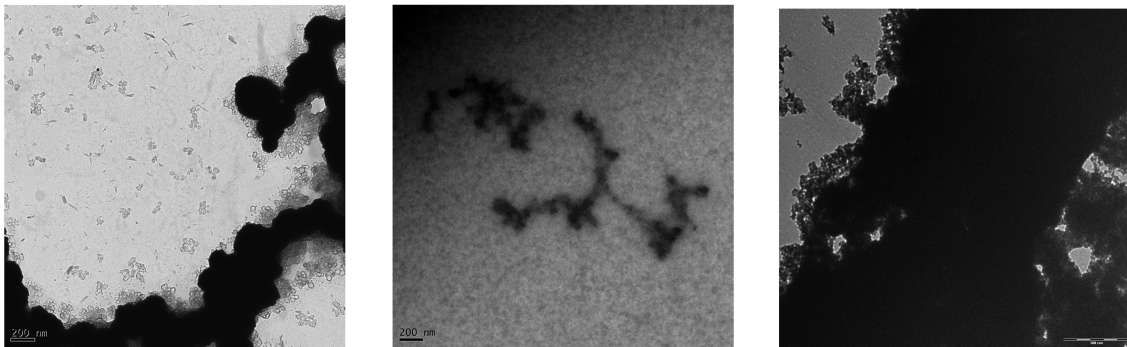


Figure 2.10. TEM images of the control experiments without the employment of plasmid DNA as a template. Aqueous solutions of (A) Me_3PAuCl , (B) NiCl_2 , and (C) CoCl_2 were irradiated with UV light. Neither narrowly dispersed sizes nor disc-like shapes are observed.

2.5. TWO-PARTICLE LITHOGRAPHY

We established a collaboration with Professor J. Garno from Louisiana State University to use the cobalt and nickel nanoparticles produced with the plasmid method to pattern a surface with magnetic rings. This technique employed the use of macroscopic silica or latex particles and therefore has been baptized 'two-particle lithography'.

The silica or latex nanoparticles are premixed in water with metallic nanoparticles (either cobalt or nickel). A drop of this dispersion is placed on MICA and the sample is dried in air. During the drying process, the metallic nanoparticles tend to ordinate around the bigger silica (or latex) particles creating rings. Once the samples are dried, the large templating particles are removed by rinsing with water, while the rings of the small NPs persist on the surface. Published in NOBCChE proceedings 2008.

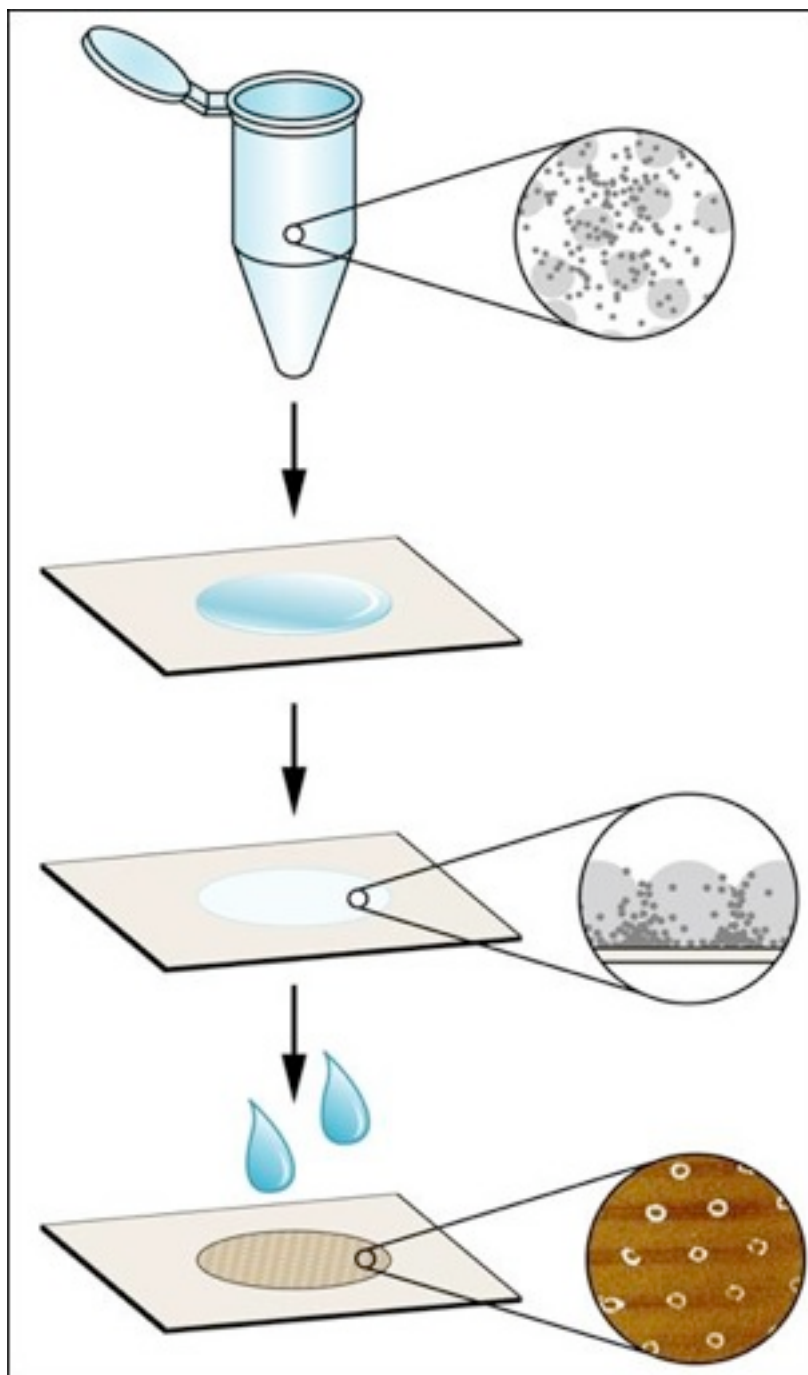


Figure 2.11. Schematic steps of the ring nanopatterning. The 2-size particles - silica (bigger) and cobalt or nickel (smaller)- are premixed in water. A drop of the dispersion is placed on MICA and let dry. While the water evaporates, the smaller particles decorate the perimeter of the bigger silica particles forming rings. The silica particles are washed off the surface leaving magnetic rings on MICA.

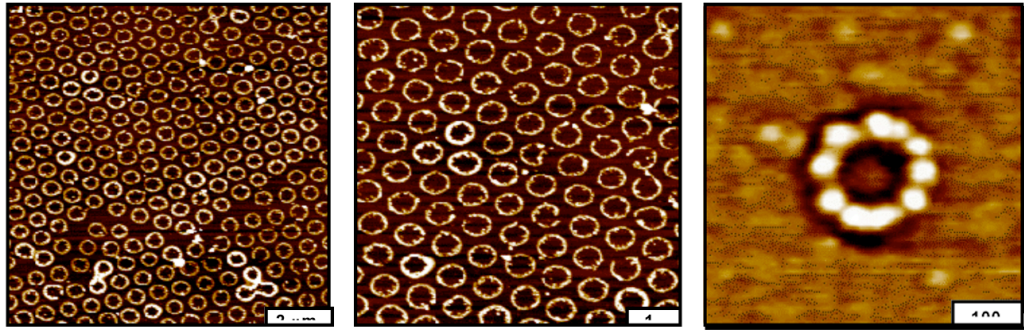


Figure 2.12. AFM images of the nanorings of MICA – successive zooms. From left to right the scale bar is 2 μm , 1 μm , 100 nm.

Patterns of nickel nanoparticles produced with two-particle lithography are displayed in Figure 12. There are about 11 rings within a $2 \times 2 \mu\text{m}^2$ frame AFM image, which would scale up to approximately 280 million rings produced within a square centimeter of sample area. The arrays of nickel nanoparticles cover approximately 24% of the mica surface in this example.

2.6. CONCLUSIONS

Two-particle lithography provides a high-throughput approach to manufacture arrays of nanopatterns of magnetic nanoparticles as test platforms for AFM measurements. Conventional bench chemistry steps, such as mixing, centrifuging, drying and rinsing are sufficient to accomplish nanofabrication. Both amplitude and phase signals acquired when using contact-mode AFM can be used to selectively and precisely map the location of magnetic nanoparticles when an AC electromagnetic field is applied to the sample surface.

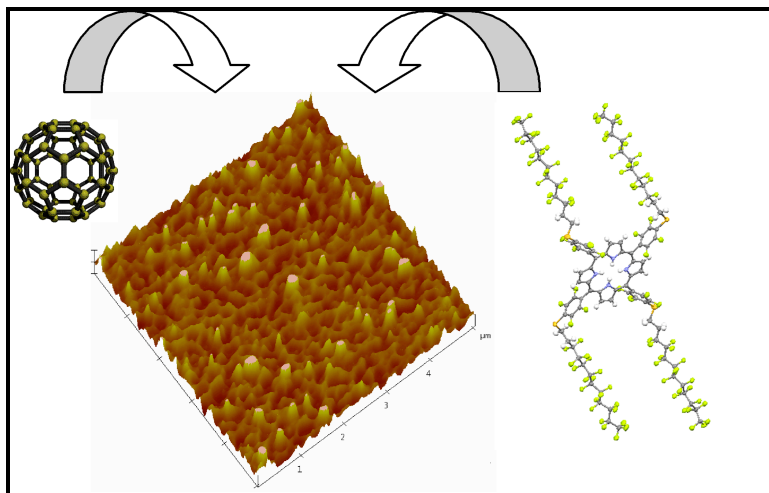
References.

1. Lu, A.-H.; Salabas, E. L.; Schuth, F., *Angew. Chem. Int. Ed.* **2007**, *46*, 1222-1244.
2. Vanden Bout, D. A., *Metal Nanoparticles: Synthesis, Characterization, and Applications*. Marcel Dekker, Inc.: New York and Basel, 2002.
3. Drain, C. M.; Smeureanu, G.; Patel, S.; Gong, X.; Garno, J.; Arijeloye, J., *New J. Chem.* **2006**, *30*, 1834-1843.
4. Frenkel, J.; Doefman, J., *Nature* **2003**, *426*, 274-275.
5. Guo, F.; Zheng, H.; Yang, Z.; Qian, Y., *Mater. Lett.* **2002**, *56*, 906-909.
6. Puentes, V. F.; Krishnan, K.; Alivisatos, A. P., *Topics in Catalysis* **2002**, *19* (2), 145-148.
7. Puentes, V. F.; Krishnan, K. M., *Appl. Phys. Lett.* **2001**, *78*, 2187-2189.
8. Kim, S. W.; Park, J.; Jang, Y.; Chung, Y.; Hwang, S.; Hyeon, T.; Kim, Y. W., *Nano Lett.* **2003**, *3*, 1289-1291.
9. Takami, A.; Kurita, H.; Koda, S., *J. Phys. Chem. B* **1999**, *103*, 1226-1232.
10. Kazakevich, P. V.; Simakin, A. V.; Voronov, V. V.; Shafeev, G. A., *Appl. Surf. Sci.* **2006**, *252*, 4373-4380.
11. Vesperinas, A.; Eastoe, J.; Jackson, S.; Wyatt, P., *Chem. Commun.* **2007**, 3912-3914.
12. Fang, Q.; He, G.; Cai, W. P.; Zhang, J.-Y.; Boyd, I. W., *Appl. Surf. Sci.* **2004**, *226*, 7-11.
13. Chen, P.; Wu, X.; Lin, J.; Tan, K. L., *J. Phys. Chem. B* **1999**, *103*, 4559-4561.
14. Ipsita A. Banerjee; Yu, L.; Matsui, H., *Proc. Natl. Acad. Sci.* **2003**, *100*, 14678-14682.
15. Sun, L.; Wei, G.; Song, Y.; Liu, Z.; Wang, L.; Li, Z., *Appl. Surf. Sci.* **2006**, *252*, 4969-4974.
16. Aldaye, F. A.; Palmer, A. L.; Sleiman, H. F., *Science* **2008**, *321*, 1795-1799.
17. Coffey, J. L.; Bigham, S. R.; Li, X.; Pinizzotto, R. F.; Rho, Y. G.; Pirtle, R. M.; Pirtle, I. L., *Appl. Phys. Lett.* **1996**, *69*, 3851-3853.
18. Flynn, C. E.; Lee, S.-W.; Peelle, B. R.; Belcher, A. N., *Acta Materialia* **2003**, *51*, 5867-5880.
19. Maruszewski, K.; Jasiorski, M.; Hreniak, D.; Strk, W.; Hermanowicz, K.; Heiman, K., *J. Sol-Gel Science and Technology* **2003**, *26*, 83-88.
20. Antonietti, M.; Ozin, G. A., *Chem. Eur. J.* **2004**, *10*, 28-41.
21. Zhong, Z.; Sim, D.; Teo, J.; Luo, J.; Zhang, H.; Gedanken, A., *Langmuir* **2008**, *24*, 4655-4660.
22. Ganesan, R.; Gedanken, A., *Nanotechnology* **2008**, *19*, 025702.
23. Djalali, R.; Samson, J.; Matsui, H., *J. Am. Chem. Soc.* **2004**, *126*, 7935-7939.
24. Lipps, G., *Plasmids: Current Research and Future Trends*. Caister Academic Press: Norfolk UK, 2008.
25. QIAGEN. QIAGEN PlasmidAmp Kit-For direct amplification of plasmid DNA from bacterial colonies, www1.qiagen.com.

26. Conwell, C. C.; Vilfan, I. D.; Hud, N. V., *Proc. Nat. Ac. Sci.* **2003**, *100*, 9296-9301.
27. He, S.; Arscott, P. G.; Bloomfield, V. A., *Biopolymers* **1999**, *53*, 329-241.
28. Bartolini, W. P.; Johnston, M. V., *J. Mass Spectrom.* **2000**, *35*, 408-416.
29. Boerner, L. J.; Zaleski, J. M., *Current Opinion in Chemical Biology* **2005**, 135-144.
30. Sinha, R. P.; Hader, D.-P., *Photochem. Photobiol. Sci.* **2002**, *1*, 225-236.
31. Schnell, J. R.; Berman, J.; Bloomfield, V. A., *Biophys. J.* **1998** *74* 1484-1491.
32. Davey, C. A.; Richmond, T. J., *Proc. Nat. Ac. Sci. USA* **2002**, *99* 11169-11174.
33. Liu, C.; Wang, M.; Zhang, T.; Sun, H., *Coord. Chem. Rev.* **2004**, *248*, 147-168.
34. Berti, L.; Alessandrini, A.; Facci, P., *J. Am. Chem. Soc.* **2005**, *127*, 11216-11217.
35. Burley, G. A.; Gierlich, J.; Mofid, M. R.; Nir, H.; Tal, S.; Eichen, Y.; Carell, T., *J. Am. Chem. Soc.* **2006**, *128*, 1398-1399.
36. Horcas, I.; Fernandez, R.; Gomez-Rodriguez, J. M.; Colchero, J.; Gomez-Herrero, J.; Baro, A. M., *Rev. Sci. Instruments* **2007**, *78*, 013705.
37. Wong, C.; West, P. E.; Olson, K. S.; Mecartney, M. L.; Starostina, N., *JOM* **2007**, *59*, 12-16.
38. web.archive.org/web/20070518092613/http://www.northland.cc.mn.us/Chemistry/standard_reduction_potentials.htm Standard reduction potentials.

CHAPTER 3

SELF-ORGANIZATION OF A NEW FLUOROUS PORPHYRIN AND C₆₀ FILMS ON INDIUM-TIN-OXIDE ELECTRODE

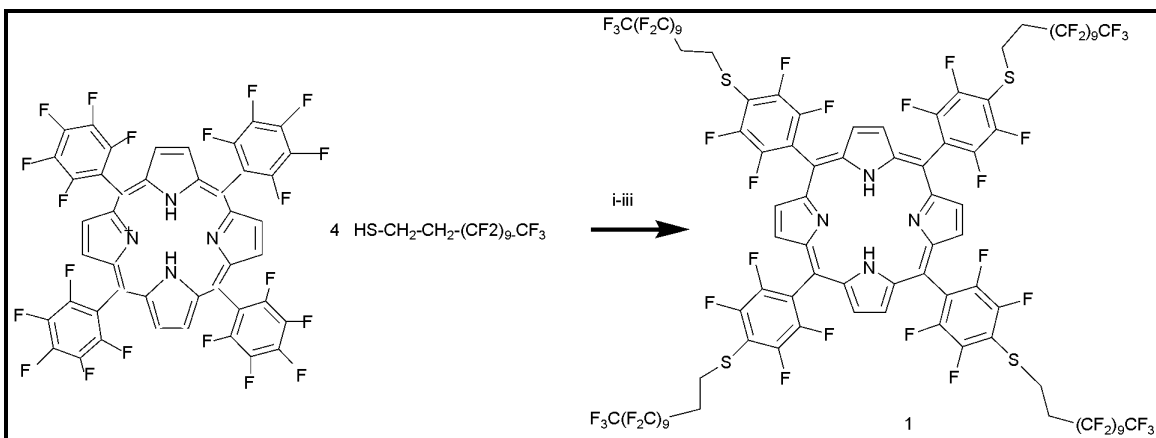


3.1. INTRODUCTION

The supramolecular self-organization of porphyrin derivatives on conductive surfaces has been widely investigated¹⁻⁷ because they are promising building blocks for the fabrication of photoactive materials. There are numerous studies on the spontaneous interactions between the π system of the porphyrin macrocycle and the curved surface of a fullerene.⁸⁻¹⁰ The porphyrin–fullerene complexes are appealing as materials for solar-energy conversion and energy storage because they can form long-lived charge separated states. The large spherical shape and polarizability of C₆₀ make it an excellent π -acceptor molecule.¹¹ Moreover, because of the small reorganization energy involved in

electron transfer reactions (ET), the charge transfer complex formed between C₆₀ and a porphyrin can be remarkably stable.¹² The oxidation and reduction potentials as well as the photophysical properties of porphyrins can be dictated by a variety of means such as metal coordination and exocyclic groups. While the porphyrin macrocycle is a good electron donor/acceptor, it is remarkably robust to oxidative damage, e.g. as films on surfaces.¹³ However, most of the exocyclic groups used to self-assemble and/or self-organize porphyrins can be oxidized, thus causing disassembly or reorganization of porphyrinic materials. Thus in applications wherein the nanoarchitecture of the chromophores is essential for the function of the materials, oxidation of the peripheral functional groups poses a limitation to their usefulness as a photoactive material. This latter consideration then limits the use of many porphyrinoid systems in photonic materials under ambient conditions. Herein the facile synthesis of a new highly fluorinated porphyrin that forms robust self-organized thin films with fullerene C₆₀ on indium-tin-oxide coated glass is presented. The C–F bond imparts stability to the exocyclic groups, and the small polarizability of fluorine atoms confers a low surface energy to materials¹⁴ composed of this porphyrin. This chapter was adapted from Alessandro Varotto, Louis Todaro, Mikki Vinodu, Jessica Koehne, Gang-yu Liu and Charles M. Drain ‘Self-organization of a new fluorinated porphyrin and C₆₀ films on indium-tin-oxide electrode’, *Chem. Commun.* **2008**, 4921– 4923.

3.2. SYNTHESIS



Scheme 3.1. Reagents and conditions: (i) ethyl acetate–DMF (2 : 1 v/v); (ii) DEA; (iii) nitrogen, room temperature, 5 min, 97% yield.

5,10,15,20-Tetrakis[4-(10H,10H,20-H, 20H-perfluorododecyl) - 2,3,5,6 - tetrafluorophenyl] porphyrin (TPPF₁₀₀) **1** is readily synthesized by reacting 5,10,15, 20-tetrakis(2,3,4,5,6-pentafluorophenyl)porphyrin (TPPF₂₀) and 1H,1H,2H,2H-perfluorododecane-1-thiol (Scheme 3.1). The high yield and purity minimize the need for column chromatography. Compound **1** was crystallized from acetone in the form of purple hexagonal plates, in the triclinic crystal

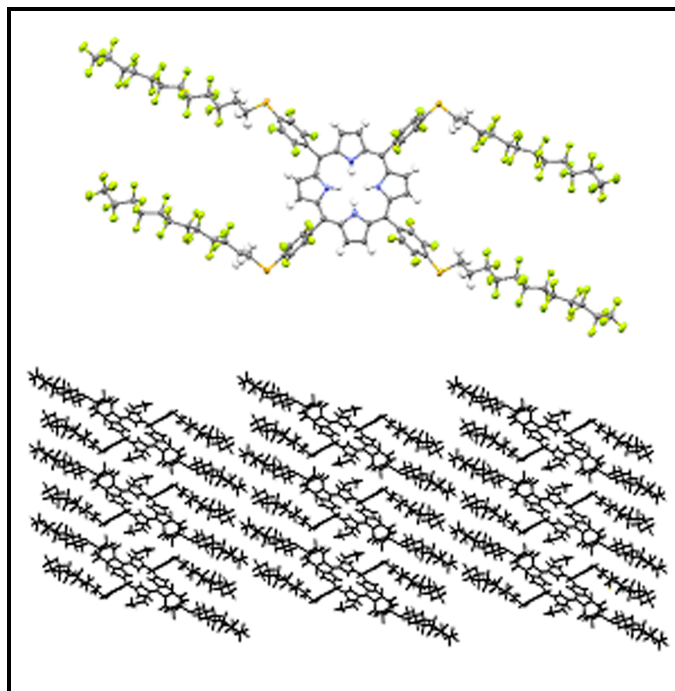


Figure 3.1. Ellipsoid model of TPPF₁₀₀ **1** (above) and its packing diagram (below), 50% probability level.

system, space group $P\bar{1}$ (Figure 3.1). This molecule has internal crystallographic symmetry. One half of the molecule is related to the other half by inversion symmetry. The strong intermolecular forces between the fluorinated alkanes appended to the porphyrin mediate the formation of a densely packed material as seen in the packing diagram. Similar dispersion interactions allow formation of robust thin films on surfaces¹⁵ (see below). Note the preference for the extended conformation of the fluorous alkane moieties, and that the 0.52 nm spacing between porphyrins indicates π - π interactions between the chromophores. The interactions between some of the fluoroalkanes in the crystal are strong enough to force two of the opposing aryl groups to adopt a 60° dihedral angle relative to

the porphyrin, whereas for the parent TPPF₂₀ these are at 90° because of steric interactions between the pyrrole β-H and the ortho F groups.

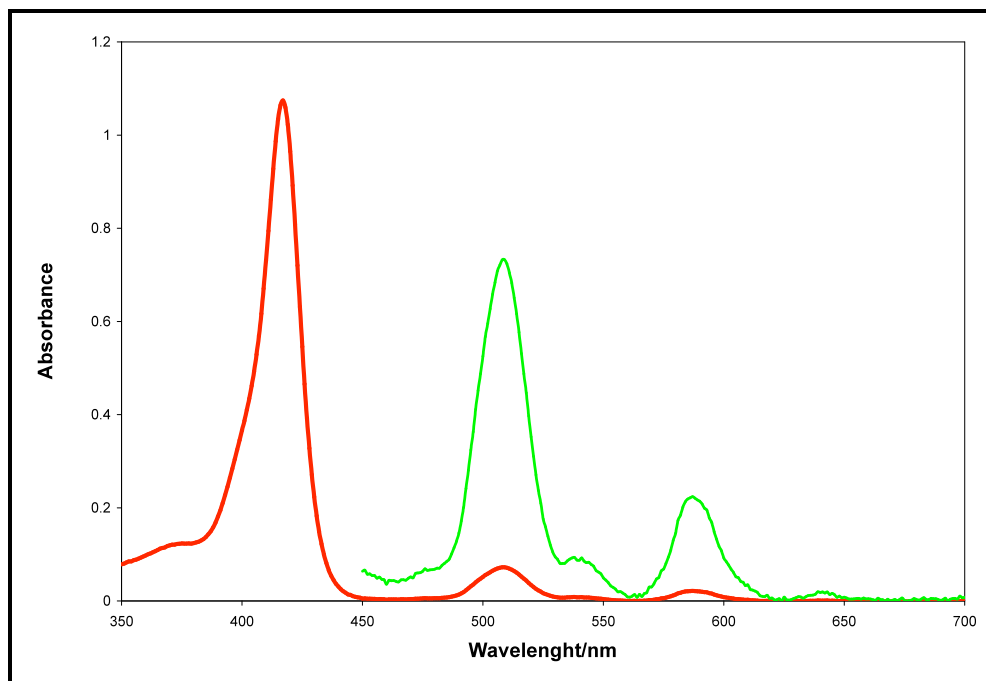


Figure 3.2. Absorption spectrum of **1** in CCl₄ (red); expansion of the Q band region (10X; green)

3.3 PREPARATION OF THE FILMS ON ITO AND CHARACTERIZATION

The solution of **1** was prepared by dissolving approximately 5 mg in 10 mL of CCl₄ and heating the solution in a water bath at 50°C for the time necessary to dissolve the porphyrin, ca. 30 seconds. The concentration was calculated by UV-Vis spectroscopy using the extinction coefficient and then diluted to $6 \cdot 10^{-5}$ M. The solution of C₆₀ was prepared by sonication of approximately 5 mg of fullerene (C₆₀, Aldrich, 99.5%) in 20 mL of CCl₄ for 3 hours obtaining a pale purple

solution, which was filtered through filter paper. Similarly the concentration was determined using the extinction coefficient.¹⁸

The 1:1 mole ratio solution of **1** and C₆₀ was prepared by mixing the two solutions in the proper ratio and the final concentration of each was calculated using the extinction coefficients. The solutions were stored in the dark and used within one month. The thin films samples were prepared as follows: a slide of ITO coated glass (Aldrich, 70-100 Ω/sq surface resistivity) was ozone cleaned for 20 minutes, rinsed with ethyl alcohol (Pharmacia 200 proof, ACS/UPS grade) and thoroughly washed with nano-pure water. The slide was immersed vertically into the solution of **1** and C₆₀ for 60 minutes, dried vertically in air, and then rinsed with nanopure water. The ITO coated slide was imaged by AFM before and after immersion using a Veeco Multimode, which was also used for nanoshaving experiments.

3.3.1 OPTICAL PROPERTIES: UV-VISIBLE AND FLUORESCENCE SPECTROSCOPY

UV-visible spectroscopy of the interaction between **1** and fullerene C₆₀ was first studied in solution at the greatest concentrations allowed by the solubility of the compounds; however, the electronic spectrum of the complex is the sum of the spectra of the individual chromophores, which is consistent with previous reports.¹⁶ Nonetheless, the interaction between the two chromophores in the solid state can be substantially greater.⁸ The interactions and electronic

communication between the chromophores in the solid state such as thin films are readily observable by fluorescence spectroscopy and microscopy. Therefore we have developed a means for forming a co-deposited film of **1** and C₆₀ on indium-tin-oxide (ITO) by immersing the electrode in a solution containing both (6·10⁻⁵ M each) at room temperature. CCl₄ is a good solvent in which both the chromophores are soluble together at concentrations up to ca. 10⁻⁴ M. Deposition from half this concentration results in similar films. The pale orange 10⁻⁵ M solution of **1** in CCl₄ was prepared just prior to use. The solution of C₆₀ was prepared by sonication in CCl₄ (1 mg/4 mL) for 3 h to yield a pale purple solution that was filtered. All concentrations were determined using the extinction coefficients.¹⁷ The 1:1 mole ratio solution of **1** and C₆₀ was prepared by mixing the two solutions in the proper ratio and the final concentration of each was determined. The thin films samples were prepared on a slide of ITO coated glass that had been ozone cleaned, rinsed with ethyl alcohol and thoroughly washed with nanopure water. After drying, the slide was immersed vertically into the solution of **1** and C₆₀ for 60 min, dried vertically in air, and then rinsed with nanopure water. The ITO coated slide was imaged by atomic force microscopy (AFM) before and after immersion. In addition to intermolecular interactions, solvent, concentration, evaporation rate, surface properties, and mode of deposition combine to dictate the morphology of self-organizing systems on surfaces.^{18,19} In this case the fluororous alkanes drive the formation of the thin films with C₆₀, since similar films are not observed using an analogue with

hydrocarbon chains and the same deposition conditions, *vide infra*. In order to assure the same amount of **1** is deposited in all the experiments, UV-visible spectra were recorded after each immersion. The Soret band of **1** on ITO is weakly red-shifted to 422 nm. The fluorescence of **1** is strongly quenched in the presence of C₆₀ in the self-organized thin film on the substrate (Figure 3.2). These data can be interpreted as photoinduced electron transfer from the porphyrin to the fullerene, as observed previously for por-C₆₀ systems.

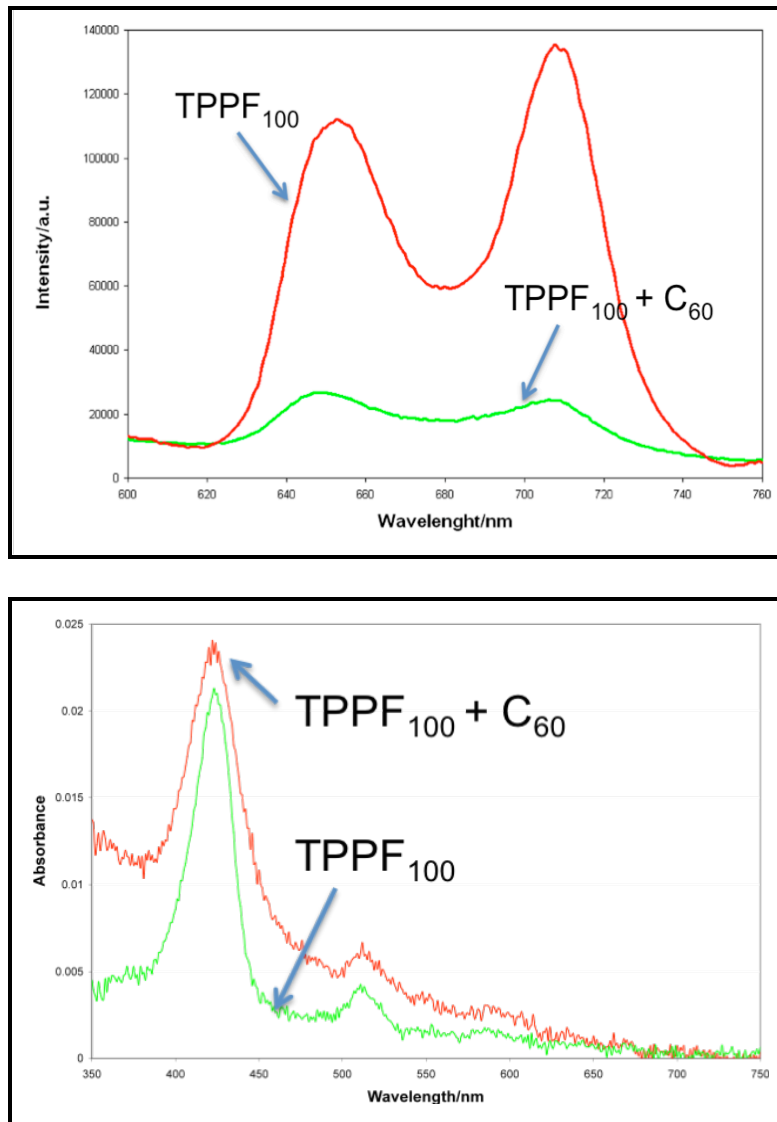


Figure 3.3. Top. Fluorescence spectra of film of **1** on ITO (red) and film of **1**-C₆₀ formed by dipping the ITO into a 1 : 1 solution once (green). Spectra are normalized to porphyrin absorption at the 422 nm excitation and baselines are corrected. Bottom. Electronic spectra of **1** on ITO (green) and a film of **1** and C₆₀ on ITO (red).

3.3.3. ATOMIC FORCE MICROSCOPY (AFM) AND LASER SCAN CONFOCAL MICROSCOPY (LSCM) COMBINED STUDIES

In order to characterize the morphology and the thickness of the films, AFM studies of the films on the substrates were conducted. As expected, AFM experiments reveal that the overall morphologies of the films of **1** alone and the film from dipping in the **1**-C₆₀ mixture are significantly different. The morphology of the material deposited on ITO (rms roughness of 0.5 nm) from immersion in a 6·10⁻⁵ M solution of **1** in CCl₄ appears as irregular flat domains of different horizontal and vertical sizes. Similar immersions in C₆₀ yield sporadic aggregates. Conversely, immersion in a solution containing both components results in thin films with a granular morphology. In order to determine the thickness of the **1**-C₆₀ film, a 4 mm² well was shaved on the surface using a contact mode imaging tip and applying a force equal to 619 nN. The well was then imaged in tapping mode. Three nanoshaving experiments were conducted on each of five films prepared by the same methods, and the average thickness of the films was 7±0.4 nm. Due to the asperities in the substrate and film surfaces (film rms roughness of ca. 1 nm), the averages of each were used, as calculated by the Veeco software. A second dipping in the 1:1 solution yields ca. 12 nm thick films with analogous granular morphologies, which is consistent with the ca. double absorbance of the Soret band. A second deposition of only **1** yields more complete films with similar flat topologies. Further dipping of either does not add any material to the substrate. AFM in combination with laser scanning confocal

microscopy was used to correlate film morphology to photonic activity of the material. For films of **1** only on ITO, the intensity of the fluorescence is inhomogeneously distributed across the ITO surface. Areas with strong fluorescence have corresponding AFM images that show large flat domains, with an average lateral dimension of 1.5 μm , and smaller flat domains, with an average lateral dimension of 33 nm. There is a paucity of any material observed on the substrate when only C_{60} is in the dipping solution. In contrast, when the ITO is immersed in a 1: 1 solution of **1**– C_{60} , a thin film is formed (Figure 3.3), with characteristic features observed neither for **1** nor for C_{60} alone. The co-deposition of **1** and C_{60} results in films with a high coverage and granular texture on ITO surfaces. Consistent with the fluorescence spectra of the films (Figure 3.2), the confocal fluorescence microscopy reveals that the porphyrin fluorescence is strongly quenched. Thus both the AFM and fluorescence experiments confirm that the C_{60} resides close to the porphyrin and that the two components do not separate into domains of each. This observation indicates that the interactions between TPPF₁₀₀ and C_{60} , which are expected to increase significantly as the solvent evaporates, dictate the morphology of the material deposited onto the ITO surface and the photophysical properties are consistent with other solid state porphyrin– C_{60} constructs.⁸ Larger AFM scans at multiple positions of the co-deposited film indicate the morphology persists over large areas. Samples stored in air and ambient light are stable for more than one month with no observed decomposition of the chromophores indicated by UV-visible spectroscopy.

Considering the previous crystallographic data,⁹ one possible molecular arrangement is with C₆₀ sandwiched between porphyrin molecules. Using the crystal data (fullerene diameter of 0.75 nm, and a porphyrin–C₆₀ distance of 0.26 nm) a 7 nm thick film would have ca. seven layers. Alternatively the C₆₀ could reside between the fluororous chains. Since sequential dipping of the substrate in separate solutions of **1** and C₆₀ does not lead to films, there must be some intermolecular interactions and pre-organization in the evaporating solvent during deposition beyond π -stacking.

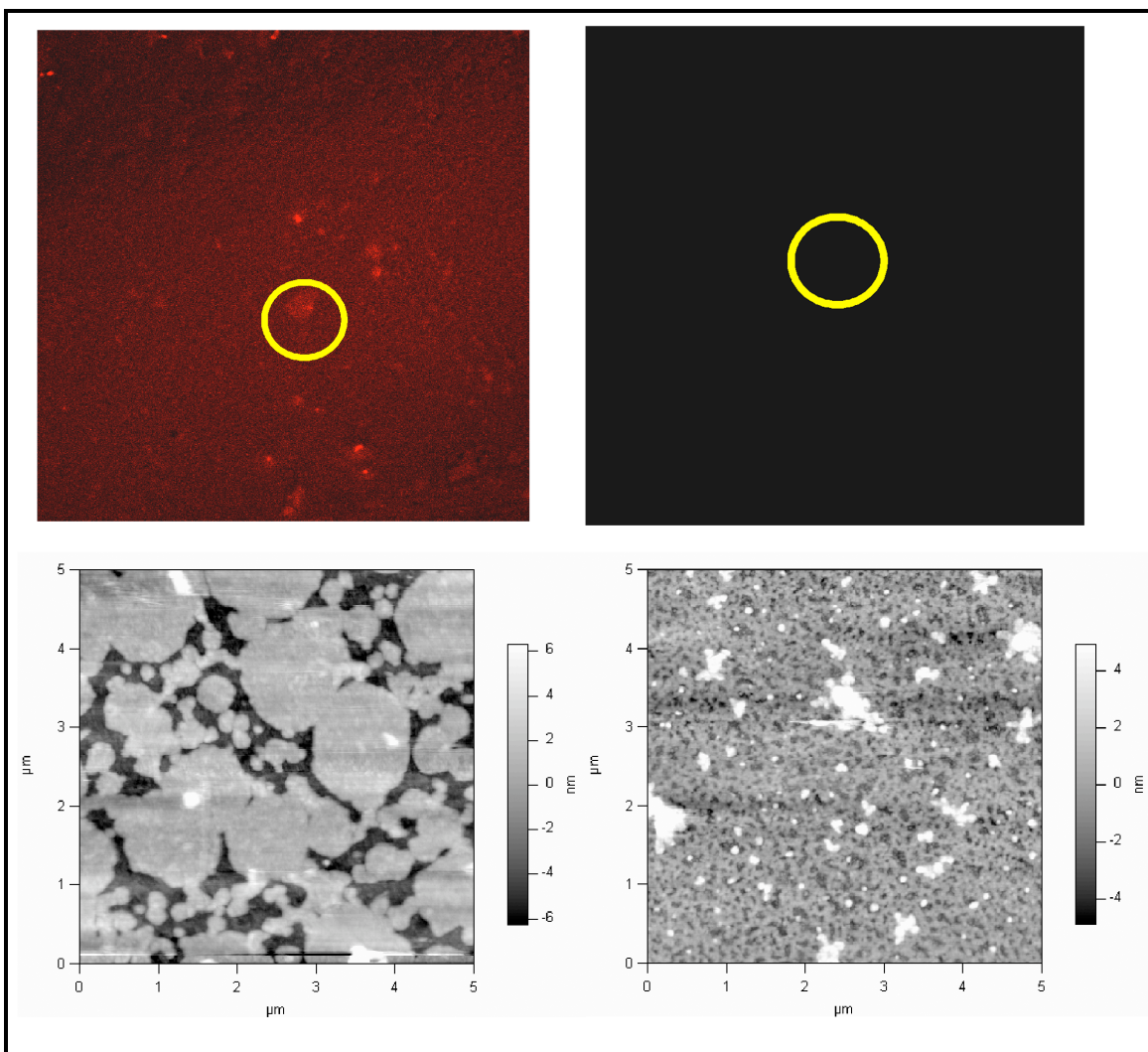


Figure 3.4. Combined laser scanning and atomic force microscopy characterization of films. Left: deposition of **1** on ITO results in an incomplete film with observable fluorescence (top left) and corresponding flat features (bottom left). Right: deposition from a 1 : 1 solution of **1** and C₆₀ in CCl₄ results in a high coverage film with no observable fluorescence (top right) and a granular topology (bottom right). Confocal data: all samples excited with a 488 nm laser. Five frames (317.2 × 317.2 m, 60× objective) were collected and averaged in order to reduce background noise. AFM data: all samples were imaged with a Park 0.1 silicon nitride tip ($k = 0.1 \text{ N m}^{-1}$) in contact mode.

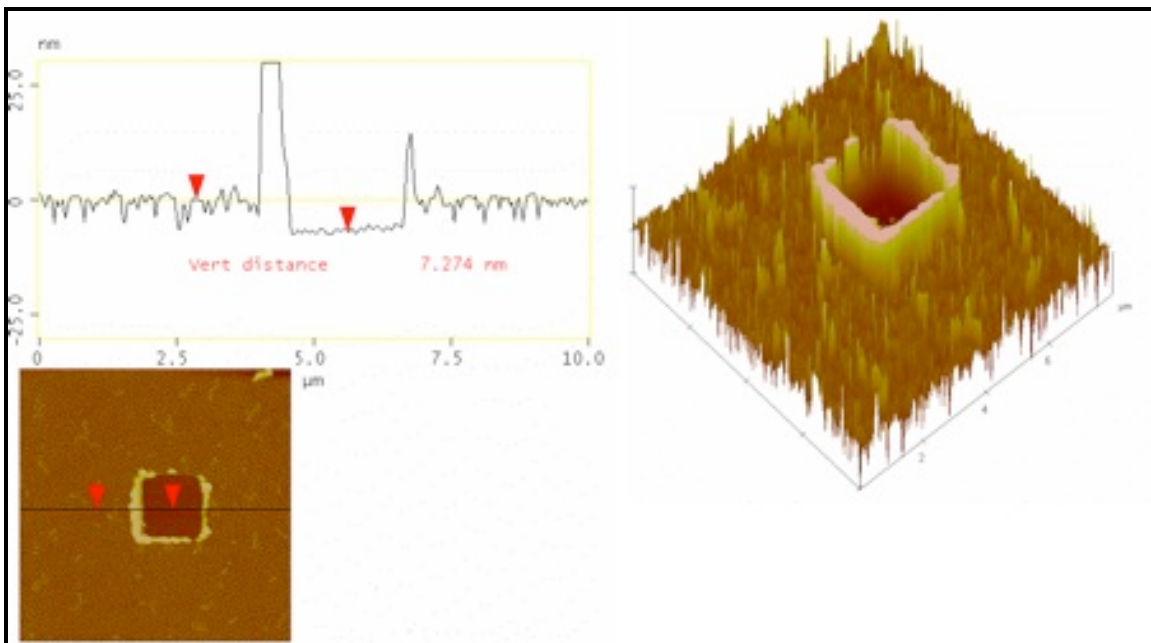


Figure 3.5. Nanoshaving of a film of **1** and C₆₀ ratio 1:1 on ITO electrode. The AFM image shows the granular morphology of film and the section analysis the thickness. A three dimensional version of the film on the right. Tapping/Height mode. Veeco Multimode AFM. Tip rectangular cantilever from Mikromasch NSC15 series Al BS (325 kHz, 40 N/m). Backside Al-coated. The well is shaved using a contact mode imaging tip with triangular cantilever from Mikromasch CSC21 series 100 kHz (2 N/m). Backside Al-coated. Spring constant calculated equal to 2.92 N/m. Force applied to shave off the film equal to 617.87 nN.

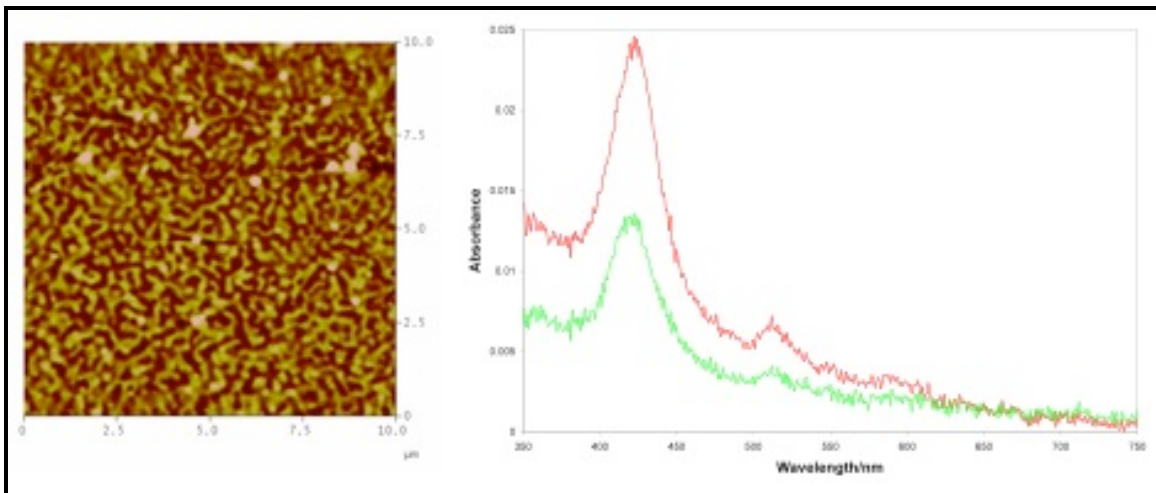


Figure 3.6. Right: 10x10 μm AFM image of a film of **1** and C₆₀ on ITO after two dipping in solution of 60 minutes each. Left: Corresponding absorbance after the first (green) and second (red) dipping.

3.4 ROLE OF THE FLUORINE ON THE MOIETIES AND STABILITY OF THE FILMS

To understand the role of the fluorocarbon chains, the corresponding porphyrin bearing four hydrocarbon chains of the same length was synthesized (compound **2**, see experimental section 3.6). The same co-deposition experiments with **2** and C₆₀ on ITO were conducted, and quite different results were found. Though UV-Vis data indicate the presence of some **2**-C₆₀ material on the surface, AFM experiments demonstrated that thin films are not formed, but only sporadic, amorphous aggregates. To compare the robustness of the two surface deposited films, the slides were sonicated in water and in 50 mM NaCl aqueous solution for 10 min. Remarkably, UV-Vis spectra show that only ca. 5% of the **1**-C₆₀ film is removed while nearly 70% of the **2**-C₆₀ film is lost and the presence of the fullerene is barely detectable. This indicates that the increased intermolecular interactions of the fluorocarbon moieties between the porphyrins and C₆₀, and the surface drive the self-organization of these films.

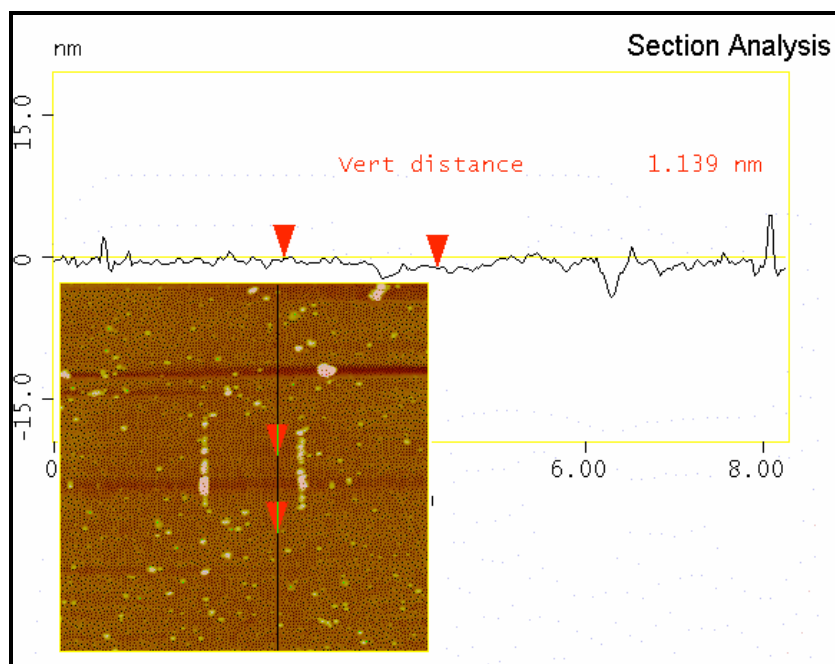


Figure 3.7. AFM image with section analysis of co-deposition of **2** and C_{60} ratio 1:1 on ITO. Tapping/Height mode. Veeco Multimode AFM. Tip rectangular cantilever from Mikromasch NSC15 series Al BS (325 kHz, 40 N/m). Backside Al-coated. The well is shaved using a contact mode imaging tip with triangular cantilever from Mikromasch CSC21 series 100 kHz (2 N/m). Backside Al-coated. Spring constant calculated equal to 2.92 N/m. Force applied to shave off the film equal to 617.87 nN.

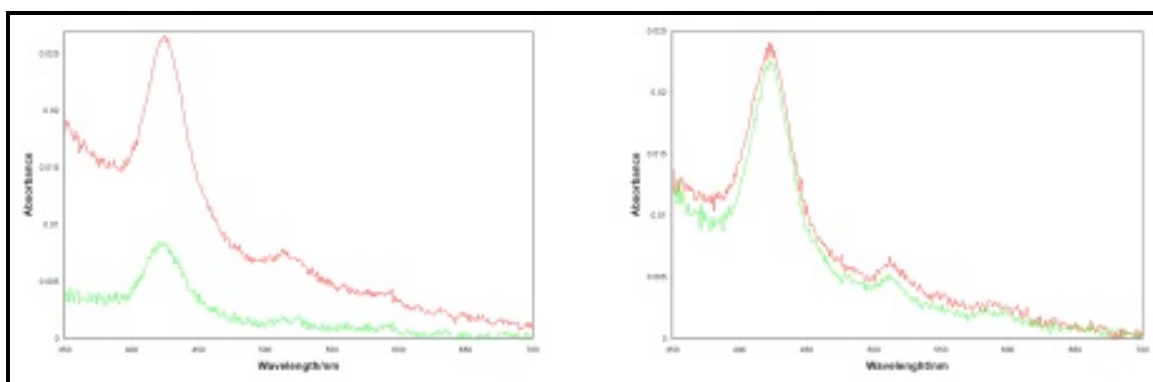


Figure 3.8. Left: UV-Vis spectra of the co-deposition of compound **2** and C_{60} on ITO before (red) and after (green) sonication in a 50 mM NaCl aqueous solution. Right: the co-deposited material composed of **1** and C_{60} before (red) and after (green) sonication in an aqueous solution of 50 mM NaCl. The slides completed immersed in the solution were sonicated for 10 minutes (Fisher Scientific FS15 sonicator).

3.5 CONCLUSIONS

In conclusion we synthesized a new porphyrin bearing fluorinated alkanes through a facile and efficient procedure. The properties of the fluoroalkane groups allow the porphyrin chromophore to self-organize with C₆₀ via a co-deposition process into thin films. The films are characterized by significant quenching of the porphyrin fluorescence by electron transfer to the fullerene.²¹

3.6. EXPERIMENTAL SECTION: SYNTHESSES AND CHARACTERIZATION OF THE COMPOUNDS

Synthesis of compound 1. 1H,1H,2H,2H-perfluorododecane-1-thiol (65 mg, 112 μ mol, FluoroFlash) was dissolved in 3 mL of ethyl acetate/DMF (2:1 v/v) with diethylamine (DEA) (20 μ L, 194 μ mol) under nitrogen. Pentafluoro-tetraphenylporphyrin TPPF20 (11.5 mg, 11.8 μ mol, TCI America), dissolved in approximately 1 mL of dimethylformamide (DMF) was added to this solution. The product **1** precipitated after 5 minutes and was filtrated, re-dissolved in acetone and purified by silica gel chromatography using hexane/acetone (9:1 v/v). The yield was 36.8 mg (11.4 μ mol, 97%). High resolution MS: $C_{92}H_{27}N_4F_{100}S_4$ 0.2688 ppm error. 1H -NMR ($CDCl_3$ 5% TFA) ppm: -0.81 (broad s, 2H, pyrrole NH); 2.78 to 2.73 (m, 8H, 2'H); 3.50 (t, 8H, 1'H); 8.98 (s, 8H, pyrrole β H). ^{19}F NMR ($CDCl_3$ 5% TFA) ppm: -137.88 to -137.78 (m, 8F, Ar-*o*-F); -132.20 to -132.12 (m, 8F, Ar-*m*-F); -126.61 to -126.10 (m, 8F, 3'F); -123.40 to -126.10 (m, 8F, 4'F); -123.00 to -122.70 (m, 8F, 5'F); -122.20 to -121.50 (m, 40 F, 6'-10'F); -114.20 to -114.12 (m, 8F, 11'F); -81.05, -81.07, -81.10 (t, 12F, 12'F).

Single-Crystal X-ray Diffraction. The intensity data for **1** were measured on an Bruker-Nonius KappaCCD diffractometer (graphite-monochromated Mo *K α* radiation, $\lambda = 0.71073$ Å, *f-w* scans) at 100 (1) K. The data were corrected for absorption. Details of the solution and refinements for this compound are presented below:

C92H26N4F100S4.4C3H6O (I): The crystal of **1**, with approximate dimensions 0.080 X 0.20 X 0.20 mm, were triclinic with space group *P*-1. The final unit-cell constants of **1** were $a = 9.357(2)$, $b = 10.938(2)$, $c = 30.832(6)$ Å, $\alpha = 87.69(3)$ $b = 88.34(3)$ $\gamma = 77.124(3)^\circ$ $V = 3073.1(11)$ Å³, $Z = 1$, $D_x = 1.863$ g cm⁻³, $\mu = 0.28$ mm⁻¹, formula weight = 3447.72. The crystal contained acetone, which was the solvent of crystallization. The structure of **1** was solved with SHELXS-97 and refined by full-matrix least squares on F^2 with SHELXL-97. The hydrogen atoms (riding model) were included in the structure-factor calculations, but their parameters were not refined. The final discrepancy indices for ρ (max) = 27.56° were $R = 0.1011$ (calculated on F with 6936 reflections [$I > 2s(I)$]) and $R_w = 0.1913$ (calculated on F^2 with 12247 reflections) with 973 parameters varied. The major peaks of the final difference map (< 0.47 e Å⁻³) are near the sulfur atoms.

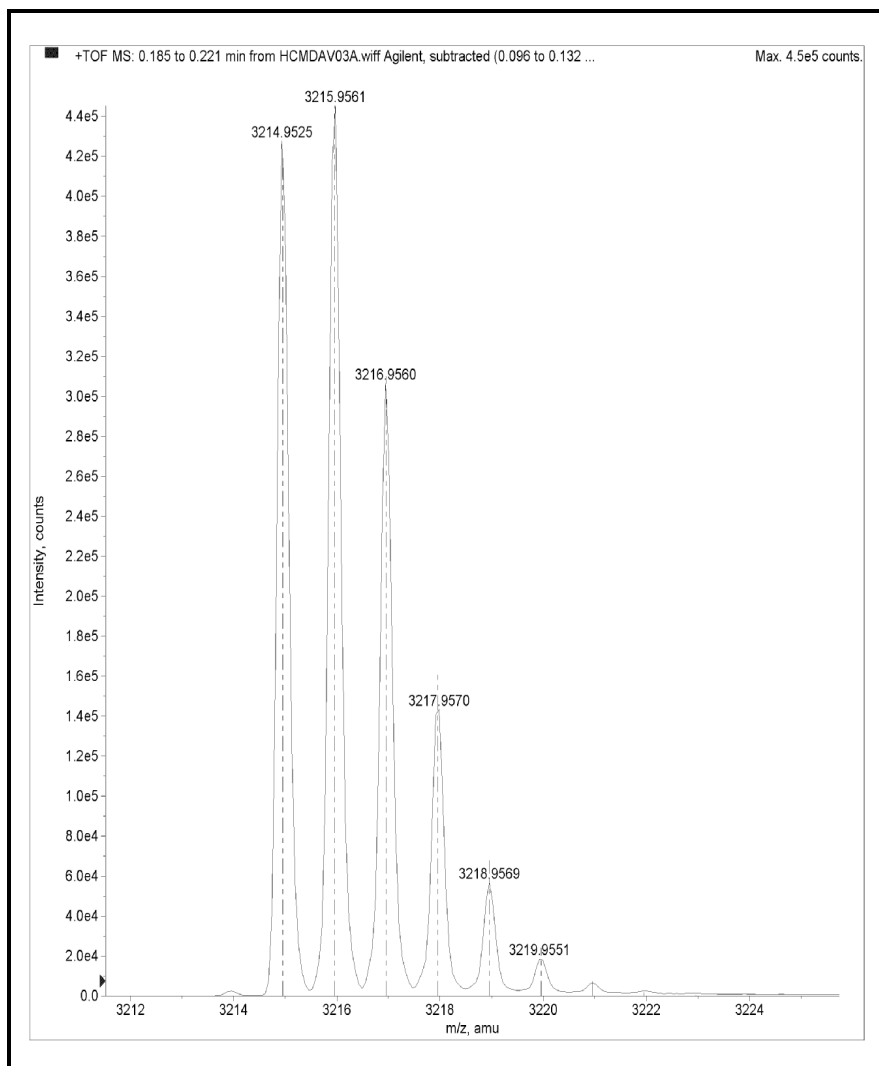


Figure 3.9. High resolution ESI-MS of compound 1.

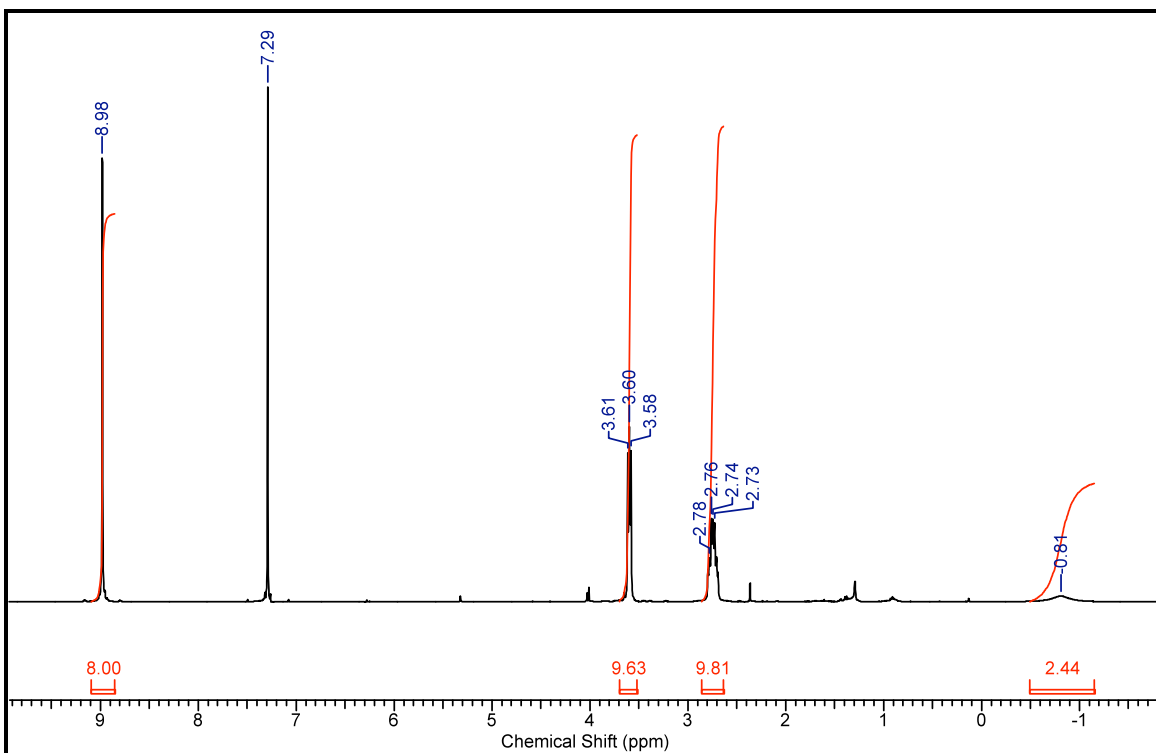


Figure 3.10. ^1H NMR of **1** in CDCl_3 5% TFA.

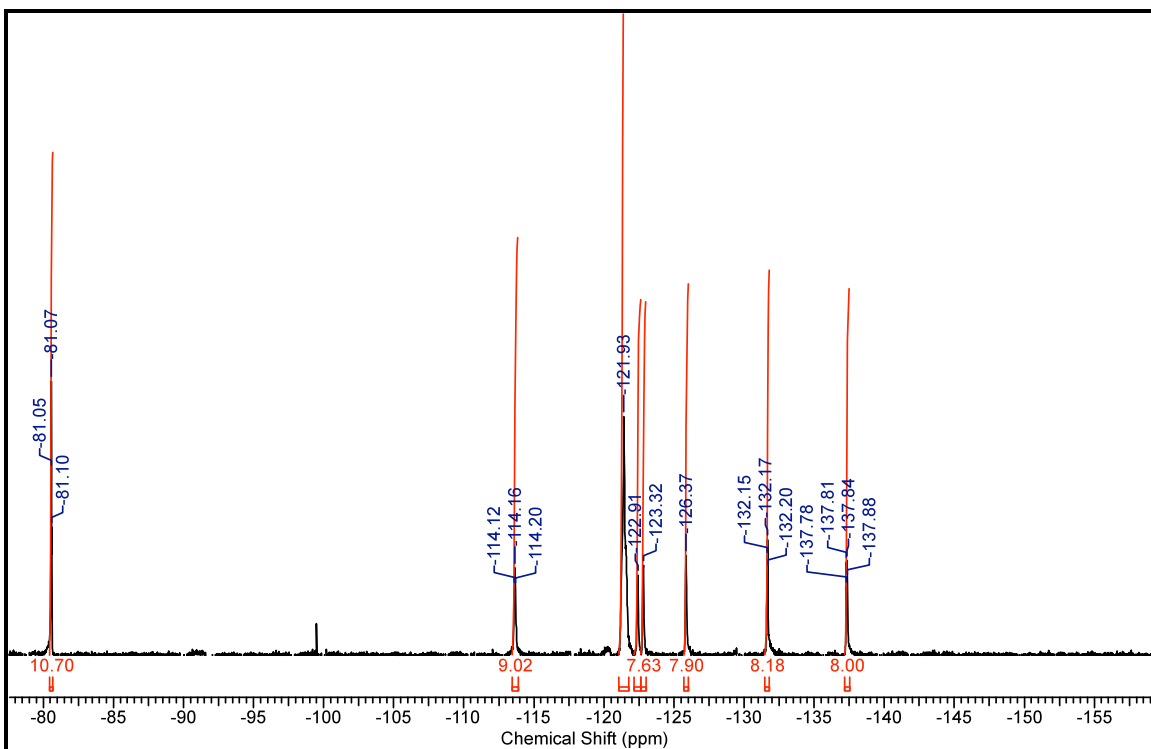


Figure 3.11. ^{19}F NMR of **1** in CDCl_3 5% TFA.

Synthesis of compound 2. 45 mg (220 μmol) of dodecanethiol were dissolved in 3 mL of DMF/Ethyl acetate 2:1 (v/v). 40 mg (40 μmol) of perfluorotetraphenylporphyrin TPPF₂₀ (TCI America) was added and the solution was stirred under nitrogen in presence of DEA (20 μL) for 8 hours. The reaction mixture was washed with water and the product was extracted with 3 portions of CH_2Cl_2 , concentrated and purified by column chromatography on silica gel using hexane/ethyl acetate (9/1, v:v). The yield was 62 mg (36 μmol , 90%). High resolution FAB: $\text{C}_{92}\text{H}_{110}\text{F}_{16}\text{N}_4\text{S}_4$, Measured mass 1702.7364, 0.6 ppm error (Service from University of Illinois, SCS Mass Spectrometry Laboratory). ^1H -NMR (CDCl_3) ppm: -2.86 (broad s, 2H, pyrrole); 0.85 to 0.87 (t, 12 H, 12'H); 1.28 to

1.44 (m, 64 H, 11-4 'H), 1.57 to 1.61 (m, 8H, 3'H), 1.83 to 1.89 (m, 8H, 2'H), 3.27 to 3.30 (t, 12H, 1'H); 8.93 (s, 8H, pyrrole β H).

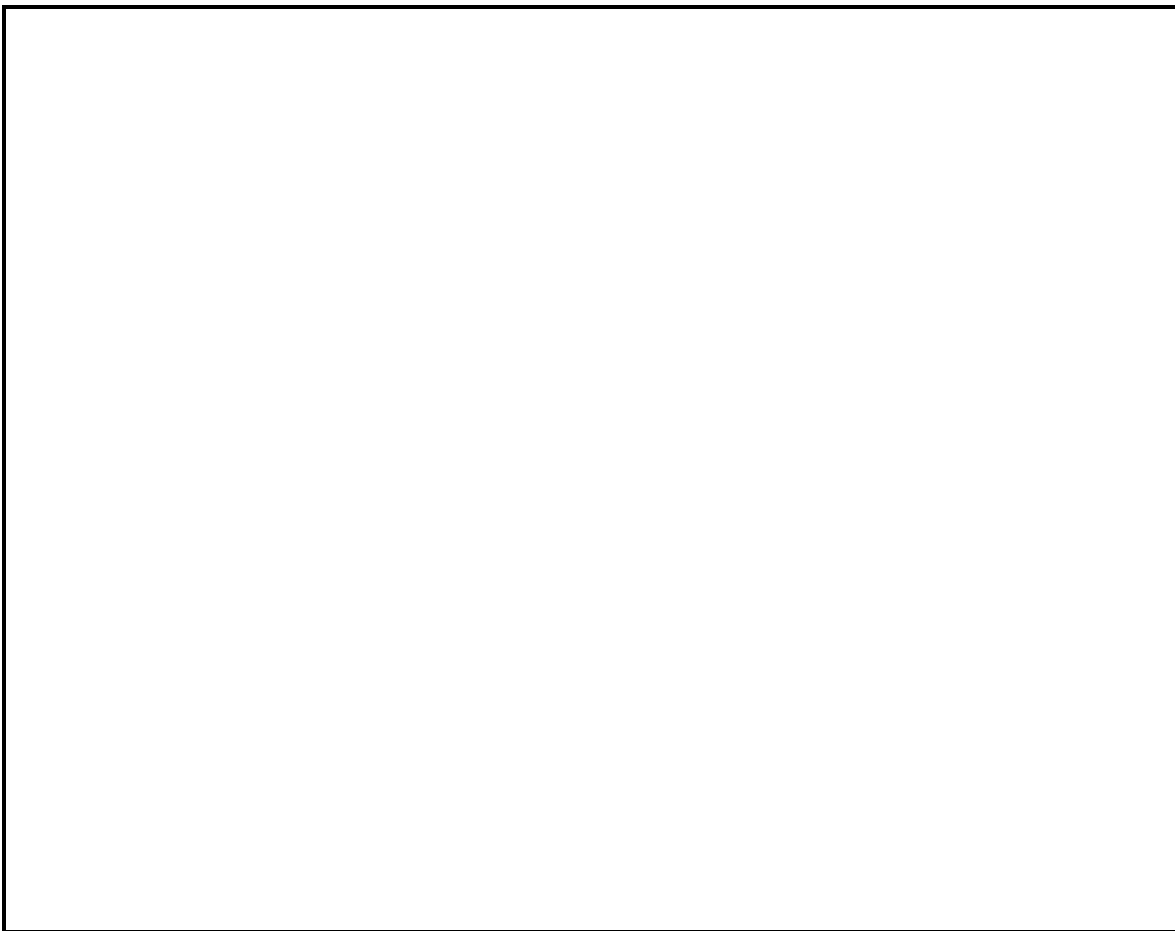


Figure 3.12. ^1H -NMR of compound **2**.

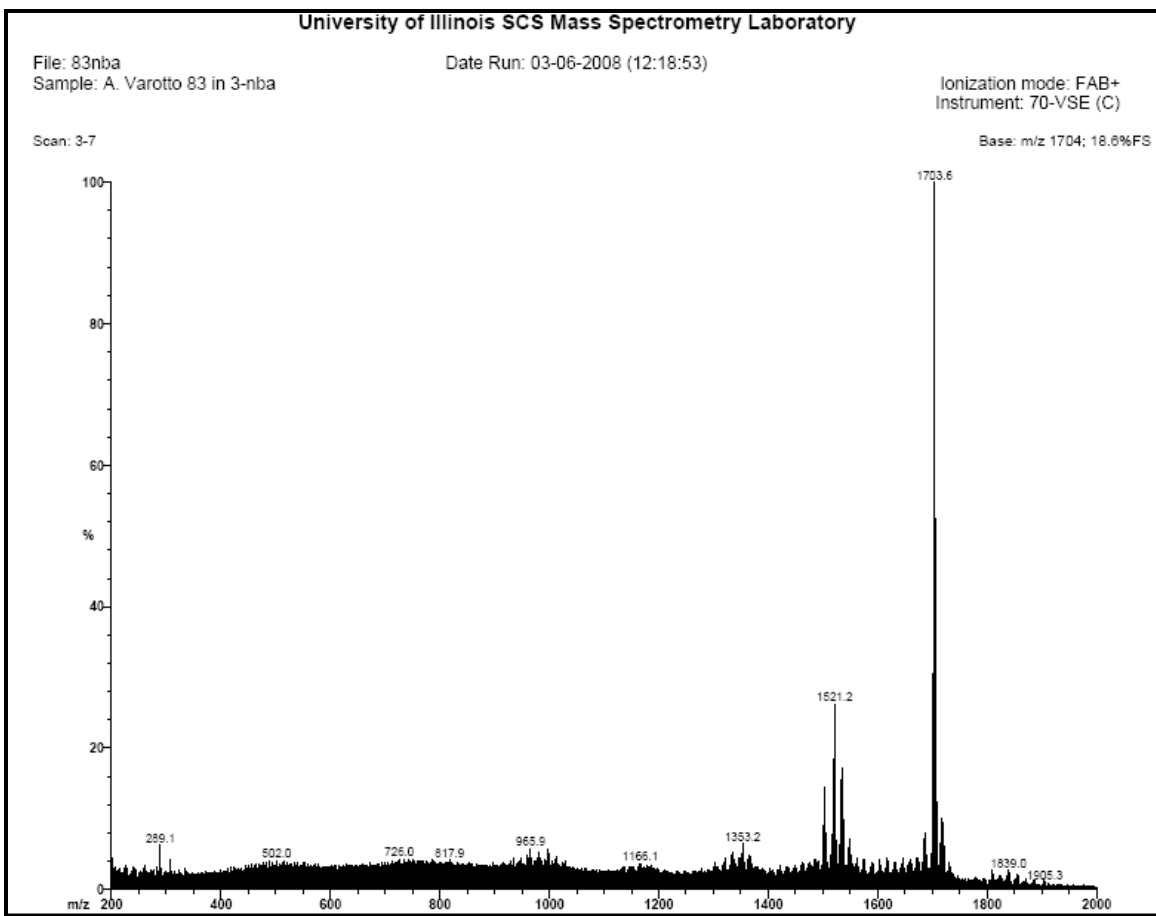


Figure 3.13. FAB spectrum of compound 2

Figure 3.14. ¹H-NMR of compound **2**.

Crystallographic data for 1. C₉₂H₂₆F₁₀₀N₄S₄•4C₂H₆O, M = 3447.72,

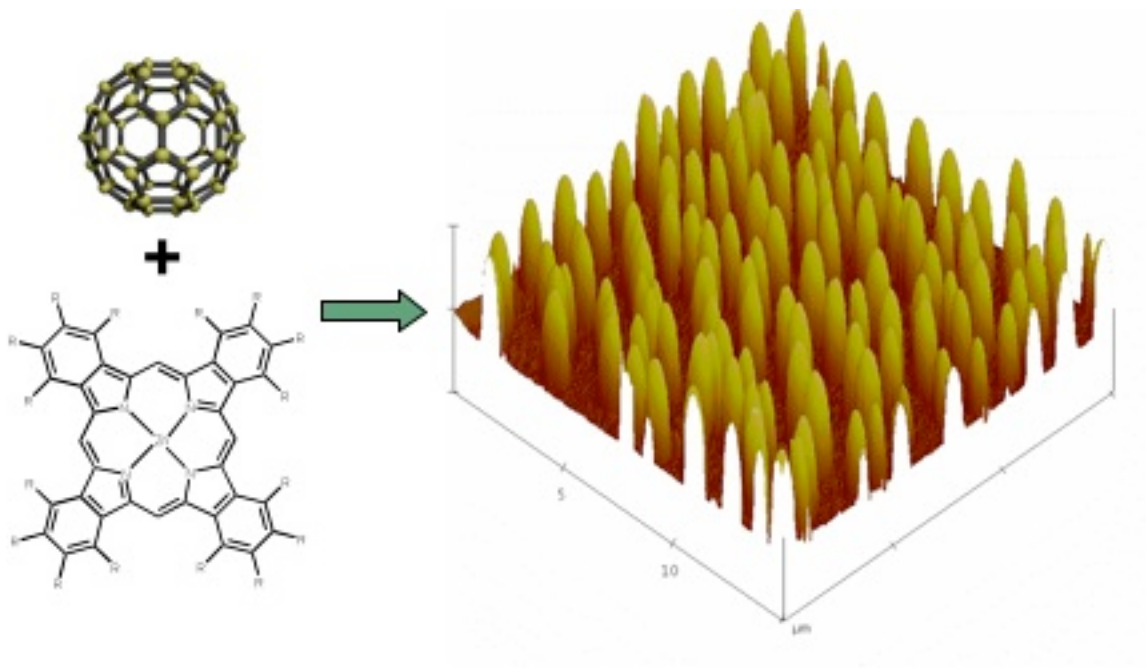
T = 100 K, triclinic, P $\bar{1}$, a = 9.3570(19), b = 10.938(2), c = 30.832(6) Å, α = 87.69(3), β = 88.34(3), γ = 77.12(3)°, V = 3073.1(11) Å³, Z = 1, D_c = 1.8634 g cm⁻³, m = 0.284 mm⁻¹, F(000) = 1698, crystal 0.20x0.20x0.08 mm³, Y_{max} = 27.56, ranges -12 ≤ h ≤ 12, -14 ≤ k ≤ 14, -39 ≤ l ≤ 38, R_{int} = 0.086, wR₂ = 0.191, reflections collected = 12247, independent reflections = 6936, parameters = 973.

References.

1. D. Bonifazi, H. Spillmann, A. Kiebele, M. de Wild, P. Seiler, F. Cheng, H.-J. Güntherodt, T. Jung and F. Diederich, *Angew. Chem., Int. Ed.*, 2004, **43**, 4759-4763.
2. H. Imahori, A. Fujimoto, S. Kang, H. Hotta, K. Yoshida, T. Umeyama, Y. Matano, S. Isoda, M. Isosomppi, N. V. Tkachenko and H. Lemmetyinen, *Chem. Eur. J.*, 2005, **11**, 7265-7275.
3. H. Imahori, H. Yamada, S. Ozawa, K. Ushidab and Y. Sakata, *Chem. Comm.*, 1999, 1165-1166.
4. A. Ikeda, T. Hatano, S. Shinkai, T. Akiyama and S. Yamada, *J. Am. Chem. Soc.*, 2001, **123**, 4855-4856.
5. T. Hasobe, H. Imahori, P. V. Kamat and S. Fukuzumi, *J. Am. Chem. Soc.*, 2003, **125**, 14962-14963.
6. M. Isosomppi, N. V. Tkachenko, A. Efimov, K. Kaunisto, K. Hosomizu, H. Imahorib and H. Lemmetyinen, *J. Mater. Chem.*, 2005, **15**, 4546-4554.
7. T. Umeyama and H. Imahori, *Photosynthesis Research*, 2006, **87**, 63-71.
8. P. D. W. Boyd and C. A. Reed, *Acc. Chem. Res.*, 2005, **38**, 235-242.
9. A. Hosseini, M. C. Hodgson, F. S. Tham, C. A. Reed and P. D. W. Boyd, *Crystal Growth&Design*, 2006, **6**, 397-403.
10. A. Hosseini, S. Taylor, G. Accorsi, N. Armaroli, C. A. Reed and P. D. W. Boyd, *J. Am. Chem. Soc.*, 2006, **128**, 15903-15913.
11. D. M. Guldi, *Chem. Comm.*, 2000, 321-327.
12. D. M. Guldi, *Chem. Soc. Rev.*, 2001, **31**, 22-36.
13. C.-y. Liu, H.-l. Pan, M. A. Fox and A. J. Bard, *Chem. Mater.*, 1997, **9**, 1422-1429.
14. P. Kirsch, *Modern Fluoroorganic Chemistry: Synthesis, Reactivity, Applications*, Wiley, 2004.
15. T. N. Milic, N. Chi, D. G. Yablon, G. W. Flynn, J. D. Batteas and C. M. Drain, *Angew. Chem.*, 2002, **41**, 2117-2119.
16. P. D. W. Boyd, M. C. Hodgson, C. E. F. Rickard, A. G. Oliver, L. Chaker, P. J. Brothers, R. D. Bolskar, F. S. Tham and C. A. Reed, *J. Am. Chem. Soc.*, 1999, **121**, 10487-10495.
17. S. Sawamura and N. Fujita, *Carbon*, 2007, **45**, 965-970.
18. C. M. Drain and X. Chen., in *Encyclopedia of Nanoscience & Nanotechnology*, ed. H. S. Nalwa, American Scientific Press, New York, 2004, pp. 593-616.
19. C. M. Drain, G. Smeareanu, J. Batteas and S. Patel, in *Dekker Encyclopedia of Nanoscience and Nanotechnology*, eds. J. A. Schwartz, C. I. Contescu and K. Putyera, Marcel Dekker, Inc., New York, 2004, pp. 3481-3502.
20. F. Wessendorf, J. F. Gnichwitz, G. H. Sarova, K. Hager, U. Hartnagel, D. M. Guldi and A. Hirsch, *J. Am. Chem. Soc.*, 2007, **129**, 16057-16071.
21. F. Oswald, D.-M. S. Islam, Y. Araki, V. Troiani, R. Caballero, P. de la Cruz, O. Ito and F. Langa, *Chem. Commun.*, 2007, 4498-4500.

CHAPTER 5

SELF-ORGANIZATION OF Pc787 AND FULLERENE C₆₀ ON ITO

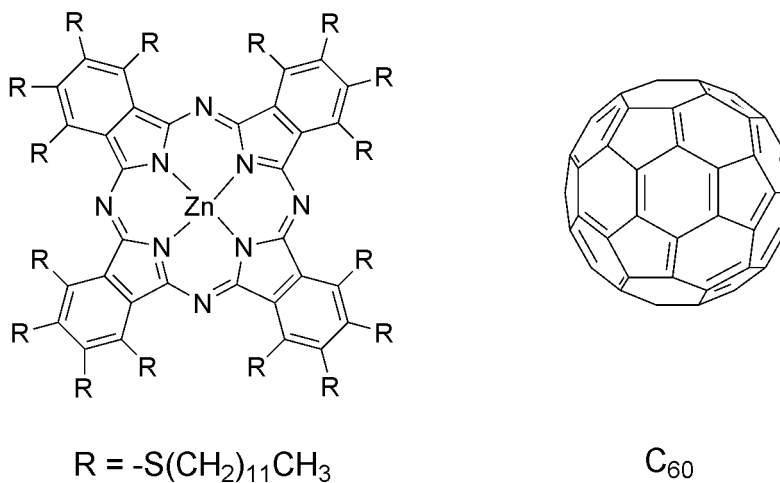


5.1. INTRODUCTION

Long alkane moieties are known to help the self-organization of small molecules on a surface within thin films. For example, flat phthalocyanines (Pc) bearing alkyl chains on the periphery of the ring are reported to form a mesogenic material when cast onto glass.^{1, 2} These Pc materials are interesting because of the way they supramolecularly organize to promote vectoral electron transfer.³ Thus, Pc-based functional materials have found application in organic electronics, photonic devices, and sensors. Other nanoarchitectures of dyes,

such as nanoparticles or nanotubes, are also interesting because they often display enhanced or exotic optical, electrical and/or magnetic properties. There are a number of reports on the formation of these nanostructured porphyrinoids^{4, 5} driven by axial coordination,⁶ coordination chemistry, or H-bonding.⁷ There are fewer reports on specifically self-organized materials of different chromophoric and/or photonic molecules, such as porphyrinoids with fullerenes, which are appealing as functional materials, for example as described in the previous chapters. Simple blends of porphyrinoids with fullerenes are even less studied because the interactions between the two are generally weak.

As with porphyrins, the flat core of a phthalocyanine is spontaneously attracted to the curved surface of a fullerene and this interaction has been described.⁸ In this chapter we will describe the growth of blended Pc787/C₆₀ nanoparticles on ITO driven by the π - π interactions between the two types of molecules and the van Der Waal's forces between the 16 alkyl chains (Figure 1) . The synthesis and properties of Pc787 can be found in chapter 4 of this thesis



Scheme 5.1. Structures of phthalocyanine Pc787 and fullerene C₆₀

5.2. PREPARATION OF THE SLIDES

The samples were prepared according to the following procedure. Slides of ITO are cleaned as follows: (1) -20 minutes ozone stream; (2) -rinsing with 10 ml of ethanol; (3)-dried with a paper towel; (4)-rinsing with 20 mL of nanopure water; (5) -dried over nitrogen stream. The material is deposited on the surface by dipping the slides in a solution containing the chromophores at a specific concentration/ratio and for an amount of time detailed below for each case.

5.3. Pc787 AND FULLERENE C₆₀

When deposited on ITO electrodes, either pure or as a blend with C₆₀, Pc787 exhibited very interesting and unique characteristics that none of the other derivatives showed. In fact, when a slide of ITO coated glass is dipped in a solution of Pc787 in toluene, it forms thin films over large areas, whereas the other derivatives (Pc735 or Pc707) tend to form sporadic and shapeless aggregates. Typical films of the hexadecaalkylphthalocyanine P787 are illustrated by the following AFM scan.

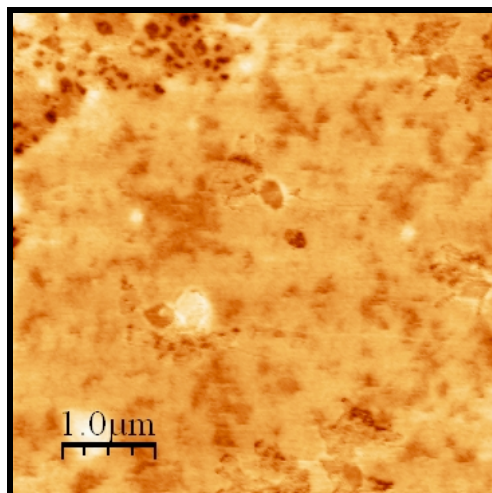


Figure 5.1. AFM heights analysis (tapping mode) of a film formed by immersing a glass slide with an ITO electrode on one face into a solution of Pc787 in toluene.

Figure 5.1 show the height analysis of a film of Pc787. The films are formed by dipping the ITO slide in solution for 1 hour and letting the solvent evaporate and dry in air. The depth of the film was approximately 10 nm. If dipped an additional hour, the slide can accumulate more material, reaching a thickness of approximately 20 nm and the coverage is more uniform. This is also confirmed by the increased absorbance of the Q-band. Additional soaking or additional times of immersion increase neither the thickness, nor the absorbance of the films.

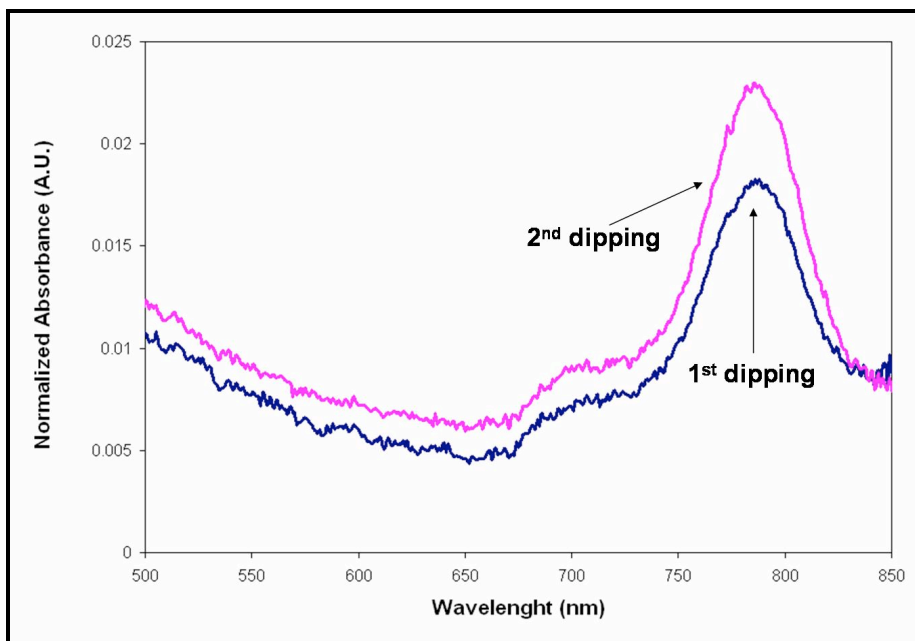


Figure 5.2. UV-Vis absorption spectra of Pc787 on ITO electrode after 1 and 2 emersions of 1 hour each (ca. 10 nm and 20 nm thick films).

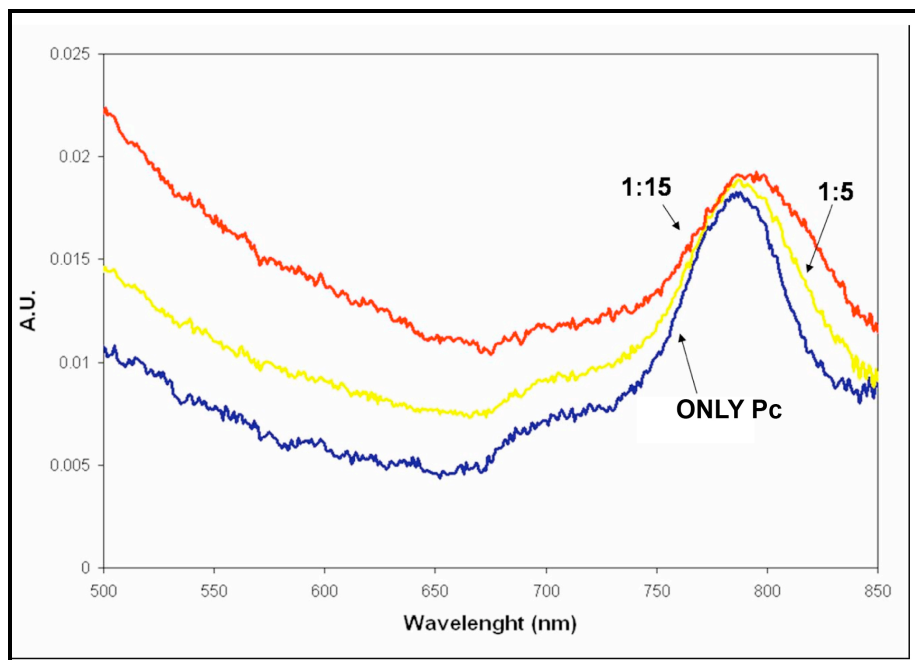


Figure 5.3. UV-Vis absorption spectra of Pc787 and Pc787 blended with fullerene C₆₀ on ITO, showing the Q-bands, with blends of two different mole ratios of the chromophores. The maximum absorption peaks tend to broaden and red-shift at increasing content of fullerene.

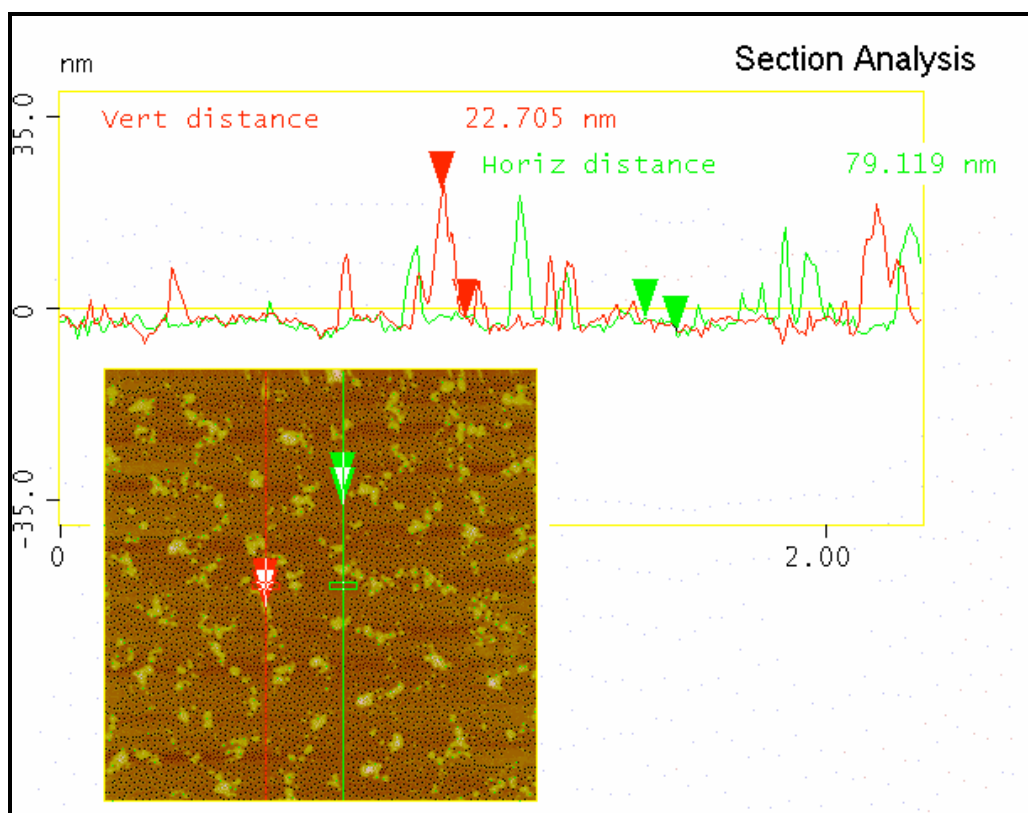


Figure 5.4. AFM height analysis of Pc735 on ITO shows that Pc with eight alkyl groups organizes differently than Pc787, when deposited on ITO under the same conditions. Pc735 does not form films but only sporadic aggregates.

As anticipated above, the property of forming films in these conditions is not shared by the other derivatives, Pc735, Pc707 and Pc677. Figure 4 shows the sporadic aggregates formed when a slide of ITO is immersed into a solution of Pc735. More surprisingly, we found out that when the ITO slides are dipped in a toluene solution containing a blend of Pc787 and fullerene C_{60} monodispersed particles formed on the surface after the solvent dries. Even though the mechanism of formation and the composition of these nanocomposites are still unclear, the following experiments suggest that the interaction between the

chromophores drive the formation of the particles and that the C₆₀ must reside between the phthalocyanines.

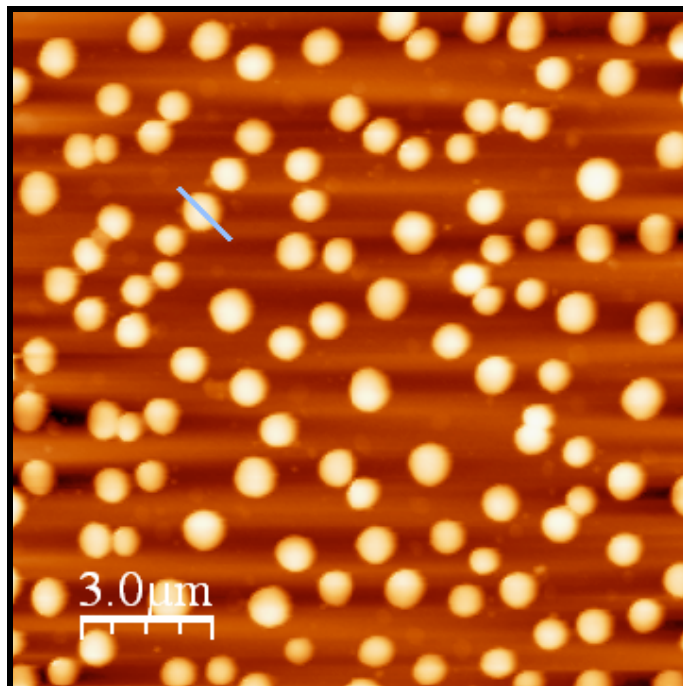


Figure 5.5. Nanoparticles formed by soaking a slide of ITO in a solution of Pc787/C₆₀ ratio 1/15 in toluene. The concentration of Pc787 is 0.3 mM, and AFM height analysis used tapping mode.

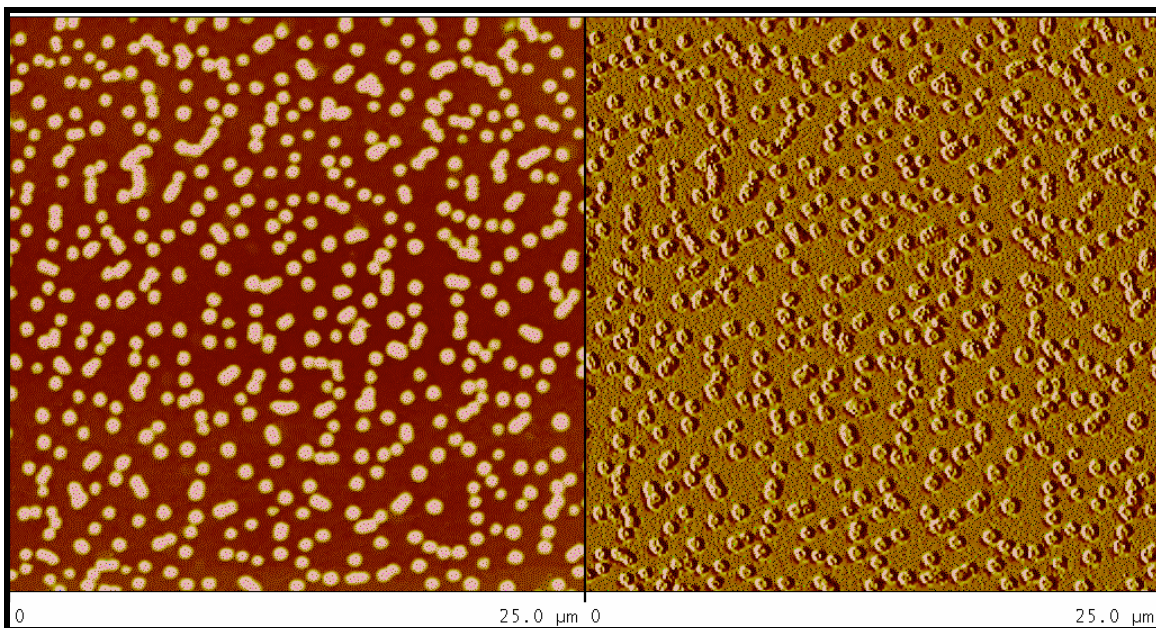


Figure 5.6. Larger scan of the same sample described in Figure 5.5. Height (left) and Amplitude (right) analyses, tapping mode.

5.3.1. RATIO WITH C_{60}

The effect of changing the ratio between the fullerene and Pc787 was studied to understand the mechanism of formation of the particles. We find that a large molar excess of C_{60} is needed to drive the formation of the particles, in fact as illustrated in the following images, they seem to form only when the mole ratio between Pc787 and C_{60} is less than 1/10 (Figure 5.7). As described above, Pc787 alone forms large area thin films on ITO. When Pc787 : C_{60} are premixed in solution in ratios of 1:2 or 1:5, we found that the films were less uniform (ratio 1:2) or showed additional features (ratio 1:5) that are indicative of phase separation of the component molecules into domains. When the Pc787: C_{60} ratio was decreased to 1:10, the formation of the nanoparticles started to be noticeable, though they are less defined nor are they monodispersed. At a ratio

of Pc787/C₆₀ 1:15, particles of well defined size and shape patterned the ITO surface, as shown in Figure 5.5.

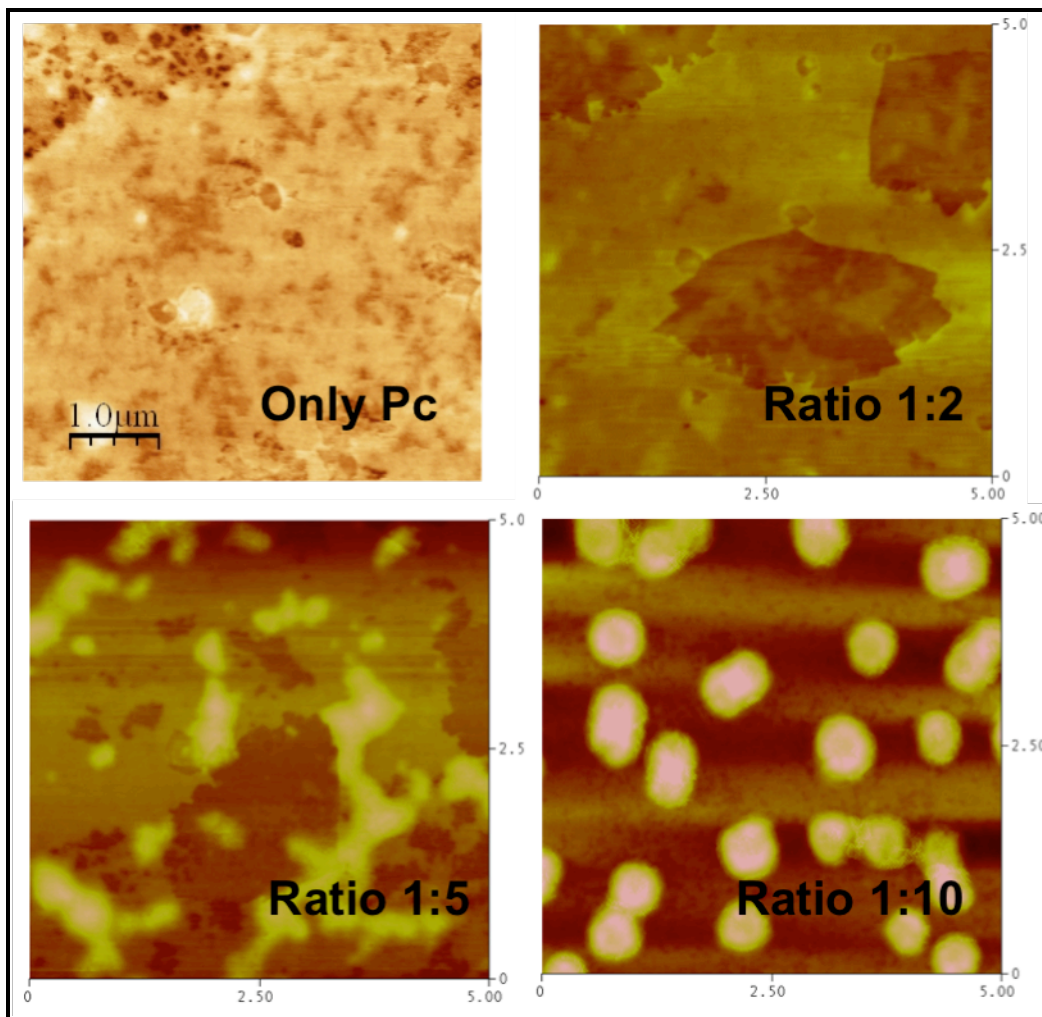


Figure 5.7. AFM height analysis of four different samples obtained by immersing ITO slides in solutions of Pc787 with increasing amounts of fullerene C₆₀. These images indicate that the formation of the nanoparticles results only at ratios of Pc/Fullerene less than 1:10. All scans are 5X5 μm.

5.3.2.SIZE OF THE PARTICLES

We investigated the effect of changing the concentration of Pc787 and found that the concentration dictates the size of the nanoparticles. Particles formed from 0.1 mM solution in phthalocyanine were significantly smaller than those formed from 0.3 mM as shown in Figure 5.8, 5.9 and 5.10

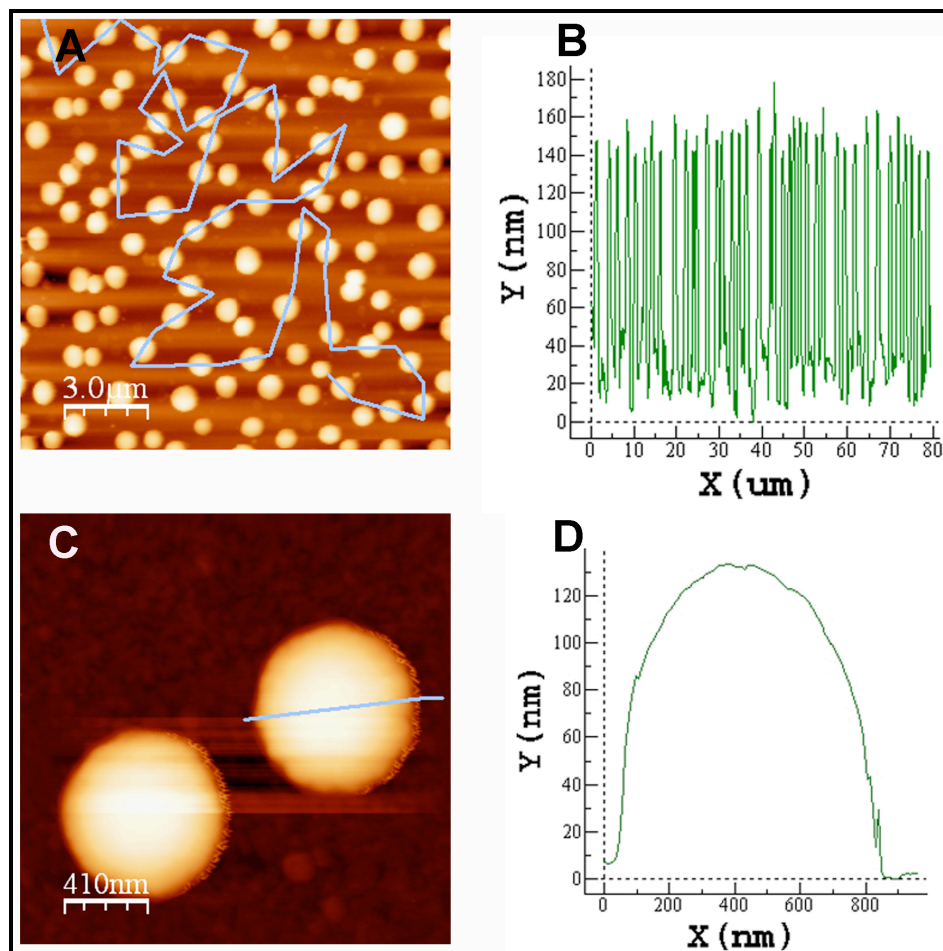


Figure 5.8. (A) AFM images of nanoparticles obtained from Pc787/C₆₀ ratio 1/15 and Pc concentration 0.3 mM. (B) Height analysis showing that the nanoparticles are monodispersed and they are ca. 130 nm high. (C) AFM macro of the same sample and (D) size of one particle showing the height (ca. 130 nm) and diameter (ca. 700 nm).

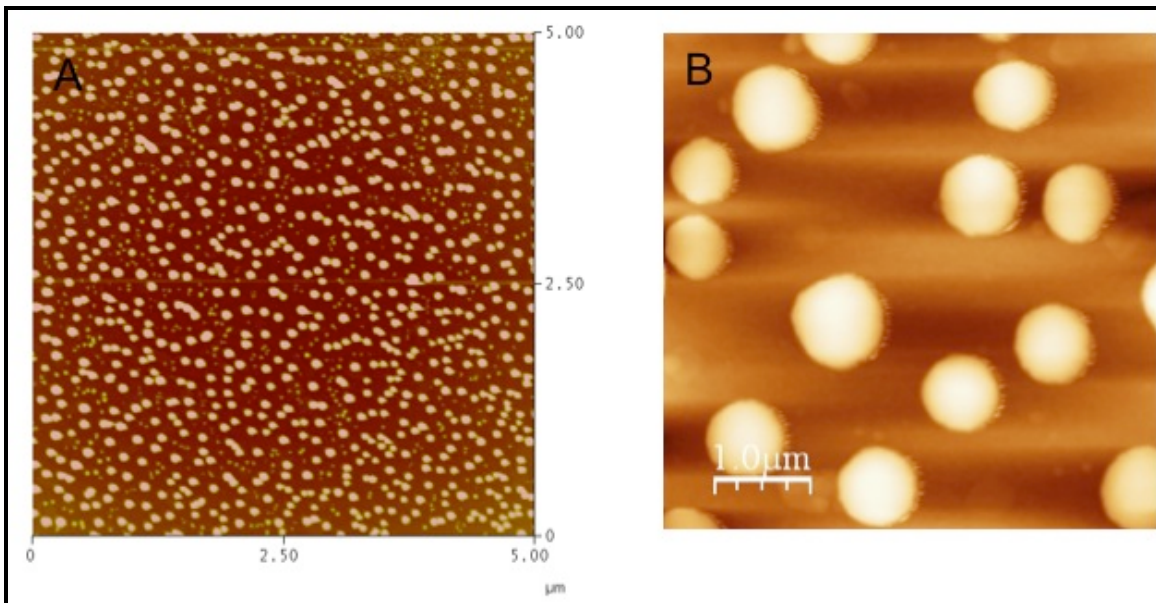


Figure 5.9. AFM images (5x5 microns, height mode) of nanoparticles formed from Pc787/C₆₀ in ratio 1/15 at different concentration of Pc: (A) 0.1 mM, where the average height is 75 and width is ca. 60 nm, compared to (B) 0.3 mM. All scans are 5X5 μm .

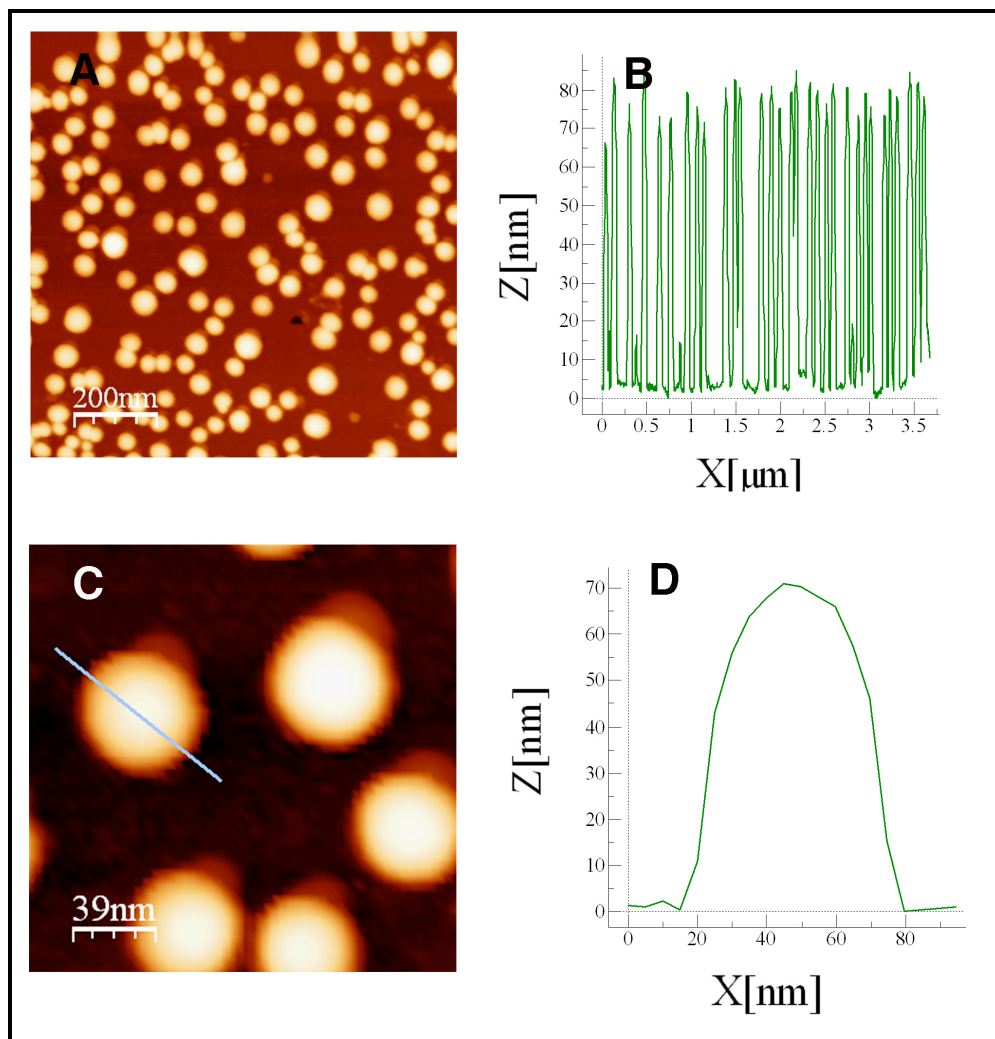


Figure 5.10. (A) AFM images of nanoparticles obtained from Pc787/C₆₀ ratio 1/15 and Pc concentration 0.1 mM. (B) Height analysis showing that the nanoparticles are monodispersed and they are ca. 75 nm high. (C) AFM macro of the same sample and (D) size of one particle showing the width (ca. 60 nm).

5.3.3. TIME OF IMMERSION

From the experiments described so far it appears that the particles are scattered on the surface and they do not coat the entire area of the substrate. In an effort to cover a wider region we tried to soak the ITO for a longer time. The following images show that after two hours of immersion the substrate reaches

equilibrium and it is not possible to accumulate more materials. We left a sample soaking for 2 days and we found the same amount of materials deposited after 2 hours. Even successive dipping do not allow for more material to coat the surface.

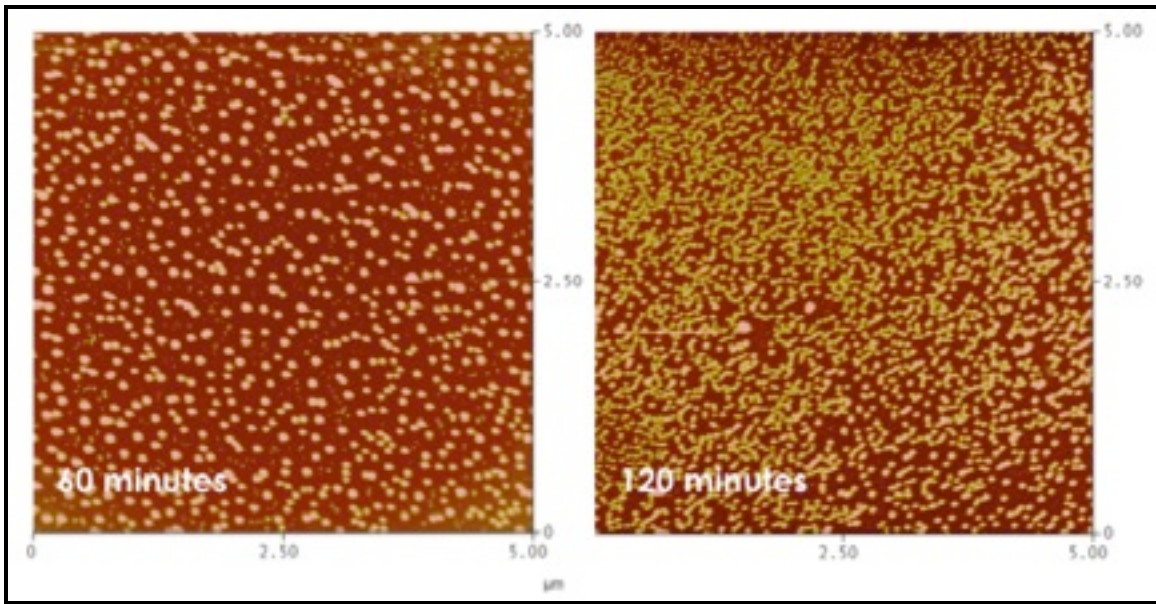


Figure 5.11. AFM images of nanoparticles formed from Pc787/C₆₀ ratio 1:15, Pc concentration 0.1 mM, after 60 and 120 minutes of soaking in solution.

5.3.4. ALTERNATE DIPPING

UV-visible and fluorescence experiments conducted in solution indicate little or no interaction between the phthalocyanine and the fullerene; therefore it is reasonable to conclude that the particles are forming on the surface. We then carried out an experiment in which we first dipped the ITO substrate in a solution containing only Pc787, let it dry, and then soak it in a solution containing only fullerene. We found that islands of materials are formed under these conditions, but they are not as uniform and monodispersed as when the chromophores are pre-mixed in the same solution. The morphologies of materials formed by dipping the substrate in solution containing only one of the chromophores appear very different from AFM images: thin films for Pc and much smaller sporadic particles (ca. 15 nm) for fullerene.

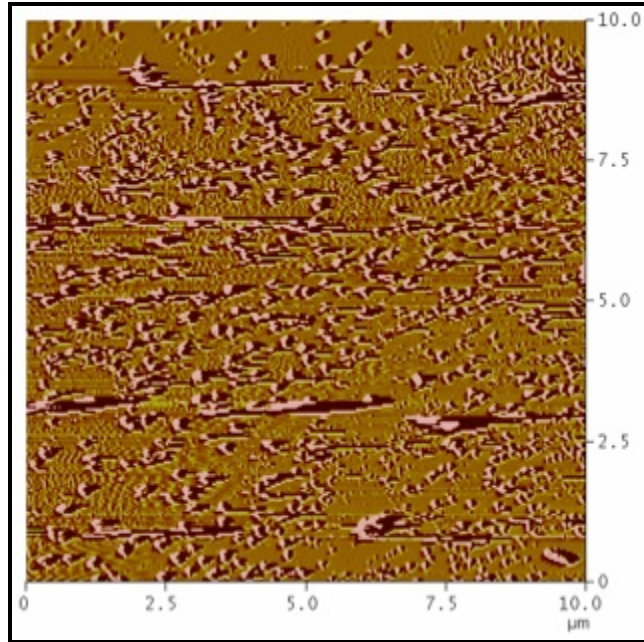


Figure 5.12. AFM image (Amplitude, tapping mode) of particles formed by dipping the ITO first in a solution of Pc787 and then in a solution of fullerene C₆₀.

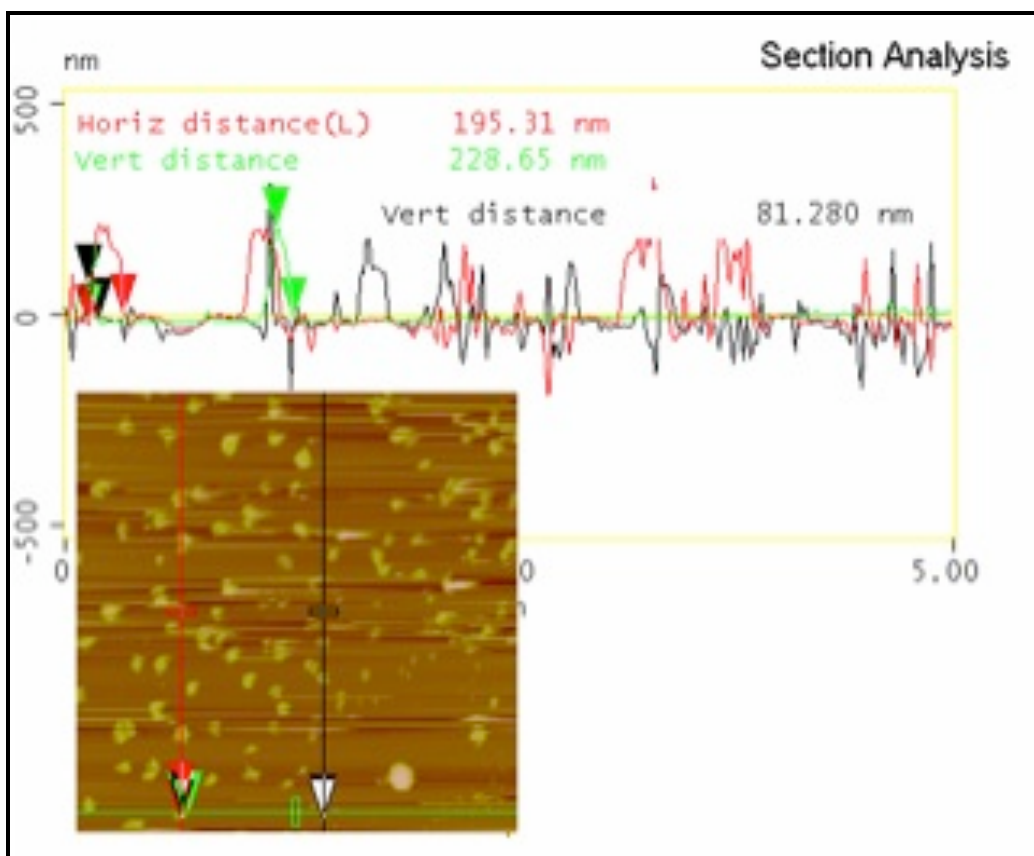


Figure 5.13. AFM height analysis of the particles described in Figure 5.12. Size and shape are not as homogeneous as when the chromophores are pre-mixed in solution.

5.4. CONCLUSION AND OUTLOOK

We have synthesized a phthalocyanine bearing 16 long alkane moieties to promote self-organization on a surface and showed how to pattern ITO electrode with a blend of this phthalocyanine and fullerene C₆₀ by using a simple electrode immersion method. The particles are highly monodispersed and changing the concentration of the chromophores in solution can control their size. More studies need to be conducted to investigate on the properties of these nanostructures.

References.

1. Sabine, L.; Angelika, B.; Nelli, S.; Frank, G.; Constanze, H.; Giusy, S.; Roxana, J.; Elisabeth, K.; Sven, S.; Alina, S.; Martin, T., Discotic Liquid Crystals: From Tailor-Made Synthesis to Plastic Electronics. *Angew. Chem. Int. Ed.* **2007**, 46, (26), 4832-4887.
2. de la Escosura, A.; Martinez-Diaz, M. V.; Barbera, J.; Torres, T., Self-Organization of Phthalocyanine and [60]Fullerene Dyads in Liquid Crystals. *J. Org. Chem.* **2008**, 73, (4), 1475-1480.
3. Schumacher, Amy L.; Sandanayaka, A. S. D.; Hill, Jonathan P.; Ariga, K.; Karr, Paul A.; Araki, Y.; Ito, O.; D'Souza, F., Supramolecular Triad and Pentad Composed of Zinc-Porphyrin(s), Oxoporphyrinogen, and Fullerene(s): Design and Electron-Transfer Studies. *Chem. Eur. J.* **2007**, 13, (16), 4628-4635.
4. Guldi, D. M.; Gouloumis, A.; Vazquez, P.; Torres, T.; Georgakilas, V.; Prato, M., Nanoscale Organization of a Phthalocyanine-Fullerene System: Remarkable Stabilization of Charges in Photoactive 1-D Nanotubules. *J. Am. Chem. Soc.* **2005**, 127, (16), 5811-5813.
5. Georgakilas, V.; Pellarini, F.; Prato, M.; Guldi, D. M.; Melle-Franco, M.; Zerbetto, F., Supramolecular self-assembled fullerene nanostructures. *PNAS* **2002**, 99, (8), 5075-5080.
6. D'Souza, F.; Ito, O., Photoinduced electron transfer in supramolecular systems of fullerenes functionalized with ligands capable of binding to zinc porphyrins and zinc phthalocyanines. *Coord. Chem. Rev.* **2005**, 249, (13-14), 1410-1422.
7. Drain, C. M.; Varotto, A.; Radivojevic, I., Self-Organized Porphyrinic Materials. *Chem. Rev.* **2009**, 109, (5), 1630-1658.
8. Boyd, P. D. W.; Reed, C. A., Fullerene-Porphyrin Constructs. In *Acc. Chem. Res.*, 2005; Vol. 38, pp 235-242.

CHAPTER 6

SYNTHESIS OF NOVEL CHROMOPHORES FOR THE PREPARATION OF ORGANIC SOLAR CELLS

6.1 SYNTHESIS OF PORPHYRIN-PHTHALOCYANINE DYADS

The aim of this synthesis was to build a molecule made of two chromophores absorbing at different wavelength to use as a light-harvesting materials for photovoltaics. The idea was to use cyanuric chloride as a scaffold to mount an aminoporphyrin, which is a blue absorber, and an aminophthalocyanine, which is a red absorber, following the synthesis described below. The choice for cyanuric chloride as the scaffold to mount the chromophores was for the easiness of replacement of the chlorines with amino-groups that can be tuned by changing the temperature, as described elsewhere.¹ We synthesized the two chromophores, **3** and **7**, following procedures described in the literature.^{2, 3}

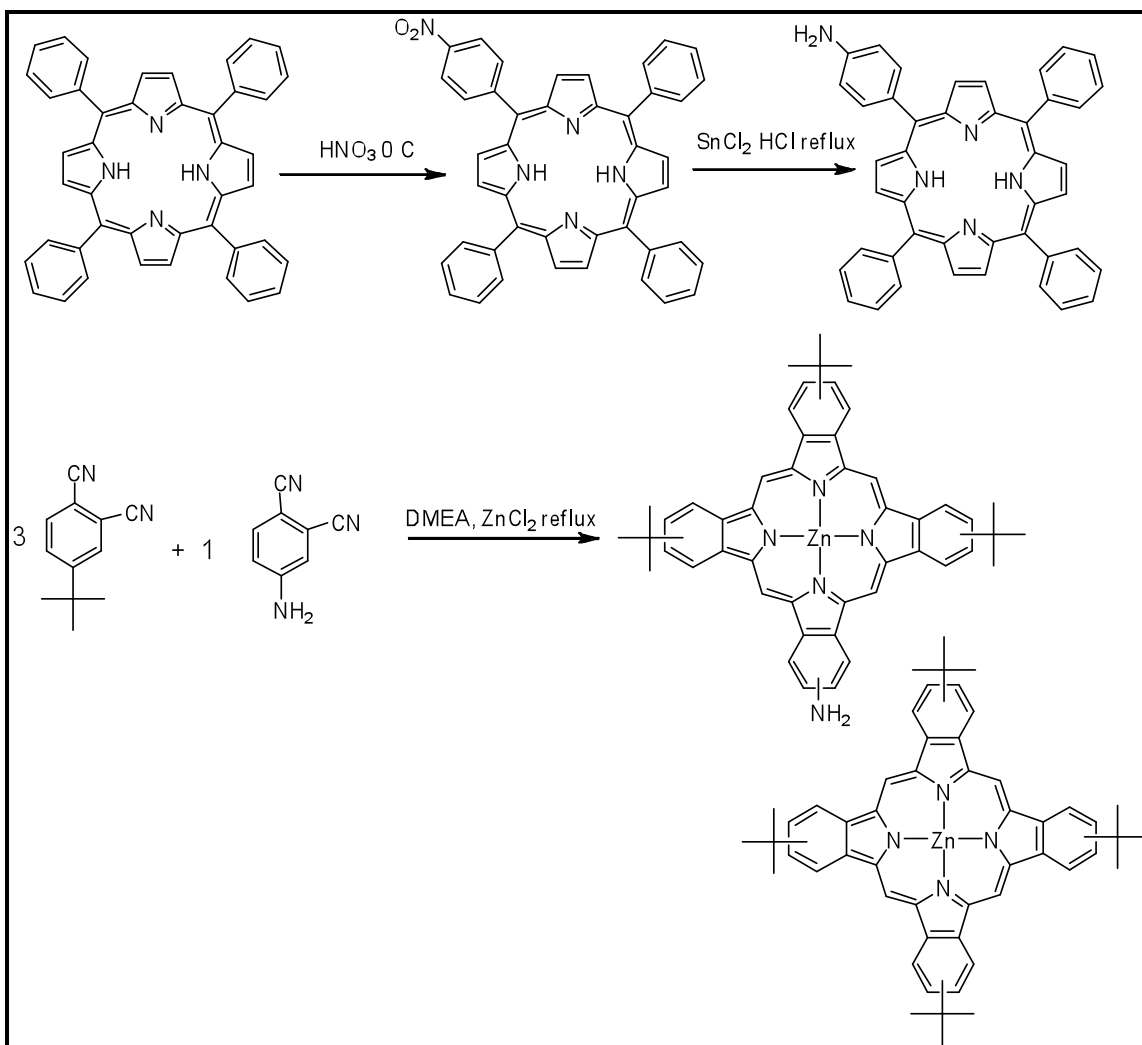


Figure 6.1. Synthetic schemes: for 5(4-aminophenyl)-10,15,20-triphenylporphyrin, which nitrates the commercially available tetraphenylporphyrin followed by the reduction to the amine;² and the preparation of the tri-*tert*-butylaminophthalocyanine from a 3:1 mixture of the malononitriles results in the statistical mixture of products which are then separated by chromatography. DMEA=dimethylethanolamine.^{3, 4}

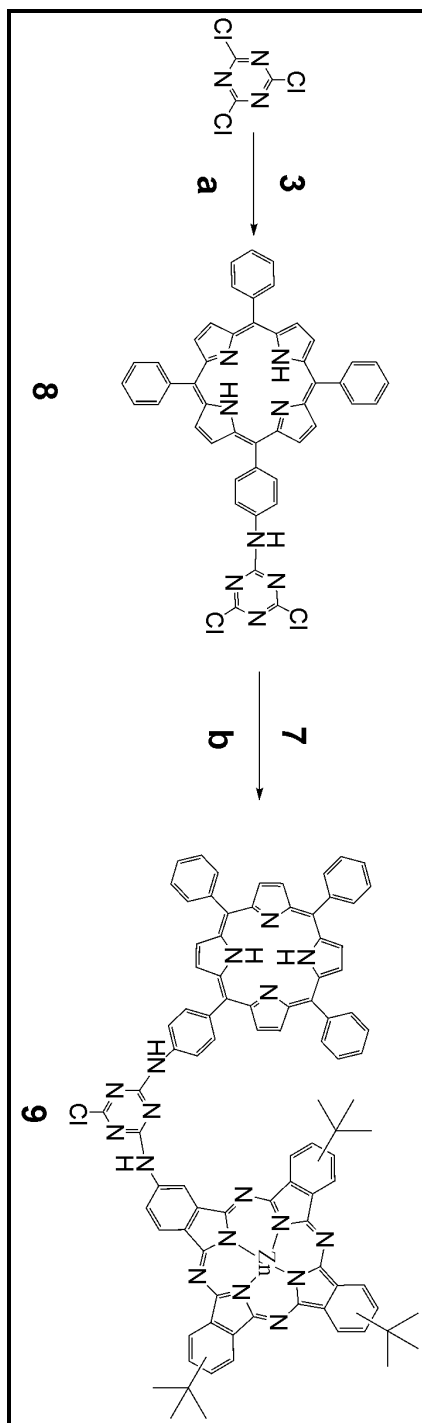


Figure 6.2. Synthesis of the porphyrin-phthalocyanine conjugate using a cyanuric chloride linker.^{2, 3, 5}

The first chloride substitution must be done at 0° C to avoid adding a second porphyrin unit, whereas addition of the second subunit, the aminophthalocyanine occurs at room temperature (ca. 25° C). The third position can be substituted with a primary amine with a long alkylic group to increase the solubility. We tried both the routes: starting with aminoporphyrin **3** followed by aminophthalocyanine **7**, or **7** followed by **3**. We witnessed that **3** is a much stronger nucleophile than **7**, likely due to the fact that the amino group is not bound to a conjugated macrocycle. Thus we were able to substitute the cyanuric chloride with **3** but we do not have indication that we formed a conjugate with **7**.

6.2 SYNTHETIC PROCEDURES.

Synthesis of compound 2

400 mg of TPP were dissolved in 15 mL CHCl_3 and cooled in an ice bath. 5 mL of HNO_3 69% were added drop wise over a 30 minute period. The solution was stirred for an additional hour. 30 mL of H_2O were poured into the solution and the pH was adjusted to 8 by adding a saturated solution of NaHCO_3 . The organic phase was extracted with CHCl_3 (3X20 mL). The solvent was removed under reduced pressure. TCL of the crude in CHCl_3 showed the starting material ($R_f = 0.88$) and TPPNO_2 ($R_f = 0.78$) in about a 40:60 ratio of starting material to nitrophenylporphyrin. The mixture was not separated but was further reacted to synthesize compound 3.

Synthesis of compound 3

250 mg of the mixture of TPP and TPPNO_2 were dissolved in 8 mL of HCl and stirred under N_2 . 260 mg of SnCl_2 were added and the solution was refluxed for 1 hr. The mixture was cooled down to room temperature, neutralized to pH 7 with NaHCO_3 and extracted with CH_2Cl_2 (3x20 mL). The solvent was removed under reduced pressure. The solid was chromatographed with silica gel using CH_2Cl_2 as eluent (R_f $\text{TPPNH}_2 = 0.3$). The overall yield of the aminophenylporphyrins was The R_f was consistent with literature values.²

Synthesis of compound 7

2-aminotri-*tert*-butylphthalocyaninatozinc(II). A mixture of 4-*tert* butylphthalonitrile (552 mg, 3 mmol) and 4-aminophthalonitrile (143 mg, 1 mmol) was refluxed in dimethylethanolamine (DMEA) 2 mL under argon for 12 h in the presence of ZnCl₂ (1 mmol). After the solution cooled, the crude product was washed by centrifugation with water/methanol (10:1) and dried under vacuum. The compound was purified by column chromatography (silica gel, toluene/methanol 25:1 v/v) to yield 7 as a green solid (76 mg, 10%). The tetra-*tert*-butylphthalocanaine is the other major macrocyclic product. Characterized by UV-Vis spectroscopy and consistent with reported values.⁴

6.3 SYNTHESIS OF Zn-Pc BEARING LONG PERFLUOROALKANE

As described earlier in this manuscript, appending long alkylated and perfluoroalkylated moieties on the periphery of small molecules help their self-organization into thin films. A characteristic of perfluoroalkanes is that, due to the larger size of fluorine with respect to hydrogen, they form very compact clusters due to increased van der Waal's forces between the chains. Fluorous films and materials are usually neither soluble in organic nor aqueous solvents. These films tend to be less permeable to moisture and more stable to oxidation; therefore, are more stable than films composed of regular alkanes. We studied the substitution of ZnPc-F₁₆ with 1H,1H,2H,2H-perfluorodecane-1-thiol. Due to the higher nucleophilicity of the perfluorothioalkane when compared to the regular thioalkane, the reaction proceeds faster and required a lower ratio of thiol/Pc to substitute the same or larger number of fluorines. When we stirred ZnPc-F₁₆ with 1H,1H,2H,2H-perfluorodecane-1-thiol (molecular ratio 1:8) at 60° C the reaction started after 20 minutes, as witnessed from the color change. After 12 hours the reaction was stopped and MALDI MS showed a mixture of ZnPc's bearing mostly 4,5 and 6 substituents. For comparison, we ran the reaction keeping all the same conditions but using dodecanethiol instead of the perfluorinated thiol and we obtained a mixtures of ZnPc's with mostly 1,2 and 3 substituents and unreacted ZnPcF₁₆, as indicated by MALDI MS.

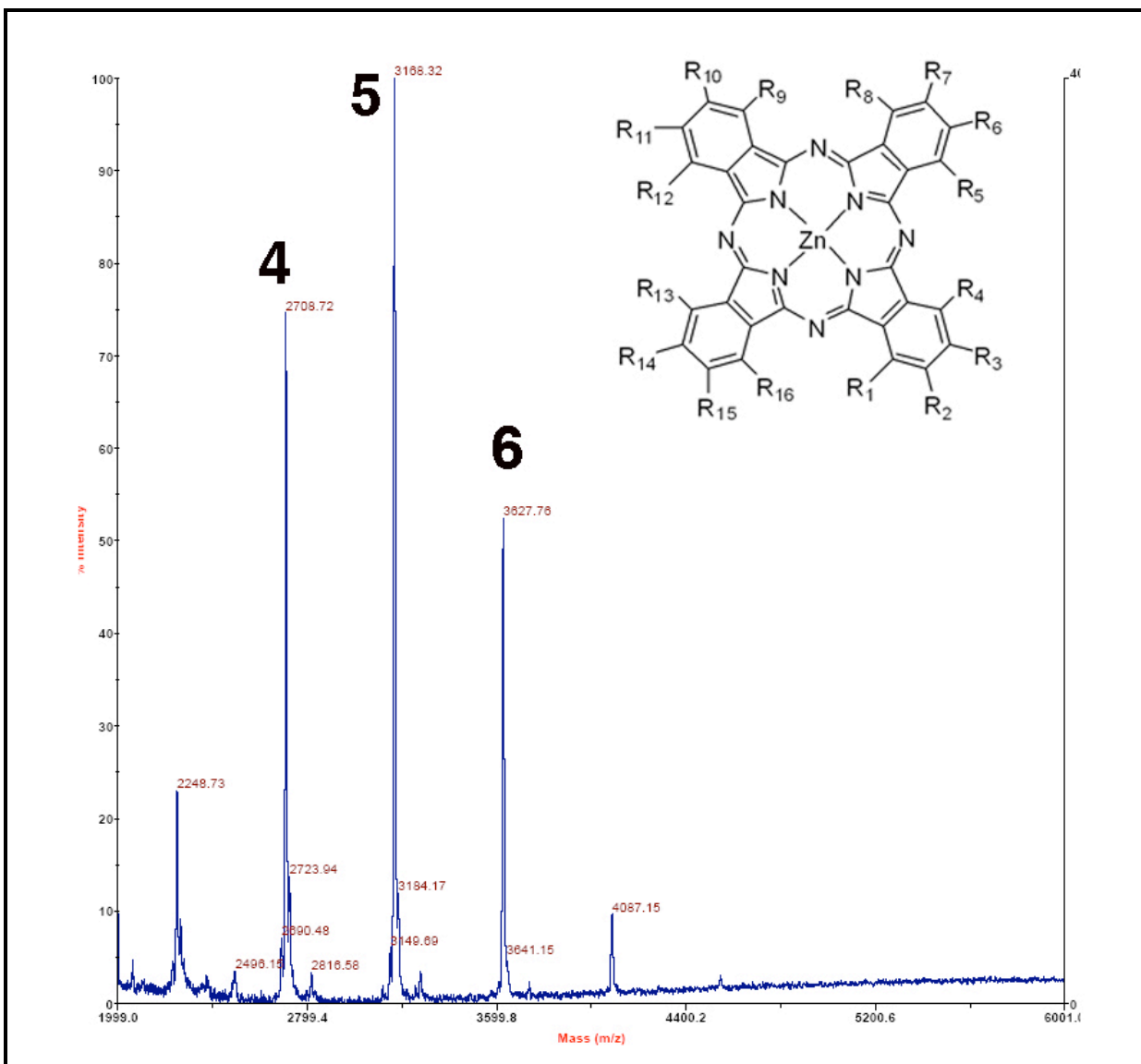


Figure 6.3. Maldi of perfluoroalkylated ZnPc. R's can be either F or $S(CH_2)_2(CF_2)_7CF_3$. Numbers indicate the # of perfluoroalkanes appended.

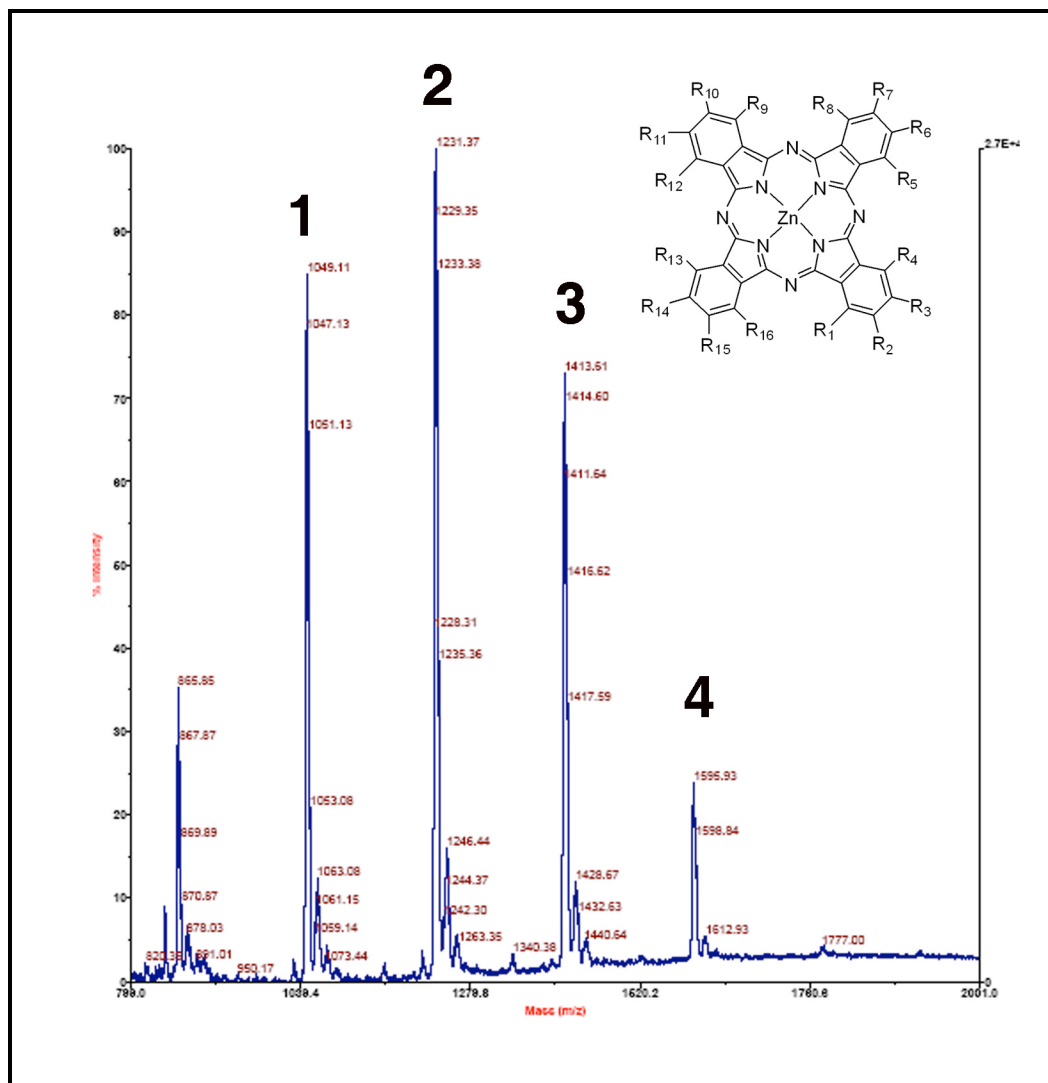


Figure 6.4. MALDI of alkylated ZnPc. R's can be either F or S(CH₂)₁₁CH₃. Numbers indicate the # of alkanes appended.

References

1. Blotny, G., Recent applications of 2,4,6-trichloro-1,3,5-triazine and its derivatives in organic synthesis. *Tetrahedron* **2006**, 62, 9507–9522.
2. Kruper, W. J.; Chamberlin, T. A.; Kochanny, M., Regiospecific aryl nitration of meso-substituted tetraarylporphyrins: a simple route to bifunctional porphyrins. *J. Org. Chem.* **2002**, 54, (11), 2753-2756.
3. Soares, A. R. M.; Martinez-Diaz, M. V.; Bruckner, A.; Pereira, A. M. V. M.; Tome, J. P. C.; Alonso, C. M. A.; Faustino, M. A. F.; Neves, M. G. P. M. S.; Tome, A. C.; Silva, A. M. S.; Cavaleiro, J. A. S.; Torres, T.; Guldi, D. M., Synthesis of Novel N-Linked Porphyrin-Phthalocyanine Dyads. *Org. Lett.* **2007**, 9, (8), 1557-1560.
4. Gonzalez-Cabello, A.; Vazquez, P.; Torres, T.; Guldi, D. M., Highly Coupled Dyads Based on Phthalocyanine-Ruthenium(II) Tris(bipyridine) Complexes. Synthesis and Photoinduced Processes. *J. Org. Chem.* **2003**, 68, (22), 8635-8642.
5. Carofiglio, T.; Varotto, A.; Tonellato, U., One-Pot Synthesis of Cyanuric Acid-Bridged Porphyrin-Porphyrin Dyads. *J. Org. Chem.* **2004**, 69, (23), 8121-8124.

Bibliography

Chapter 1.

1. Kadish, K.; Smith, K. M.; Guillard, R., *The Porphyrin Handbook*. Academic Press: New York, 2000, 2003; Vol. 1-20.
2. Kimura, M.; Shirai, H., *The Porphyrin Handbook*. In Kadish, K. M.; Smith, K. M.; Guillard, R., Eds. Academic Press: New York, 2003; Vol. 19, pp 151-174.
3. Dolphin, D., *The Porphyrins*. Academic Press: New York, 1978.
4. Rio, Y.; Rodríguez-Morgade, M. S.; Torres, T., Modulating the electronic properties of porphyrinoids: a voyage from the violet to the infrared regions of the electromagnetic spectrum. *Org. Biomol. Chem.* **2008**, 6, 1877-1894.
5. Ceulemans, A.; Oldenhof, W.; Gorller-Walrand, C.; Vanquickenborne, L. G., Gouterman's "four-orbital" model and the MCD spectra of high-symmetry metalloporphyrins. *J. Am. Chem. Soc.* **2002**, 124, (6), 1155-1163.
6. Alstrum-Acevedo, J. H.; Brennaman, M. K.; Meyer, T. J., Chemical Approaches to Artificial Photosynthesis. 2 *Inorg. Chem.* **2005**, 44, 6802-6827.
7. Wasielewski, M. R., Energy, Charge, and Spin Transport in Molecules and Self-Assembled Nanostructures Inspired by Photosynthesis. *J. Org. Chem.* **2006**, 71, (14), 5051-5066.
8. Cogdell, R. J.; Isaacs, N. W.; Howard, T. D.; McLusky, K.; Fraser, N. J.; Prince, S. M., How Photosynthetic Bacteria Harvest Solar Energy. *J. Bacteriol.* **1999**, 181, 3869–3879.

9. Law, C. J.; Roszak, A. W.; Southall, J.; Gardiner, A.; Isaacs, N. W.; Cogdell, R. J., The structure and function of bacterial light harvesting complex. *Mol. Membr. Biol.* **2004**, 21, 183-191.
10. Zuber, H.; Brunisholz, R. A., *Chlorophylls*. CRC: Boca Raton: 1991; p 627-704.
11. Zuber, H.; Cogdell, R. J., *An oxygenic photosynthetic Bacteria*. Kluwer Academic: Boston, 1995; p 315-348.
12. Byrn, M. P.; Curtis, C. J.; Hsiou, Y.; Khan, S. I.; Sawin, P. A.; Tendick, S. K.; Terzis, A.; Strouse, C. E., Porphyrin sponges: conservative of host structure in over 200 porphyrin-based lattice clathrates *J. Am. Chem. Soc.* **1993**, 115, (21), 9480-9497.
13. Shmilovits, M.; Vinodu, M.; Goldberg, I., Porphyrin clathrates. Crystal structures of two unexpected products obtained by solvothermal reactions of Pt-tetra(4-carboxyphenyl)porphyrin with copper acetate. *J. Inclu. Phenom. Macro. Chem.* **2004**, 48, (3-4), 165-171.
14. Vinodu, M.; Goldberg, I., Complexes of hexamethylenetetramine with zinc-tetraarylporphyrins, and their assembly modes in crystals as clathrates and hydrogen-bonding network polymers. *New J. Chem.* **2004**, 28, (10), 1250-1254.
15. Abrahams, B. F.; Hoskins, B. F.; Michail, D. M.; Robson, R., Assembly of porphyrin building blocks into network structures with large channels. *Nature* **1994**, 369, 727-729.

16. Fleischer, E. B.; Shachter, A. M., Coordination oligomers and a coordination polymer of zinc tetraarylporphyrins. *Inorg. Chem.* **1991**, 30, 3763-3769.
17. Goldberg, I., Crystal engineering of porphyrin framework solids. *Chem. Commun.* **2005**, (10), 1243-1254.
18. Goldberg, I., Crystal engineering of nanoporous architectures and chiral porphyrin assemblies. *CrystEngComm* **2008**, 10, 637-645.
19. Drain, C. M.; Christensen, B.; Mauzerall, D. C., Photogating of ionic currents across a lipid bilayer. *Proc. Natl. Acad. Sci. USA* **1989**, 86, 6959-6962.
20. Drain, C. M.; Mauzerall, D. C., Photogating of ionic currents across lipid bilayers: hydrophobic ion conductance by an ion chain mechanism. *Biophys. J.* **1992**, 63, 1556-1563.
21. Drain, C. M.; Mauzerall, D. C., Photogating of ionic currents across lipid bilayers: electrostatics of ions and dipoles inside the membrane. *Biophys. J.* **1992**, 63, 1544-1555.
22. Drain, C. M.; Russel, K. C.; Lehn, J.-M., Self-assembly of a multi-porphyrin supramolecular macrocycle by hydrogen bond molecular recognition. *Chem. Commun.* **1996**, 337-338.
23. Drain, C. M.; Batteas, J. D.; Flynn, G. W.; Milic, T.; Chi, N.; Yablon, D. G.; Sommers, H., Designing supramolecular porphyrin arrays that self-organize into nanoscale optical and magnetic materials. *Proc. Natl. Acad. Sci. U S A* **2002**, 99 Suppl 2, 6498-6502.

24. Samaroo, D.; Soll, C. E.; Todaro, L. J.; Drain, C. M., Efficient Microwave-Assisted Synthesis of Amine-Substituted Tetrakis(pentafluorophenyl)porphyrin. *Org. Lett.* **2006**, *8*, 4985-4988.
25. Drain, C. M.; Lehn, J., M., Self-assembly of square multiporphyrin arrays by metal ion coordination. *Chem. Commun.* **1994**, 2313-2315 (correction 1995, p503).
26. Drain, C. M.; Nifiatis, F.; Vasenko, A.; Batteas, J. D., Porphyrin tessellation by design: Metal-mediated self-assembly of large arrays and tapes *Angew. Chem.* **1998**, *37*, 2344-2347.
27. Milic, T.; Garno, J. C.; Batteas, J. D.; Smeureanu, G.; Drain, C. M., Self-organization of self-assembled tetrameric porphyrin arrays on surfaces. *Langmuir* **2004**, *20*, (10), 3974-3983.
28. Drain, C. M., Self-organization of self-assembled photonic materials into functional devices: Photo-switched conductors. *Proc. Natl. Acad. Sci. USA* **2002**, *99*, 5178-5182.
29. Lipstman, S.; Muniappan, S.; Golberg, I., Supramolecular Reactivity of Porphyrins with Mixed Iodophenyl and Pyridyl mesa-Substituents. *Cryst. Growth Des.* **2008**, *8*, 1682-1688.
30. Stang, P. J.; Olenyuk, B., Self-Assembly, Symmetry, and Molecular Architecture: Coordination as the Motif in the Rational Design of Supramolecular Metallacyclic Polygons and Polyhedra. *Acc. Chem. Res.* **1997**, *30*, (12), 502-518.
31. van Hameren, R.; Schön, P.; van Buul, A. M.; Hoogboom, J.; Lazarenko, S. V.; Gerritsen, J. W.; Engelkamp, H.; Christianen, P. C.; Heus, H. A.; Maan, J.

- C.; Rasing, T.; Speller, S.; Rowan, A. E.; Elemans, J. A.; Nolte, R. J., Macroscopic hierarchical surface patterning of porphyrin trimers via self-assembly and dewetting. *Science* **2006**, 314, (5804), 1433-1436.
32. Elemans, J. A. A. W.; Van Hameren, R.; Nolte, R. J. M.; Rowan, A. E., Molecular materials by self-assembly of porphyrins, phthalocyanines, and perylenes. *Adv. Mater.* **2006**, 18, (10), 1251-1266.
33. Drain, C. M.; Chen., X., Self-Assembled Porphyrinic Nanoarchitectures. In *Encyclopedia of Nanoscience & Nanotechnology*, Nalwa, H. S., Ed. American Scientific Press: New York, 2004; Vol. 9, pp 593-616.
34. Drain, C. M.; Batteas, J. D.; Smeureanu, G.; Patel, S., Self-Assembled Porphyrinic Materials on Surfaces. In *Encyclopedia of Nanoscience and Nanotechnology*, Marcel Dekker: New York, 2004; pp 3481-3502.
35. Linares, M.; Iavicoli, P.; Psychogyiopolou, K.; Beljonne, D.; Feyter, S. D.; Amabilino, D. B.; Lazzaroni, R., Chiral Expression at the Solid-Liquid Interface: A Joint Experimental and Theoretical Study of the Self-Assembly of Chiral Porphyrins on Graphite. *Langmuir* **2008**, 24, (17), 9566–9574.
36. Drain, C. M.; Bazzan, G.; Milic, T.; Vinodu, M.; Goeltz, J. C., Formation and Applications of Stable 10 nm to 500 nm Supramolecular Porphyrinic Materials. *Isr. J. Chem.* **2005**, 45, 255–269.
37. Izquierdo, A.; Ono, S. S.; Voegel, J.-C.; Schaaf, P.; Decher, G., Dipping versus Spraying: Exploring the Deposition Conditions for Speeding Up Layer-by-Layer Assembly. *Langmuir* **2005**, 21, 7558-7567.

38. Decher, G.; B.Schlenoff, J., *Multilayer thin films*. Wiley-VCH, Weinheim: 2003.
39. Drain, C. M.; Goldberg, I.; Sylvain, I.; Falber, A., Synthesis and applications of supramolecular porphyrinic materials. *Topics in Current Chemistry* **2005**, 245, 55-88.
40. Jiang, L.; Changa, Q.; Ouyanga, Q.; Liub, H.; Wanga, Y.; Zhanga, X.; Songa, Y.; Lib, Y., Fabrication and nonlinear optical properties of an ultrathin film with acceptor–donor periodically overlapping structure *Chem. Phys.* **2006**, 324, 556-562.
41. Xiang, Y.; Wei, X.-W.; Zhang, X.-M.; Wang, H.-L.; Wei, X.-L.; Hu, J.-P.; Yin, G.; Xu, Z., Synthesis of new pyridinofullerene ligands capable of forming complexes with zinc tetraphenyl porphyrin. *Inorg. Chem. Commun.* **2006**, 9, (5), 452-455.
42. Zhang, B.; Mu, J.; Li, X., Linear assemblies of aged CdS particles and cationic porphyrin in multilayer films. *Appl. Surf. Sci.* **2006**, 252, 4990–4994.
43. Zhang, S.; Echegoyen, L., Supramolecular immobilization of fullerenes on gold surfaces: receptors based on calix[n]arenes, cyclotrimeratrylene (CTV) and porphyrins. *C. R. Chimie* **2006**, 9, (7-8), 1031-1037.
44. Zhao, S.; Zhang, K.; Yang, M.; Sun, Y.; Sun, C., Fabrication of photosensitive self-assembled multilayer films based on porphyrin and diazoresin via H-bonding. *Mater. Lett.* **2006**, 60, (19), 2406.

45. Splan, K. E.; Hupp, J. T., Permeable Nonaggregating Porphyrin Thin Films That Display Enhanced Photophysical Properties. *Langmuir* **2004**, *20*, 10560-10566.
46. Splan, K. E.; Massari, A. M.; Hupp, J. T., A porous multilayer dye-based photoelectrochemical cell that unexpectedly runs in reverse. *J. Phys. Chem. B* **2004**, *108*, 4111-4115.
47. Splan, K. E.; Stern, C. L.; Hupp, J. T., Two coordinately linked supramolecular assemblies constructed from highly electron deficient porphyrins. *Inorg. Chim. Acta* **2004**, *357*, (13), 4005-4014.
48. Badjic, J. D.; Nelson, A.; Cantrill, S. J.; Turnbull, W. B.; Stoddart, J. F., Multivalency and cooperativity in supramolecular chemistry. *Acc. Chem. Res.* **2005**, *38*, (9), 723-732.
49. Balaban, T. S.; Linke-Schaetzel, M.; Bhise, A. D.; Vanthuyne, N.; Roussel, C.; Anson, C. E.; Buth, G.; Eichhöfer, A.; Foster, K.; Garab, G.; Gliemann, H.; Goddard, R.; Javorfi, T.; Powell, A. K.; Rösner, H.; Schimmel, T., Structural characterization of artificial self-assembling porphyrins that mimic the natural chlorosomal Bacteriochlorophylls c, d, and e. *Chem. Eur. J.* **2005**, *11*, 2267-2275.
50. Ahn, S.; Hupp, J. T., Assembles of porphyrin layers on ITO and deposition of polyaniline on porphyrin layered ITO. *Bull. Kor. Chem. Soc.* **2006**, *27*, (9).
51. Jiang, L.; Lu, F.; Li, H.; Chang, Q.; Li, Y.; Liu, H.; Wang, S.; Song, Y.; Cui, G.; Wang, N.; He, X.; Zhu, D., Third-Order Nonlinear Optical Properties of an

Ultrathin Film Containing a Porphyrin Derivative. *J. Phys. Chem. B* **2005**, 109, 6311-6315.

52. Guldi, D. M., Fullerene–porphyrin architectures; photosynthetic antenna and reaction center models. *Chem. Soc. Rev.* **2002**, 31, 22-36.

53. Hasobe, T.; Fukuzumi, S.; Hattori, S.; Kamat, P. V., Shape- and Functionality-Controlled Organization of TiO₂-Porphyrin-C₆₀ Assemblies for Improved Performance of Photochemical Solar Cells. *Chem. As. J.* **2007**, 2, (2), 265-272.

54. Campbell, W. M.; Burrell, A. K.; Officer, D. L.; Jolley, K. W., Porphyrins as light harvesters in the dye-sensitised TiO₂ solar cell. *Coord. Chem. Rev.* **2004**, 248, 1363–1379.

55. Hasobe, T.; Saito, K.; Kamat, P. V.; Troiani, V.; Qiu, H.; Solladie, N.; Kim, K. S.; Park, J. K.; Kim, D.; D'Souza, F.; Fukuzumi, S., Organic solar cells. Supramolecular composites of porphyrins and fullerenes organized by polypeptide structures as light harvesters. *J. Mater. Chem.* **2007**, 17, 4160–4170.

56. Bonifazi, D.; Kiebele, A.; Stöhr, M.; Cheng, F.; Jung, T.; Diederich, F.; Spillmann, H., Supramolecular Nanostructuring of Silver Surfaces via Self-Assembly of [60]Fullerene and Porphyrin Modules. *Adv. Func. Mater.* **2007**, 17, (7), 1051-1062.

57. Tong, L. H.; Wietor, J.-L.; Clegg, W.; Raithby, P. R.; Pascu, S. I.; Sanders, J. K. M., Supramolecular Assemblies of Tripodal Porphyrin Hosts and C₆₀. *Chem. Eur. J.* **2008**, 14, (10), 3035-3044.

58. Umeyama, T.; Imahori, H., Self-Organization of Porphyrins and Fullerenes for Molecular Photoelectrochemical Devices. *Photosyn. Res.* **2006**, 87, 63-71.
59. Imahori, H.; Yamada, H.; Ozawa, S.; Ushidab, K.; Sakata, Y., Synthesis and photoelectrochemical properties of a self-assembled monolayer of a ferrocene–porphyrin–fullerene triad on a gold electrode. *Chem. Commun.* **1999**, 1165-1166.
60. Yamada, H.; Imahori, H.; Nishimura, Y.; Yamazaki, I.; Ahn, T. K.; Kim, S. K.; Kim, D.; Fukuzumi, S., Photovoltaic Properties of Self-Assembled Monolayers of Porphyrins and Porphyrin-Fullerene Dyads on ITO and Gold Surfaces. *J. Am. Chem. Soc.* **2003**, 125, (30), 9129-9139.
61. Wang, N.; Li, Y.; Lu, F.; Liu, Y.; He, X.; Jiang, L.; Zhuang, J.; Li, X.; Li, Y.; Wang, S.; Liu, H.; Zhu, D., Fabrication of novel conjugated polymer nanostructure: Porphyrins and fullerenes conjugately linked to the polyacetylene backbone as pendant groups. *J. Poly. Sci.* **2005**, 43, (13), 2851-2861.
62. Akiyama, T.; Matsuoka, K.-i.; Arakawa, T.; Kakutani, K.; Miyazaki, A.; Yamada, S., Facile Fabrication and Photoelectrochemical Properties of Porphyrin–Fullerene Assemblies by Self-Assembly and Surface Sol–Gel Processes. *Jap. J. Appl. Phys.* **2006**, 45, (4b), 3758.
63. Nakagawa, H.; Ogawa, K.; Satake, A.; Kobuke, Y., A supramolecular photosynthetic triad of slipped cofacial porphyrin dimer, ferrocene, and fullerene. *Chem. Commun.* **2006**, 14, 1560-1562.
64. Isosomppi, M.; Tkachenko, N. V.; Efimov, A.; Kaunisto, K.; Hosomizu, K.; Imahorib, H.; Lemmetyinen, H., Photoinduced electron transfer in multilayer self-

assembled structures of porphyrins and porphyrin–fullerene dyads on ITO. *J. Mater. Chem.* **2005**, 15, 4546-4554.

65. Chukharev, V.; Vuorinen, T.; Efimov, A.; Tkachenko, N. V.; Kimura, M.; Fukuzumi, S.; Imahori, H.; Lemmetyinen, H., Photoinduced Electron Transfer in Self-Assembled Monolayers of Porphyrin-Fullerene Dyads on ITO. *Langmuir* **2005**, 21, (14), 6385-6391.

66. Schuster, D. I.; Li, K.; Guldi, D. M.; Palkar, A.; Echegoyen, L.; Stanisky, C.; Cross, R. J.; Niemi, M.; Tkachenko, N. V.; Lemmetyinen, H., Azobenzene-Linked Porphyrin-Fullerene Dyads. *J. Am. Chem. Soc.* **2007**, 129, (51), 15973-15982.

67. Fazio, M. A.; Lee, O. P.; Schuster, D. I., First Triazole-Linked Porphyrin-Fullerene Dyads. *Org. Lett.* **2008**, 10, (21), 4979-4982.

68. Hayes, R. T.; Wasielewski, M. R.; Gosztola, D., Ultrafast Photoswitched Charge Transmission through the Bridge Molecule in a Donor-Bridge-Acceptor System. *J. Am. Chem. Soc.* **2000**, 122, (23), 5563-5567.

69. Kiebele, A.; Bonifazi, D.; Cheng, F.; Stohr, M.; Diederich, F.; Jung, T.; Spillmann, H., Adsorption and Dynamics of Long-Range Interacting Fullerenes in a Flexible, Two-Dimensional, Nanoporous Porphyrin Network. *Chem.Phys.Chem.* **2006**, 7, 1462-1470.

70. Conoci, S.; Guldi, D. M.; Nardis, S.; Paolesse, R.; Kordatos, K.; Prato, M.; Ricciardi, G.; Vicente, M. G. H.; Zilbermann, I.; Valli, L., Langmuir-Schäfer Transfer of Fullerenes and Porphyrins: Formation, Deposition, and Application of Versatile Films. *Chem. Eur. J.* **2004**, 10, (24), 6523-6530.

71. Zilbermann, I., Anderson, G.A., Guldi, D.M., Yamada, H., Imahori, H. and Fukuzumi, S., Layer-by-layer assembly of porphyrin-fullerene dyads. *J. Porph. Phth.* **2003**, 7, 357-364.
72. Kaunisto, K.; Vuorinen, T.; Vahasalo, H.; Chukharev, V.; Tkachenko, N. V.; Efimov, A.; Tolkki, A.; Lehtivuori, H.; Lemmetyinen, H., Photoinduced Electron Transfer and Photocurrent in Multicomponent Organic Molecular Films Containing Oriented Porphyrin-Fullerene Dyad. *J. Phys. Chem. C* **2008**, 112, (27), 10256-10265.
73. Boyd, P. D. W.; Reed, C. A., Fullerene-Porphyrin Constructs. *Acc. Chem. Res.* **2005**, 38, (4), 235-242.
74. Boyd, P. D. W.; Hodgson, M. C.; Rickard, C. E. F.; Oliver, A. G.; Chaker, L.; Brothers, P. J.; Bolskar, R. D.; Tham, F. S.; Reed, C. A., Selective Supramolecular Porphyrin/Fullerene Interactions. *J. Am. Chem. Soc.* **1999**, 121, (45), 10487-10495.
75. Hosseini, A.; Hodgson, M. C.; Tham, F. S.; Reed, C. A.; Boyd, P. D. W., Tapes, Sheets, and Prisms. Identification of the Weak C-F Interactions that Steer Fullerene-Porphyrin Cocrystallization. *Cryst. Growth Des.* **2006**, 6, (2), 397-403.
76. Olmstead, M. M.; Nurco, D. J., Fluorinated Tetraphenylporphyrins as Cocrystallizing Agents for C₆₀ and C₇₀. *Cryst. Growth Des.* **2006**, 6, (1), 109-113.
77. Sun, D.; Tham, F. S.; Reed, C. A.; Chaker, L.; Burgess, M.; Boyd, P. D. W., Porphyrin-Fullerene Host-Guest Chemistry. *J. Am. Chem. Soc.* **2000**, 122, 10704-10705.

78. Bonifazi, D.; Enger, O.; Diederich, a. F., Supramolecular [60]fullerene chemistry on surfaces. *Chem. Soc. Rev.* **2007**, 36, 390-414.
79. Imahori, H.; Fukuzumi, a. S., Porphyrin- and Fullerene-Based Molecular Photovoltaic Devices. *Adv. Funct. Mater.* **2004**, 14, (6), 525-536.
80. Sgobba, V.; Giancane, G.; Conoci, S.; Casilli, S.; Ricciardi, G.; Guldi, D. M.; Prato, M.; Valli, L., Growth and Characterization of Films Containing Fullerenes and Water Soluble Porphyrins for Solar Energy Conversion Applications. *J. Am. Chem. Soc.* **2007**, 129, (11), 3148-3156.
81. Grätzel, M., Dye-sensitized solar cells. *J. Photochem. Photobiol. C: Photochem. Rev.* **2003**, 4, 145-153.
82. Nobukuni, H.; Shimazaki, Y.; Tani, F.; Naruta, Y., A Nanotube of Cyclic Porphyrin Dimers Connected by Nonclassical Hydrogen Bonds and Its Inclusion of C₆₀ in a Linear Arrangement. *Angew. Chem., Int. Ed.* **2007**, 46, (47), 8975-8978.
83. Yamaguchi, T.; Ishii, N.; Tashiro, K.; Aida, T., Supramolecular Peapods Composed of a Metalloporphyrin Nanotube and Fullerenes. *J. Am. Chem. Soc.* **2003**, 125, (46), 13934-13935.
84. Shirakawa, M.; Fujita, N.; Shimakoshi, H.; Hisaeda, Y.; Shinkai, S., Molecular Programming of Organogelators Which Can Accept [60]Fullerene by Encapsulation. *Tetrahedron* **2006**, 62, (9), 2016-2024.
85. Dudi, M.; Lhoták, P.; Stibor, I.; Petíková, H.; Lang, K., (Thia)calix[4]arene-porphyrin conjugates: novel receptors for fullerene complexation with C₇₀ over C₆₀ selectivity. *New J. Chem.* **2004**, 28, 85-90.

86. Tashiro, K.; Aida, T., Metalloporphyrin hosts for supramolecular chemistry of fullerenes. *Chem. Soc. Rev.* **2007**, 36, (2), 189-197.
87. Imahori, H.; Fujimoto, A.; Kang, S.; Hotta, H.; Yoshida, K.; Umeyama, T.; Matano, Y.; Isoda, S.; Isosomppi, M.; Tkachenko, N. V.; Lemmetyinen, H., Host-Guest Interactions in the Supramolecular Incorporation of Fullerenes into Tailored Holes on Porphyrin-Modified Gold Nanoparticles in Molecular Photovoltaics. *Chem. Eur. J.* **2005**, 11, (24), 7265-7275.
88. Marois, J. S.; Cantin, K.; Desmarais, A.; Morin, J. F., [3]Rotaxane-Porphyrin Conjugate as a Novel Supramolecular Host for Fullerenes. *Org. Lett.* **2008**, 10, (1), 33-36.
89. Taylor, S. K.; Jameson, G. B.; Boyd, P. D. W., A New Polymeric Framework Formed by the Self Assembly of 5,10,15,20-tetra(3-pyridyl)porphyrin, Hg₂ And C₆₀. *Supramol. Chem.* **2005**, 17, 543-546.
90. Bonifazi, D.; Spillmann, H.; Kiebele, A.; Wild, M. d.; Seiler, P.; FuyongCheng; Guntherodt, H.-J.; Jung, T.; Diederich, F., Supramolecular Patterned Surfaces Driven by Cooperative Assembly of C[60] and Porphyrins on Metal Substrates. *Angew. Chem., Int. Ed.* **2004**, 43, 4759-4763.
91. Hasobe, T.; Imahori, H.; Kamat, P. V.; Fukuzumi, S., Quaternary self-organization of porphyrin and fullerene units by clusterization with gold nanoparticles on SnO₂ electrodes for organic solar cells. *J. Am. Chem. Soc.* **2003**, 125, 14962-14963.
92. Trabolsi, A.; Elhabiri, M.; Urbani, M.; Delgado de la Cruz, J. L.; Ajamaa, F.; Solladié, N.; Albrecht-Gary, A. M.; Nierengarten, J. F., Supramolecular click

chemistry for the self-assembly of a stable Zn(II)-porphyrin-C₆₀ conjugate. *Chem. Commun.* **2005**, 46, 5736-5738.

93. Zhang, S.; Echegoyen, L., Supramolecular Incorporation of Fullerenes on Gold Surfaces: Comparison of C₆₀ Incorporation by Self-Assembled Monolayers of Different Calix[n]arene (n = 4, 6, 8) Derivatives. *J. Org. Chem.* **2005**, 70, (24), 9874-9881.

94. Sánchez, L.; Sierra, M.; Martín, N.; Myles, A. J.; Dale, T. J.; Jr, J. R.; Seitz, W.; Guldi, D. M., Exceptionally Strong Electronic Communication through Hydrogen Bonds in Porphyrin-C₆₀Pairs. *Angew. Chem., Int. Ed.* **2006**, 45, (28), 4637-4641.

95. Schmittel, M.; He, B.; Mal, P., Supramolecular Multicomponent Self-Assembly of Shape-Adaptive Nanoprisms: Wrapping up C₆₀ with Three Porphyrin Units. *Org. Lett.* **2008**, 10, (12), 2513-2516.

96. Hasobe, T.; Sandanayaka, A. S. D.; Wada, T.; Araki, Y., Fullerene-encapsulated porphyrin hexagonal nanorods. An anisotropic donor-acceptor composite for efficient photoinduced electron transfer and light energy conversion. *Chem. Commun.* **2008**, 3372-3374.

97. Furutsu, D.; Satake, A.; Kobuke, Y., A giant supramolecular light-harvesting antenna-acceptor composite. *Inorg. Chem.* **2005**, 44, (13), 4460-4462.

98. Ohmura, T.; Usuki, A.; Fukumori, K.; Ohta, T.; Ito, M.; Tatsumi, K., New porphyrin-based metal-organic framework with high porosity: 2-D infinite 22.2-A square-grid coordination network. *Inorg. Chem.* **2006**, 45, (20), 7988-7990.

99. Drain, C. M.; Varotto, A.; Radivojevic, I., Self-Organized Porphyrinic Materials. *Chem. Rev.* **2009**, 109, (5), 1630–1658.
100. Marois, J.-S.; Morin, J.-F., Synthesis and Surface Self-Assembly of [3]Rotaxane-Porphyrin Conjugates: Toward the Development of a Supramolecular Surface Tweezer for C60. *Langmuir* **2008**, 24, (19), 10865-10873.
101. Sakakibara, K.; Nakatsubo, F., Effect of Fullerene on Photocurrent Performance of 6-O-Porphyrin-2,3-di-O-stearoylcellulose Langmuir-Blodgett Films. *Macromol. Chem. Phys.* **2008**, 209, (12), 1274-1281.
102. Varotto, A.; Todaro, L.; Vinodu, M.; Koehne, J.; Liu, G.-y.; Drain, C. M., Self-organization of a new fluorous porphyrin and C60 films on indium-tin-oxide electrode. *Chem. Commun.* **2008**, 4921 - 4923.
103. Regev, A.; Galili, T.; Levanon, H.; Schuster, D. I., Triplet Topology of Self-Assembled Zinc Porphyrin-Pyridylfullerene Complex. *J. Phys. Chem. A* **2006**, 110, (27), 8593-8598.
104. Sandanayaka, A. S.; Araki, Y.; Ito, O.; Chitta, R.; Gadde, S.; D'Souza, F., Electron transfer switching in supramolecular porphyrin-fullerene conjugates held by alkylammonium cation-crown ether binding. *Chem. Commun.* **2006**, 4327-4329.
105. D'Souza, F.; Chitta, R.; Gadde, S.; Rogers, Lisa M.; Karr, Paul A.; Zandler, Melvin E.; Sandanayaka, Atula S. D.; Araki, Y.; Ito, O., Photosynthetic Reaction Center Mimicry of a 'Special Pair' Dimer Linked to Electron Acceptors by a

Supramolecular Approach: Self-Assembled Cofacial Zinc Porphyrin Dimer Complexed with Fullerene(s). *Chem. Eur. J.* **2007**, 13, (3), 916-922.

106. D'Souza, F.; Chitta, R.; Gadde, S.; Zandler, M. E.; McCarty, A. L.; Sandanayaka, A. S. D.; Araki, Y.; Ito, O., Effect of Axial Ligation or pi-pi-Type Interactions on Photochemical Charge Stabilization in 'Two-Point' Bound Supramolecular Porphyrin-Fullerene Conjugates. *Chem. Eur. J.* **2005**, 11, (15), 4416-4428.

107. D'Souza, F.; E.El-Khouly, M.; Gadde, S.; Zandler, M. E.; McCarty, A. L.; Araki, Y.; Itoh, O., Supramolecular Triads Bearing Porphyrin and Fullerene via 'Two-Point' Binding Involving Coordination and Hydrogen Bonding. *Tetrahedron* **2006**, 62, (9), 1967-1978.

108. D'Souza, F.; Chitta, R.; Gadde, S.; McCarty, A. L.; Karr, P. A.; Zandler, M. E.; Sandanayaka, A. S. D.; Araki, Y.; Ito, O., Design, Syntheses, and Studies of Supramolecular Porphyrin-Fullerene Conjugates, Using Bis-18-crown-6 Appended Porphyrins and Pyridine or Alkyl Ammonium Functionalized Fullerenes. *J. Phys. Chem. B* **2006**, 110, (12), 5905-5913.

109. D'Souza, F.; El-Khouly, M. E.; McCarty, A. L.; Gadde, S.; Karr, P. A.; Zandler, M. E.; Araki, Y.; Ito, O., Self-Assembled via Axial Coordination Magnesium Porphyrin-Imidazole Appended Fullerene Dyad: Spectroscopic, Electrochemical, Computational, and Photochemical Studies. *J. Phys. Chem. B* **2005**, 109, (20), 10107-10114.

110. D'Souza, F.; Chitta, R.; Gadde, S.; Shafiqullslam, D. M.; Schumacher, A. L.; Zandler, M. E.; Araki, Y.; Ito, O., Design and Studies on Supramolecular

Ferrocene-Porphyrin-Fullerene Constructs for Generating Long-Lived Charge Separated States. *J. Phys. Chem. B* **2006**, 110, (50), 25240-25250.

111. Terazono, Y.; Kodis, G.; Liddell, P. A.; Garg, V.; Gervaldo, M.; Moore, T. A.; Moore, A. L.; Gust, D., Photoinduced Electron Transfer in a Hexaphenylbenzene-Based Self-Assembled Porphyrin-Fullerene Triad. *Photochem. Photobiol. Sci.* **2006**, 83, (2), 464-469.

112. Schmittel, M.; Kishore, R. S.; Bats, J. W., Synthesis of supramolecular fullerene-porphyrin-Cu(phen)(2)-ferrocene architectures. A heteroleptic approach towards tetrads. *Org. Biomol. Chem.* **2007**, 5, (1), 78-86.

113. Mateo-Alonso, A.; Sooambar, C.; Prato, M., Fullerene photoactive dyads assembled by axial coordination with metals. *Comptes Rendus Chimie* **2006**, 9, (7-8), 944-951.

114. Schumacher, Amy L.; Sandanayaka, A. S. D.; Hill, Jonathan P.; Ariga, K.; Karr, Paul A.; Araki, Y.; Ito, O.; D'Souza, F., Supramolecular Triad and Pentad Composed of Zinc-Porphyrin(s), Oxoporphyrinogen, and Fullerene(s): Design and Electron-Transfer Studies. *Chem. Eur. J.* **2007**, 13, (16), 4628-4635.

115. Gadde, S.; Islam, D. M. S.; Wijesinghe, C. A.; Subbaiyan, N. K.; Zandler, M. E.; Araki, Y.; Ito, O.; D'Souza, F., Light-Induced Electron Transfer of a Supramolecular Bis(Zinc Porphyrin)-Fullerene Triad Constructed via a Diacetylamidopyridine/Uracil Hydrogen-Bonding Motif. **2007**, 111, (34), 12500-12503.

116. Imahori, H.; Tamaki, K.; Guldi, D. M.; Luo, C.; Fujitsuka, M.; Ito, O.; Sakata, Y.; Fukuzumi, S., Modulating Charge Separation and Charge

Recombination Dynamics in Porphyrin-Fullerene Linked Dyads and Triads: Marcus-Normal versus Inverted Region. *J. Am. Chem. Soc* **2001**, 123, (11), 2607-2617.

Chapter 2.

1. Lu, A.-H.; Salabas, E. L.; Schuth, F., *Angew. Chem. Int. Ed.* **2007**, 46, 1222-1244.
2. Vanden Bout, D. A., *Metal Nanoparticles: Synthesis, Characterization, and Applications*. Marcel Dekker, Inc.: New York and Basel, 2002.
3. Drain, C. M.; Smeureanu, G.; Patel, S.; Gong, X.; Garno, J.; Arijeloye, J., *New J. Chem.* **2006**, 30, 1834-1843.
4. Frenkel, J.; Doefman, J., *Nature* **2003**, 126, 274-275.
5. Guo, F.; Zheng, H.; Yang, Z.; Qian, Y., *Mater. Lett.* **2002**, 56, 906-909.
6. Puentes, V. F.; Krishnan, K.; Alivisatos, A. P., *Topics in Catalysis* **2002**, 19 (2), 145-148.
7. Puentes, V. F.; Krishnan, K. M., *Appl. Phys. Lett.* **2001**, 78, 2187-2189.
8. Kim, S. W.; Park, J.; Jang, Y.; Chung, Y.; Hwang, S.; Hyeon, T.; Kim, Y. W., *Nano Lett.* **2003**, 3, 1289-1291.
9. Takami, A.; Kurita, H.; Koda, S., *J. Phys. Chem. B* **1999**, 103, 1226-1232.
10. Kazakevich, P. V.; Simakin, A. V.; Voronov, V. V.; Shafeev, G. A., *Appl. Surf. Sci.* **2006**, 252, 4373-4380.
11. Vesperinas, A.; Eastoe, J.; Jackson, S.; Wyatt, P., *Chem. Commun.* **2007**, 3912-3914.

12. Fang, Q.; He, G.; Cai, W. P.; Zhang, J.-Y.; Boyd, I. W., *Appl. Surf. Sci.* **2004**, *226*, 7-11.
13. Chen, P.; Wu, X.; Lin, J.; Tan, K. L., *J. Phys. Chem. B* **1999**, *103*, 4559-4561.
14. Ipsita A. Banerjee; Yu, L.; Matsui, H., *Proc. Natl. Acad. Sci.* **2003**, *100*, 14678-14682.
15. Sun, L.; Wei, G.; Song, Y.; Liu, Z.; Wang, L.; Li, Z., *Appl. Surf. Sci.* **2006**, *252*, 4969-4974.
16. Aldaye, F. A.; Palmer, A. L.; Sleiman, H. F., *Science* **2008**, *321*, 1795-1799.
17. Coffey, J. L.; Bigham, S. R.; Li, X.; Pinizzotto, R. F.; Rho, Y. G.; Pirtle, R. M.; Pirtle, I. L., *Appl. Phys. Lett.* **1996**, *69*, 3851-3853.
18. Flynn, C. E.; Lee, S.-W.; Peelle, B. R.; Belcher, A. N., *Acta Materialia* **2003**, *51*, 5867-5880.
19. Maruszewski, K.; Jasiorski, M.; Hreniak, D.; Strk, W.; Hermanowicz, K.; Heiman, K., *J. Sol-Gel Science and Technology* **2003**, *26*, 83-88.
20. Antonietti, M.; Ozin, G. A., *Chem. Eur. J.* **2004**, *10*, 28-41.
21. Zhong, Z.; Sim, D.; Teo, J.; Luo, J.; Zhang, H.; Gedanken, A., *Langmuir* **2008**, *24*, 4655-4660.
22. Ganesan, R.; Gedanken, A., *Nanotechnology* **2008**, *19*, 025702.
23. Djalali, R.; Samson, J.; Matsui, H., *J. Am. Chem. Soc.* **2004**, *126*, 7935-7939.
24. Lipps, G., *Plasmids: Current Research and Future Trends*. Caister Academic Press: Norfolk UK, 2008.

25. QIAGEN. QIAGEN PlasmidAmp Kit-For direct amplification of plasmid DNA from bacterial colonies, www1.qiagen.com.
26. Conwell, C. C.; Vilfan, I. D.; Hud, N. V., *Proc. Nat. Ac. Sci.* **2003**, *100*, 9296-9301.
27. He, S.; Arscott, P. G.; Bloomfield, V. A., *Biopolymers* **1999**, *53*, 329-241.
28. Bartoliniy, W. P.; Johnston, M. V., *J. Mass Spectrom.* **2000**, *35*, 408-416.
29. Boerner, L. J.; Zaleski, J. M., *Current Opinion in Chemical Biology* **2005**, 135-144.
30. Sinha, R. P.; Hader, D.-P., *Photochem. Photobiol. Sci.* **2002**, *1*, 225-236.
31. Schnell, J. R.; Berman, J.; Bloomfield, V. A., *Biophys. J.* **1998** *74* 1484-1491.
32. Davey, C. A.; Richmond, T. J., *Proc. Nat. Ac. Sci. USA* **2002**, *99* 11169-11174.
33. Liu, C.; Wang, M.; Zhang, T.; Sun, H., *Coord. Chem. Rev.* **2004**, *248*, 147-168.
34. Berti, L.; Alessandrini, A.; Facci, P., *J. Am. Chem. Soc.* **2005**, *127*, 11216-11217.
35. Burley, G. A.; Gierlich, J.; Mofid, M. R.; Nir, H.; Tal, S.; Eichen, Y.; Carell, T., *J. Am. Chem. Soc.* **2006**, *128*, 1398-1399.
36. Horcas, I.; Fernandez, R.; Gomez-Rodriguez, J. M.; Colchero, J.; Gomez-Herrero, J.; Baro, A. M., *Rev. Sci. Instruments* **2007**, *78*, 013705.
37. Wong, C.; West, P. E.; Olson, K. S.; Mecartney, M. L.; Starostina, N., *JOM* **2007**, *59*, 12-16.

38.web.archive.org/web/20070518092613/http://www.northland.cc.mn.us/Chemistry/standard_reduction_potentials.htm Standard reduction potentials.

Chapter 3.

1. D. Bonifazi, H. Spillmann, A. Kiebele, M. de Wild, P. Seiler, F. Cheng, H.-J. Güntherodt, T. Jung and F. Diederich, *Angew. Chem., Int. Ed.*, 2004, **43**, 4759-4763.
2. H. Imahori, A. Fujimoto, S. Kang, H. Hotta, K. Yoshida, T. Umeyama, Y. Matano, S. Isoda, M. Isosomppi, N. V. Tkachenko and H. Lemmetyinen, *Chem. Eur. J.*, 2005, **11**, 7265-7275.
3. H. Imahori, H. Yamada, S. Ozawa, K. Ushidab and Y. Sakata, *Chem. Comm.*, 1999, 1165-1166.
4. A. Ikeda, T. Hatano, S. Shinkai, T. Akiyama and S. Yamada, *J. Am. Chem. Soc.*, 2001, **123**, 4855-4856.
5. T. Hasobe, H. Imahori, P. V. Kamat and S. Fukuzumi, *J. Am. Chem. Soc.*, 2003, **125**, 14962-14963.
6. M. Isosomppi, N. V. Tkachenko, A. Efimov, K. Kaunisto, K. Hosomizu, H. Imahorib and H. Lemmetyinen, *J. Mater. Chem.*, 2005, **15**, 4546-4554.
7. T. Umeyama and H. Imahori, *Photosynthesis Research*, 2006, **87**, 63-71.
8. P. D. W. Boyd and C. A. Reed, *Acc. Chem. Res.*, 2005, **38**, 235-242.
9. A. Hosseini, M. C. Hodgson, F. S. Tham, C. A. Reed and P. D. W. Boyd, *Crystal Growth&Design*, 2006, **6**, 397-403.

10. A. Hosseini, S. Taylor, G. Accorsi, N. Armaroli, C. A. Reed and P. D. W. Boyd, *J. Am. Chem. Soc.*, 2006, **128**, 15903-15913.
11. D. M. Guldi, *Chem. Comm.*, 2000, 321-327.
12. D. M. Guldi, *Chem. Soc. Rev.*, 2001, **31**, 22-36.
13. C.-y. Liu, H.-l. Pan, M. A. Fox and A. J. Bard, *Chem. Mater.*, 1997, **9**, 1422-1429.
14. P. Kirsch, *Modern Fluoroorganic Chemistry: Synthesis, Reactivity, Applications*, Wiley, 2004.
15. T. N. Milic, N. Chi, D. G. Yablou, G. W. Flynn, J. D. Batteas and C. M. Drain, *Angew. Chem.*, 2002, **41**, 2117-2119.
16. P. D. W. Boyd, M. C. Hodgson, C. E. F. Rickard, A. G. Oliver, L. Chaker, P. J. Brothers, R. D. Bolskar, F. S. Tham and C. A. Reed, *J. Am. Chem. Soc.*, 1999, **121**, 10487-10495.
17. S. Sawamura and N. Fujita, *Carbon*, 2007, **45**, 965-970.
18. C. M. Drain and X. Chen., in *Encyclopedia of Nanoscience & Nanotechnology*, ed. H. S. Nalwa, American Scientific Press, New York, 2004, pp. 593-616.
19. C. M. Drain, G. Smeareanu, J. Batteas and S. Patel, in *Dekker Encyclopedia of Nanoscience and Nanotechnology*, eds. J. A. Schwartz, C. I. Contescu and K. Putyera, Marcel Dekker, Inc., New York, 2004, pp. 3481-3502.
20. F. Wessendorf, J. F. Gnichwitz, G. H. Sarova, K. Hager, U. Hartnagel, D. M. Guldi and A. Hirsch, *J. Am. Chem. Soc.*, 2007, **129**, 16057-16071.

21. F. Oswald, D.-M. S. Islam, Y. Araki, V. Troiani, R. Caballero, P. de la Cruz, O. Ito and F. Langa, *Chem. Commun.*, 2007, 4498-4500.

Chapter 4.

1. Dennler, G.; Sariciftci, N. S.; Brabec, C. J., Conjugated Polymer-Based Organic Solar Cells. In *Semiconducting Polymers: Chemistry, Physics and Engineering*, Second ed.; Hadziioannou, G.; Malliaras, G. G., Eds. WILEY-VCH Verlag GmbH & Co.: Weinheim, 2007; Vol. 1, pp 455-530.

2. Hoppe, H.; Sariciftci, N., Polymer Solar Cells. In *Photoresponsive Polymers II*, Springer-Verlag: Berlin, 2008; pp 1-86.

3. Leznoff, C. C., *Phthalocyanines Properties and Applications*. Wiley VCH publishers: New York, 1993.

4. Drain, C. M.; Varotto, A.; Radivojevic, I., Self-Organized Porphyrinic Materials. *Chem. Rev.* **2009**, 109, (5), 1630–1658.

5. Xue, J.; Uchida, S.; Rand, B. P.; Forrest, S. R., 4.2% efficient organic photovoltaic cells with low series resistances. *Appl. Phys. Lett.* **2004**, 84, (16), 3013-3015.

6. Rio, Y.; Rodriguez-Morgade, M. S.; Torres, T., Modulating the electronic properties of porphyrinoids: a voyage from the violet to the infrared regions of the electromagnetic spectrum. *Org. Biomol. Chem.* **2008**, 6, 1877-1894.

7. Leznoff, C. C.; Sosa-Sanchez, J. L., Polysubstituted phthalocyanines by nucleophilic substitution reactions on hexadecafluorophthalocyanines. *Chem. Commun.* **2004**, 338-339.
8. Jürgen, H., Cyclic Voltammetry - Electrochemical Spectroscopy. New Analytical Methods *Angew. Chem. Int. Ed.* **1984**, 23, (11), 831-847.
9. D'Souza, F.; Ito, O., Photoinduced electron transfer in supramolecular systems of fullerenes functionalized with ligands capable of binding to zinc porphyrins and zinc phthalocyanines. *Coord. Chem. Rev.* **2005**, 249, (13-14), 1410-1422.
10. Loi, M. A.; Denk, P.; Hoppe, H.; Neugebauer, H.; Winder, C.; Meissner, D.; Brabec, C.; Sariciftci, N. S.; Gouloumis, A.; Vázquez, P.; Torres, T., Long-lived photoinduced charge separation for solar cell applications in phthalocyanine–fulleropyrrolidine dyad thin films. *J. Mater. Chem.* **2003**, 13, 700-704.
11. Kim, J. Y.; Lee, K.; Coates, N. E.; Moses, D.; Nguyen, T.-Q.; Dante, M.; Heeger, A. J., Efficient Tandem Polymer Solar Cells Fabricated by All-Solution Processing. *Science* **2007**, 317, 222-225.
12. Marczak, R.; Sgobba, V.; Kutner, W.; Gadde, S.; D'Souza, F.; Guldi, D. M., Langmuir-Blodgett Films of a Cationic Zinc Porphyrin-Imidazole-Functionalized Fullerene Dyad: Formation and Photoelectrochemical Studies. *Langmuir* **2007**, 23, (4), 1917-1923.

13. El-Khouly, M. E.; Ito, O.; Smith, P. M.; D'Souza, F., Intermolecular and supramolecular photoinduced electron transfer processes of fullerene-porphyrin/phthalocyanine systems. *J. Photochem. Photobiol. C: Photochem. Rev.* **2004**, 5, (1), 79-104.
14. Troshin, P. A.; Koeppe, R.; Peregudov, A. S.; Peregudova, S. M.; Egginger, M.; Lyubovskaya, R. N.; Sariciftci, N. S., Supramolecular Association of Pyrrolidinofullerenes Bearing Chelating Pyridyl Groups and Zinc Phthalocyanine for Organic Solar Cells. *Chem. Mater.* **2007**, 19, (22), 5363-5372.
15. Sullivan, P.; Heutz, S.; Schultes, S. M.; Jones, T. S., Influence of codeposition on the performance of CuPc-C₆₀ heterojunction photovoltaic devices. *Appl. Phys. Lett.* **2004**, 84, (7), 1210-1212.
16. Milic, T.; Garino, J. C.; Batteas, J. D.; Smeureanu, G.; Drain, C. M., Self-organization of self-assembled tetrameric porphyrin arrays on surfaces. *Langmuir* **2004**, 20, (10), 3974-3983.
17. Van Keuren, E.; Bone, A.; Ma, C., Phthalocyanine Nanoparticle Formation in Supersaturated Solutions. *Langmuir* **2008**, 24, (12), 6079-6084.
18. Prato, M.; Maggini, M.; Giacometti, C.; Scorrano, G.; Sandona, G.; Farnia, G., Synthesis and Electrochemical Properties of Substituted Fulleropyrrolidines. *Tetrahedron* **1996**, 52, (14), 5221-5234.
19. Kang, J.-W.; Lee, D.-S.; Park, H.-D.; Park, Y.-S.; Kim, J. W.; Jeong, W.-I.; Yoo, K.-M.; Go, K.; Kimb, S.-H.; Kim, J.-J., Silane- and triazine-containing hole

and exciton blocking material for high-efficiency phosphorescent organic light emitting diodes. *J. Mater. Chem.* **2007**, 17, 3714–3719.

20. Kinoshita, Y.; Hasobe, T.; Murata, H., Control of open-circuit voltage in organic photovoltaic cells by inserting an ultrathin metal-phthalocyanine layer. *Appl. Phys. Lett.* **2007**, 91, 083518.

Chapter 5.

1. Sabine, L.; Angelika, B.; Nelli, S.; Frank, G.; Constanze, H.; Giusy, S.; Roxana, J.; Elisabeth, K.; Sven, S.; Alina, S.; Martin, T., Discotic Liquid Crystals: From Tailor-Made Synthesis to Plastic Electronics. *Angew. Chem. Int. Ed.* **2007**, 46, (26), 4832-4887.

2. de la Escosura, A.; Martinez-Diaz, M. V.; Barbera, J.; Torres, T., Self-Organization of Phthalocyanine and [60]Fullerene Dyads in Liquid Crystals. *J. Org. Chem.* **2008**, 73, (4), 1475-1480.

3. Schumacher, Amy L.; Sandanayaka, A. S. D.; Hill, Jonathan P.; Ariga, K.; Karr, Paul A.; Araki, Y.; Ito, O.; D'Souza, F., Supramolecular Triad and Pentad Composed of Zinc-Porphyrin(s), Oxoporphyrinogen, and Fullerene(s): Design and Electron-Transfer Studies. *Chem. Eur. J.* **2007**, 13, (16), 4628-4635.

4. Guldi, D. M.; Gouloumis, A.; Vazquez, P.; Torres, T.; Georgakilas, V.; Prato, M., Nanoscale Organization of a Phthalocyanine-Fullerene System: Remarkable Stabilization of Charges in Photoactive 1-D Nanotubules. *J. Am. Chem. Soc.* **2005**, 127, (16), 5811-5813.

5. Georgakilas, V.; Pellarini, F.; Prato, M.; Guldi, D. M.; Melle-Franco, M.; Zerbetto, F., Supramolecular self-assembled fullerene nanostructures. *PNAS* **2002**, 99, (8), 5075-5080.
6. D'Souza, F.; Ito, O., Photoinduced electron transfer in supramolecular systems of fullerenes functionalized with ligands capable of binding to zinc porphyrins and zinc phthalocyanines. *Coord. Chem. Rev.* **2005**, 249, (13-14), 1410-1422.
7. Drain, C. M.; Varotto, A.; Radivojevic, I., Self-Organized Porphyrinic Materials. *Chem. Rev.* **2009**, 109, (5), 1630-1658.
8. Boyd, P. D. W.; Reed, C. A., Fullerene-Porphyrin Constructs. In *Acc. Chem. Res.*, 2005; Vol. 38, pp 235-242.

Chapter 6.

1. Blotny, G., Recent applications of 2,4,6-trichloro-1,3,5-triazine and its derivatives in organic synthesis. *Tetrahedron* **2006**, 62, 9507–9522.
2. Kruper, W. J.; Chamberlin, T. A.; Kochanny, M., Regiospecific aryl nitration of meso-substituted tetraarylporphyrins: a simple route to bifunctional porphyrins. *J. Org. Chem.* **2002**, 54, (11), 2753-2756.
3. Soares, A. R. M.; Martinez-Diaz, M. V.; Bruckner, A.; Pereira, A. M. V. M.; Tome, J. P. C.; Alonso, C. M. A.; Faustino, M. A. F.; Neves, M. G. P. M. S.; Tome, A. C.; Silva, A. M. S.; Cavaleiro, J. A. S.; Torres, T.; Guldi, D. M., Synthesis of Novel N-Linked Porphyrin-Phthalocyanine Dyads. *Org. Lett.* **2007**, 9, (8), 1557-1560.

4. Gonzalez-Cabello, A.; Vazquez, P.; Torres, T.; Guldi, D. M., Highly Coupled Dyads Based on Phthalocyanine-Ruthenium(II) Tris(bipyridine) Complexes. Synthesis and Photoinduced Processes. *J. Org. Chem.* **2003**, 68, (22), 8635-8642.
5. Carofiglio, T.; Varotto, A.; Tonellato, U., One-Pot Synthesis of Cyanuric Acid-Bridged Porphyrin-Porphyrin Dyads. *J. Org. Chem.* **2004**, 69, (23), 8121-8124.